NORGES GEOTEKNISKE INSTITUTT

NORWEGIAN GEOTECHNICAL INSTITUTE

Publikasjon/Publication **209**

G. AAS AND S. LACASSE
Shear strength of Soft Clay in Terms of Effective Stresses

G. AAS AND S. LACASSE
K_0 as Function of Changes in Stress and Strain Conditions during Consolidation, Unloading and Reloading

G. AAS AND S. LACASSE
Vane Shear Strength in Terms of Effective Stresses

G. AAS AND S. LACASSE
Undrained Shear Strength of Overconsolidated Clays

G. AAS AND S. LACASSE
Stability of Natural Slopes in Quick Clays

G. AAS AND S. LACASSE
Yield stresses in Soft Contracting Clays

OSLO 2022

ISBN 978-82-546-1009-1

NGI Publication 209 is a special issue in the NGI Publication series published by:

Norwegian Geotechnical Institute
P.O. Box 3930 Ullevaal Stadion
N-0806 Oslo, Norway

Telephone: *+47 22 02 30 00*
Email: *ngi@ngi.no*
Webpage *http://www.ngi.no*

The six articles have not been published before.

NGI's Publication 209

Dedication

The authors wish to dedicate the six articles to Dr Elmo DiBiagio, our friend and colleague, who encouraged us to write these articles. Elmo not only insisted on having this work documented, he was also a discussion partner and contributed significantly by transcribing and coordinating much of the work. Our only regret is that he was not able to see the finished product.

Gunnar Aas
Suzanne Lacasse
Oslo, 15 July 2021/20 October 2022

Preface to NGI Publication 209

It is with special pleasure that I write the preface to the newest digital NGI Publication, number 209. It is also a thankful task because Gunnar Aas has been a pillar and pioneer in the development of NGI's foundation design expertise and has provided the basis for understanding the behaviour of soft and quick clays.

Gunnar has worked at NGI for over 33 years. After he retired, he, at last, found the time to bring together his seminal contributions throughout his years at NGI, It all started with Gunnar Aas preparing an invited keynote paper for the American Society of Civil Engineers (ASCE) "In situ 1986" conference hosted by Professor J. Michael Duncan at Virginia Tech, and then giving the 10th Laurits Bjerrum Lecture (1987) on the "Undrained shear strength of clay as a function of effective stresses". Throughout the years he worked on the unification and systematisation of the description of the behaviour of soft clays, yielding, the effective stress shear strength parameters to use for both normally and overconsolidated clays, and the derivation of the coefficient of earth pressure at rest K_0 and the undrained shear strength ratio s_u/σ'_{vc} of clays. The papers are easy and enjoyable to read and are witness of a detailed and thorough analysis that will live through the test of time.

Well done, Gunnar, for a lifelong expertise on soft clays!

Oslo, 2022-10-20
Lars Andresen
Managing Director
NGI

Introduction

NGI's Publication 209 brings together the concepts and experience developed by the first author, Gunnar Aas, throughout his 33-year career at NGI and thereafter as geotechnical consultant on construction projects. During all those years, the first author accumulated data and developed novel concepts of shear strength, effective stress parameters and behaviour of soft clays.

The cooperation between the two authors on this topic started in 1985 when Kaare Höeg, then Managing Director of NGI, was asked by Professor J. Michael Duncan to prepare a keynote lecture for the ASCE "In situ 1986" conference, and delegated the task to the authors. This resulted in the paper: Aas, G., Lacasse, S., Lunne, T. and Höeg, K.: "Use of in Situ Tests for Foundation Design on Clay".

Gunnar Aas gave the 10th Laurits Bjerrum Lecture (1987) on the "Undrained shear strength of clay as a function of effective stresses". The papers in this NGI Publication present and expand the concepts presented in the Bjerrum Lecture. In the years following the Bjerrum Lecture, the first author continued to develop his concepts on yielding and effective stress shear strength parameters for both normally and overconsolidated clays, and established a model to derive theoretically the coefficient of earth pressure at rest K_0 and the undrained shear strength ratio s_u/σ'_{vc} of clays. These concepts were then applied to the analysis of the stability of natural slopes.

The idea of writing up the papers came up after the first author retired. Originally, the plan was two papers. The work progressed slowly because of other geotechnical commitments. Finally, the first author and Elmo DiBiagio took the matter in hand, and gradually the two papers became six papers as the developments were more numerous than originally anticipated:

- *Shear strength of Soft Clay in Terms of Effective Stresses*
- *K_0 as Function of Changes in Stress and Strain Conditions during Consolidation, Unloading and Reloading*
- *Vane Shear Strength in Terms of Effective Stresses*
- *Undrained Shear Strength of Overconsolidated Clays*
- *Stability of Natural Slopes in Quick Clays*
- *Yield stresses in Soft Contracting Clays*

The authors are indebted to many colleagues at NGI who throughout the years have contributed with data, discussions and ideas, and especially to Dr Elmo DiBiagio for taking the initiative of transforming the thoughts onto paper. The authors are especially grateful to NGI and Dr Lars Andresen for supporting the idea of this special NGI Publication and for the financial support with the drafting of all the figures. The diligent help in this regard of Mr Tim Gregory and Ms Maren Kristine Johnsen is greatly appreciated.

Gunnar Aas
Suzanne Lacasse
2021-07-15/October 2022

Shear Strength of Soft Clay in Terms of Effective Stresses

Gunnar Aas[1] and Suzanne Lacasse[2]
[1] formerly Norwegian Geotechnical Institute (NGI), [2] NGI

Abstract

It is commonly understood and accepted today that soft, contractant soils, when sheared under undrained conditions, develop high pore pressures that result in failure at a critical shear stress, occurring before the soil has been able to fully mobilize its effective stress strength parameters. This has led to the conclusion that in this type of clay, stability analyses, even for natural slopes, should be based on undrained, active and passive triaxial or plane strain strengths and possibly direct simple shear strength (Bjerrum, 1973; Ladd and Foott, 1974). The present study included an analysis of the results from undrained shear strength tests on high quality samples, and aimed at developing an expression for the undrained shear strength and "critical" shear stress as functions of effective stresses. The study demonstrates the importance of considering the effect of shear deformations, the contribution of friction and attraction to undrained strength, and how undrained shear strength is a unique result of the consolidation history of the clay. A procedure is proposed to express the undrained shear strengths measured in active and passive triaxial tests and in direct simple shear tests as functions of the effective stresses and a set of generally valid effective stress strength parameters. The framework also provides a new explanation of the notion of attraction (and cohesion) in soft clays). The study demonstrates how a set of effective stress paths from an active and a passive triaxial test can be used together to establish the consolidation conditions and to determine the effective stress strength parameters, friction angle and attraction. Using tests on clays with plasticity between 5 and 90%, the new framework provides a clear, simple and logical relationship, with decreasing friction angle and increasing attraction with increasing plasticity.

Introduction

In soft, contractant clays, yielding and failure takes place at a critical stress value occurring before the clay has been able to fully mobilize its effective stress strength parameters. The present study puts forward a theory describing how friction and attraction contribute to mobilize the undrained shear strength. In this connection, it was important to focus on the relationship between shear strain and mobilization of strength, and to demonstrate that undrained shear strength is a unique result of the consolidation history of the clay. The new framework was tested with several different clays from around in the world.

The paper first discusses the undrained shear strength for a soft, contractant clay, as determined from triaxial active and passive tests and from direct simple shear tests. A framework to determine the effective stress shear strength parameters from undrained shear tests on soft, contractant clay is then presented. The proposed approach is tested for a number of case records in Norway and abroad. The shear strength parameters are then correlated to plasticity index for 25 clays at 14 locations.

Determination of the undrained shear strength

The undrained shear strength, s_u, along a well-defined, but arbitrary failure plane can be expressed as:

$$s_u = {}^1/_2\,(\sigma'_{ULS} - \sigma'_{LLS}) \qquad (1)$$

where σ'_{ULS} and σ'_{LLS} denote the effective, compressive failure stresses acting at angles of ±45° with the failure plane. In the following, these two failure stresses will be denoted the *upper limiting stress* (ULS) and the *lower limiting stress (LLS)*. The meaning of these limiting stresses is that they represent stress-values that cannot be exceeded without yielding occurring. This study wanted to clarify how these two limiting stresses can be determined from the knowledge of the effective stress/deformation history of the soil. In this way, the undrained strength could then be expressed directly in terms of the effective stresses, without having to involve changes in total stresses and pore pressures.

The relationship between undrained shear strength and effective stresses was taken to be governed by two fundamental strength parameters, the *material friction angle*, φ'_M, and the *relative material attraction*, χ. These parameters are believed to be pure material constants and, hence, independent of stress level, stress directions and stress history.

Friction

The build-up of friction in a soil under shear loading constitutes physical work. In physics, a force is said to do work if, when acting, there is a displacement of the point of application in the direction of the force. Work transfers energy from one form to another. In a soil, a soil volume under the influence of an external force mobilizes resistance against being strained and, as strains increase, against failure. Mobilization of friction requires that a plastic (nonreversible) deformation takes place, and that the conditions of work equal to force times distance, with associated deformations, do exist, with coincidence in directions of stresses and strains.

Small elastic strains and larger plastic strains act differently in the process of mobilizing frictional shear strength.

When a clay deposit consolidates without undergoing net lateral strain (K_0-conditions), the ratio between the horizontal and vertical effective stress is equal to the coefficient of earth pressure at rest, K_0 ($K_0 = \sigma'_{h0}/\sigma'_{v0}$). Without lateral expansion, only the vertical consolidation stress contributes to building up frictional resistance capacity. Consequently, the mobilized active frictional strength (along a 45° plane) is limited to the value ${}^1/_2\sigma'_{vo}\cdot\sin\varphi'_M$, where M is the mobilized effective friction angle. The stress conditions for this clay represent the final stage of a yielding process and are dictated by a simple requirement of static equilibrium. Hence, the mobilized frictional resistance has to be equal to the applied shear stress:

$$s_{uA} = {}^1/_2(\sigma'_{v0} - \sigma'_{h0}) = {}^1/_2\,\sigma'_{v0}\cdot\sin\varphi'_M \qquad (2)$$

which gives:

$$K_o = \sigma'_{ho} / \sigma'_{vo} = 1 - \sin\varphi'_M \qquad (3)$$

Equation (3) represents the well-known Jaky's formula (Jaky, 1948) expressing the coefficient of earth pressure at rest for a normally consolidated soil.

In clays, mineral to mineral contacts are supposed to occur only between sand and silt particles. Clay particles are dissociated in the contact points by a thin, firmly bounded layer of pore water. This layer is thought to be of viscous nature, which means that it can transfer, to a certain degree, both compressive stresses and shear stresses. This ability is, however, strongly dependent on the applied rate of strain. In the present study, all shear strengths are, for simplicity, related to a "standard" strain rate corresponding to what is conventionally used in laboratory testing.

The ratio between ultimate friction resistance and effective normal stress at the contact points is substantially higher for the sand and silt fraction than for the clay fraction. Consequently, a plastic clay exhibiting a relatively high content of active clay particles will show a low friction angle compared to a lean (silty) clay.

Attraction

In clays, one assumes that the net attractive forces act at the contact points between clay particles across the water-film. The resulting attractive force in any direction is denoted the *material attraction*, σ_a. This attraction acts like a tension reinforcement in the clay. Compared to an attraction-free soil where the undrained shear strength is governed by friction alone, the attraction force enables the clay to withstand an additional reduction of the lower limiting stress at failure, and thereby increases the undrained shear strength. As the attractive forces already exist prior to any undrained shearing process, practically no strain is necessary to activate the attraction. In a given clay soil, the attractive forces increase with decreasing distance between clay particles. Consequently, the attraction, believed to reflect the effective stresses to which the clay is subjected, can be expressed as follows:

$$\sigma_a = \chi \cdot \sigma'_{na} \tag{4}$$

where σ'_{na} denotes the effective stress in the direction normal to the direction of the attractive force. For undrained shear under active triaxial loading on a young, normally consolidated clay, the effective vertical consolidation stress σ'_{vo} is σ'_{na}, and the contribution to the active undrained shear strength from the attraction is $^1/_2\,\chi\cdot\sigma'_{vo}$.

As the material attraction is a function of exclusively the clay mineral fraction, its magnitude will increase with increasing content of active clay particles and thereby plasticity.

Failure in soft, contractant soils

An *in situ* clay element consolidated under a vertical stress of σ'_{vo} will undergo a uniaxial plastic deformation and mobilize an active frictional strength equal to $^1/_2\cdot\sigma'_{vo}\cdot\sin\varphi'_M$. A successive unloading of the clay by reducing the deviator stress to zero results in elastic strains only, which does not influence the clays ability to mobilize friction. A further vertical unloading leads to plastic shear strains and a gradual mobilization of the passive shear strength until σ'_v equals σ'_{ho} $(1-\sin\varphi'_M)$. The passive shear stress and strength are then both $^1/_2\cdot\sigma'_{ho}\cdot\sin\varphi'_M$.

These values of active and passive strength assume that no additional plastic deformation has taken place to mobilize friction due to σ'_{ho} in either active or passive shear. Such mobilization

implies an important change compared with the previous stage, as the directions of shear deformations here are reversed in relation to the frictional supporting stress component. These reversed conditions in contractant soils are believed to be responsible for a structural reorganization among the clay particles, high pore pressures and decreasing shear strength with increasing strain.

If reconsolidated in the laboratory under *in situ* stresses, the young clay will have upper limiting stresses equal to σ'_{vo} and $\sigma'_{ho} = \sigma'_{vo}(1 - \sin\varphi'_M)$ under active and passive shear. Taking into consideration the contribution from attraction, the lower limiting stresses then become under active and passive shear $\sigma'_{vo}(1 - \chi - \sin\varphi'_M)$ and $\sigma'_{ho}(1 - \chi - \sin\varphi'_M)$, respectively.'

Active shear strength of loose sand

A loose fine sand may have properties similar to that of a contractant clay, and, in a similar manner, undergo a structural collapse at a critical strain before reaching a classic Mohr-Coulomb failure. As an example of this, Figure 1 reproduces the results from a series of undrained, active triaxial tests on the saturated, loose Ham River Sand (Bishop *et al.*, 1965; Bishop, 1966). All tests gave a friction angle close to 34°, corresponding to the maximum value of σ'_v/σ'_h reached at large strains. However, the peak points on the effective stress paths occur at small strains (about 1 %) and fall approximately on the line describing $\sigma'_h/\sigma'_v = 1 - \sin\varphi'_M$ (line added in diagram by authors). One test was run under drained conditions (initial average stress $\frac{1}{2}(\sigma'_1 + \sigma'_3)$ of 990 psi) until the shear stress by far exceeded the value corresponding to the $\sigma'_h/\sigma'_v = 1 - \sin\varphi'_M$ line, and then continued as an undrained test. No additional shear resistance could be mobilized. A second test was run drained (initial average stress $\frac{1}{2}(\sigma'_1 + \sigma'_3)$ of 500 psi), and the shear stress also here exceeded considerably the value corresponding to the $\sigma'_h/\sigma'_v = 1 - \sin\varphi'_M$ line.

These results support the above results for soft contractant clay, where the upper limiting active stress for a young, normally consolidated clay is σ'_{vo}, and that the active, undrained shear strength of an (attraction-free) contractant soil is limited to the contribution to friction from the vertical stress alone.

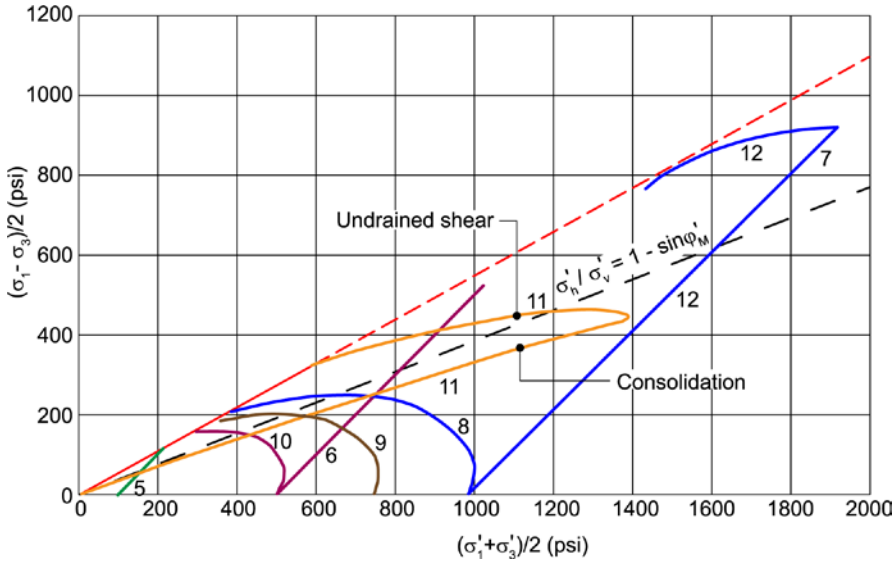

Figure 1. Effective stress paths from undrained active triaxial tests on Ham River Sand (after Bishop et al., 1965; Bishop, 1966)

Undrained shear strength of contractant clays

A perfect, young, normally consolidated clay is rarely encountered in practice. As both frictional resistance and attraction are closely related to consolidation strains, one needs to distinguish among different types of load applications and load history. The following four categories of clays were established for this study:

- Young, normally consolidated clay.
- Aged, normally consolidated clay, which has undergone secondary consolidation.
- Weathered clay, previously subjected to alternating capillary stresses due to, e.g., evaporation or freeze-thaw action.
- Overconsolidated clay, previously subjected to considerably larger loads than at present.

In the following discussion, the clay is assumed, in all cases, to have been consolidated, and if unloaded, under conditions of no lateral yield (K_0-conditions).

As a result of ageing, weathering or overconsolidation, an *in situ* clay deposit has experienced a supplementary vertical strain and behaves correspondingly as if it had been a young clay consolidated under a vertical stress σ'_{vE} higher than σ'_{v0} (Fig. 2). This vertical stress implies an increased horizontal stress of σ'_{vE} (1-sinφ'_M). The earlier strain history enables the clay to activate these "equivalent" stresses without undergoing plastic strains. Hence, the stresses represent an upper stress regime which enables one to determine the upper limiting stresses under active and passive triaxial shear and even under direct simple shear, as will be illustrated in examples later.

Because the existing vertical and horizontal effective stresses are σ'_{v0} and $K_0\sigma'_{v0}$, these stresses form in the same way the basis for the lower limiting stresses under active triaxial shear. The horizontal stress can be lowered to $\sigma'_{v0}(1 - \sin\varphi'_M)$, which means that the shear stress is balanced by the friction due to the vertical stress alone, and further reduced with the activation of the attraction. Hence, the lower limiting stress in active shear is in this case $\sigma'_{v0}(1 - \chi - \sin\varphi'_M)$, where $\chi\cdot\sigma'_{v0}$ reflects the contribution from attraction.

In the same way the lower limiting stress under passive shear becomes equal to $K_0\sigma'_{v0}(1 - \chi - \sin\varphi'_M)$. Coefficient K_0 is equal to $1 - \sin\varphi'_M$ for aged and overconsolidated clays. In the case of weathered clays, however, where the clay has been subjected to an alternating isotropic stress change, K_0 may differ from this value, as seen below for one of the case records.

In direct simple shear, where the principal stresses rotate 45°, the same way of reasoning as above leads to values of upper and lower limiting stress equal to $^1/_2(\sigma'_{vE} + \sigma'_{vE}(1\text{-}\sin\varphi'_M))$ and $^1/_2(\sigma'_{vo} + K_0\sigma'_{v0}(1 - \sin\varphi'_M - \chi))$, respectively.

Combining the above limiting stresses with Eqs. 1 and 2, the expressions for the undrained shear strength under active (s_{uA}), passive (s_{uP}) and simple shear (s_{uD}) loadings become:

$$s_{uA} = {}^1/_2\sigma'_{vo}[(\chi + \sin\varphi'_M) + \sigma'_{vE}/\sigma'_{vo} - 1] \quad (5)$$

$$s_{uP} = {}^1/_2\sigma'_{vo}[K_0(\chi + \sin\varphi'_M) + \sigma'_{vE}/\sigma'_{vo}(1 - \sin\varphi'_M) - K_0] \quad (6)$$

$$s_{uD} = {}^1/_4\sigma'_{vo}[(1 + K_0)(\chi + \sin\varphi'_M) + \sigma'_{vE}/\sigma'_{vo}(2 - \sin\varphi'_M) - (1 + K_0] \quad (7)$$

The expressions above state the following relationship (for a 45° rotation):

$$s_{uD} = {}^1/_2(s_{uA} + s_{uP}) \tag{8}$$

The expression for the undrained strength on any inclination β (in degrees) of the failure plane ($s_{u\,\beta}$) is then:

$$s_{u\,\beta} = s_{uA}\cdot\cos^2(\beta - 45°) + s_{uP}\cdot\sin^2(\beta - 45°) \tag{9}$$

In reality, Eqs 5, 6 and 7 are of limited practical importance: it is more convenient to determine the stress-strength parameters directly from the effective stress paths in a Mohr diagram.

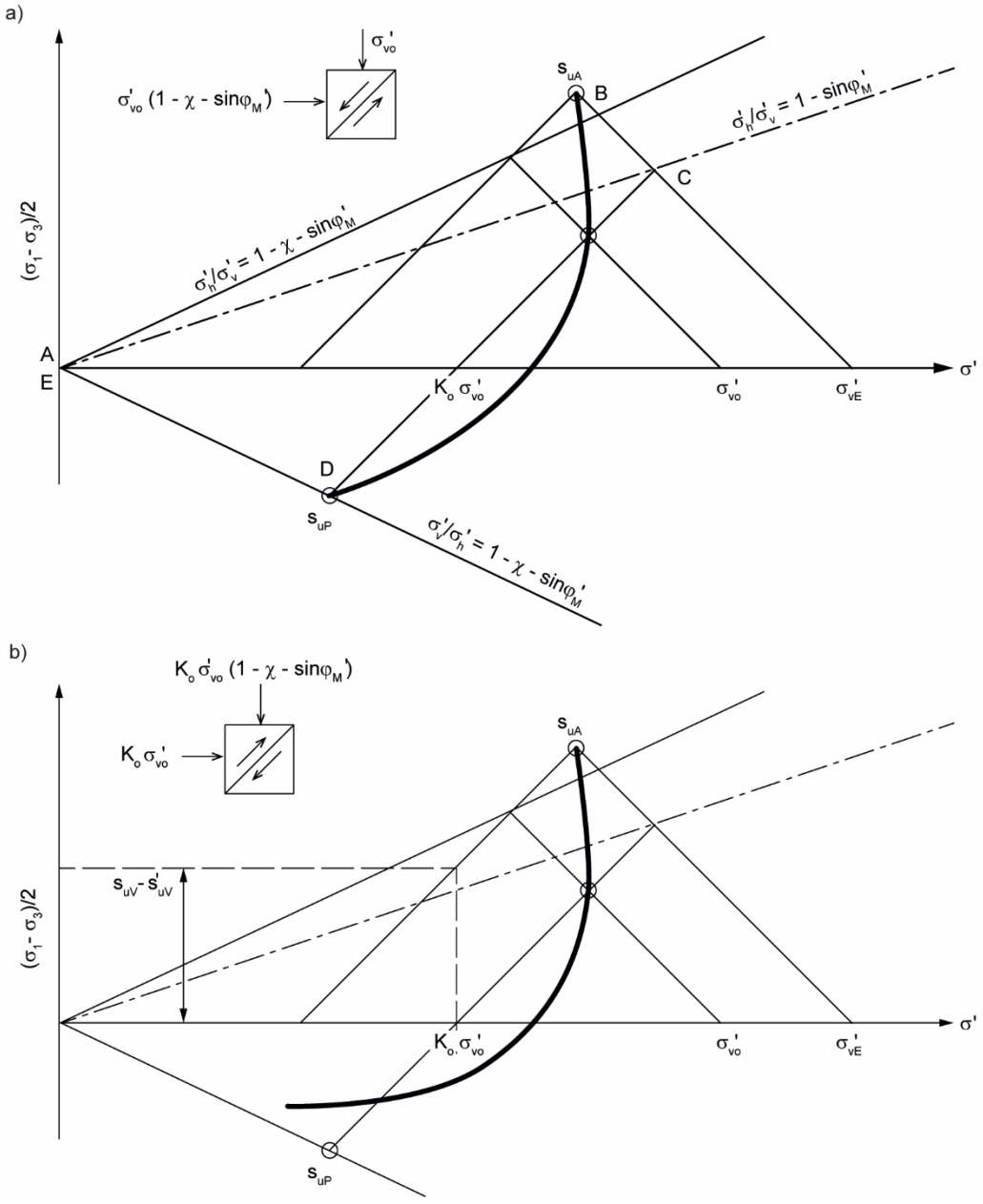

Figure 2. Determination of effective stress and strength parameters on effective stress path from triaxial tests

Framework to determine effective stress strength parameters from undrained shear tests

Figure 2 gives an example of how the effective shear strength parameters φ'_M and χ can be determined from the results of active and passive triaxial tests on an aged, normally consolidated clay. Known are the position of the active and passive shear strengths, s_{uA} and s_{uP} in the Mohr-Coulomb diagram and the effective vertical stress, σ'_{vo}.

The intersection between an upward 45° line from s_{uP} and a downward 45° line from s_{uA} gives a point on the $\sigma'_h/\sigma'_v = (1 - \sin\varphi'_M)$ line. The upward gradient n:1 of this line gives the relation: $\sin\varphi'_M = 2n/(1+n)$.

In the same manner, the intersection between an upward 45° line from σ'_{vo} and a downward 45° line from s_{uA} gives a point on the $\sigma'_h/\sigma'_v = (1 - \chi - \sin\varphi'_M)$ line. The relation between χ and the gradient of this line is $\chi = 2n/(1+n) - \sin\varphi'_M$.

The above derivation requires the knowledge of a sufficiently accurate peak value on the passive effective stress path, which in turn will be used to determines the value of K_0. The determination of the K_0-value may often be problematic in practice, especially in highly sensitive and nearly attraction-free clays. Aas *et al*. (1986) suggested that the data from passive triaxial tests can be replaced by strength data from *in situ* vane shear tests performed at the same depths where the laboratory test specimen was taken. This interpretation is based on the simplified assumption that a clay element in the cylindrical failure zone circumscribing the vane, fails in the same manner as the sample in an active triaxial test. Hence, the vertical vane strength (which in soft clays does not differ much from $s_{uv} - s_{uv}'$ (Fig. 2), is determined by assuming equal lower limiting stress in the two tests:

$$\sigma'_{vo}(1 - \chi - \sin\varphi'_M) = K_o\sigma'_{vo} - (s_{uv} - s_{uv}') \qquad (10)$$

which gives:

$$K_o\sigma'_{vo} = (1 - \chi - \sin\varphi'_M)\sigma'_{vo} + (s_{uv} - s_{uv}') \qquad (11)$$

Here s_{uv} and s_{uv}' denote undisturbed and remolded vane strength, respectively.

Figure 2a shows a hypothetical example of laboratory tests on a clay where the passive shear strength is sufficiently well defined, and thereby a true value of K_o can be obtained without the need for supporting vane data. There are however numerous examples of research data where vane results has been able to confirm such "constructed" values of K_o. Figure 2b gives an example of such, where a representative vane strength value is necessary to complete the determination of the K_o–value.

In the case of weathered clays. The coefficient of earth pressure at rest, K_o, cannot be determined unless with the help of vane data. This will be examined in more detail in the Calabar case record below.

The lines forming the quadrilateral ABCDE in Figure 2a define the limiting stresses in active and passive shear These have been formerly presented as yield envelopes (e.g. Larsson and Sällfors, 1981). They represent the ultimate value before yield, when one stress is kept constant, while the other one is either reduced or increased. In practice, full mobilization of active and

passive shear strength requires in principle that a stress reduction takes place in one direction simultaneously with a stress increase in the other, resulting in points in the diagram located outside the yield envelopes.

The graphic method for the determinations of effective stress strength parameters using these upper and lower limit stresses is illustrated further with a presentation of actual test data on four different clays. It should be noted that the notation of the limiting stresses has been simplified in the forthcoming figures to ULSA, ULSP, ULSD for the upper limiting stresses in active, passive and direct simple shear and to LLSA, LLSP, LLSD for the lower limiting stresses in active, passive and direct simple shear.

Case records

New Jersey Clay (Koutsoftas and Ladd, 1983)

Figure 3 shows the normalized shear stress vs shear strain curve and effective stress paths from plane strain active and passive and direct simple shear tests on undisturbed samples of New Jersey Clay, a plastic clay with a plasticity index I_p of 43 %. The samples were consolidated anisotropically for a vertical stress about twice the *in situ* consolidation stress, and the clay thus consolidated is a "young" clay, not affected by ageing.

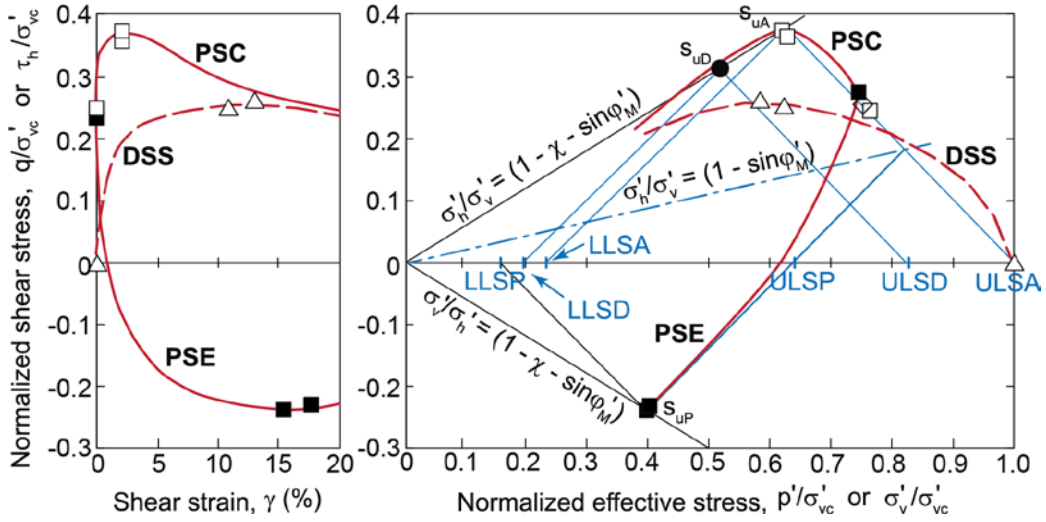

Figure 3. CK_0U plane strain (PS) and direct simple shear (DSS) test data on normally consolidated New Jersey Clay: left: Normalized shear stress vs shear strain; right: Normalized effective stress paths (Koutsoftas and Ladd, 1983) (PSC for active and PSE for passive plane strain tests)

This case, as well as a few other cases in this paper, use plain strain test data instead of triaxial data. Ladd and Edgers (1972) and Ladd *et al*. (1977) published comparisons of the two tests. They suggested higher undrained shear strength in plane strain compression (active) than in triaxial compression (active) by about 10%, and similarly higher by about 5% in extension (passive). In the present paper, the results of the two test types were considered to be equivalent.

The stress stress-shear strain data to the left in Figure 3 show a typical picture for soft, contractant clays. In the active mode of failure, the peak shear strength occurs at a low failure strain, followed by a substantial strength loss and strain-softening in active shear. In contrast, passive shear and direct simple shear, both involving a rotation of the principal stress directions,

by 90 and 45° respectively, result in a much lower peak resistance at a significantly higher failure strain, and little strain-softening.

To the right in Figure 3, the effective stress paths are shown. The peak shear stresses on the active and passive stress paths express the active and passive undrained shear strengths. The intersection of the 45° lines starting at the peak shear stress-values with the zero shear stress axis determines upper and lower limiting stresses. The intersections of the 45° lines with the $\sigma'_h/\sigma'_v = 1 - \sin\varphi'_M$ lines are also shown.

Since $\sigma'_{ULSA(=\sigma'vo)}$ equals σ'_{vo}, (see Fig. 2) for this young clay, the peak shear stress on the active stress path represents a point on the "χ-line" ($\sigma'_h/\sigma'_v = 1 - \chi - \sin\varphi'_M$). The data yield the following parameters: $\sin\varphi'_M = 0.37$, $\chi = 0.39$, $K_0 = 0.63$.

The direct simple shear test gives a peak strength significantly lower than the theoretical value s_{uD}, defined as the crossing point between the "χ-line" and a 45° line starting on the abscissa midway between σ'_{ULSP} and σ'_{ULSA}. This divergence was generally observed in the direct simple shear test. Possible explanations include the difficulty in achieving full contact between the clay and the enclosing rubber membrane (so non-K_0 conditions), the non-uniformity of stresses in the simple shear test specimen, or the rotation of the principal stresses not being exactly 45°.

Ellingsrud Clay, Oslo (Lacasse *et al.*, 1985)

Ellingsrud Clay is a quick clay exhibiting very low plasticity ($I_p = 4$ %) and vane shear strength ($s_{uv}/\sigma'_{vo} = 0.07 - 0.10$). Figure 4 shows the effective stress paths from triaxial active, triaxial passive and direct simple shear tests on a block sample from 8.1 m depth. In addition, the value of the vane strength difference ($s_{uv} - s_{uv}'$) at the same depth is shown

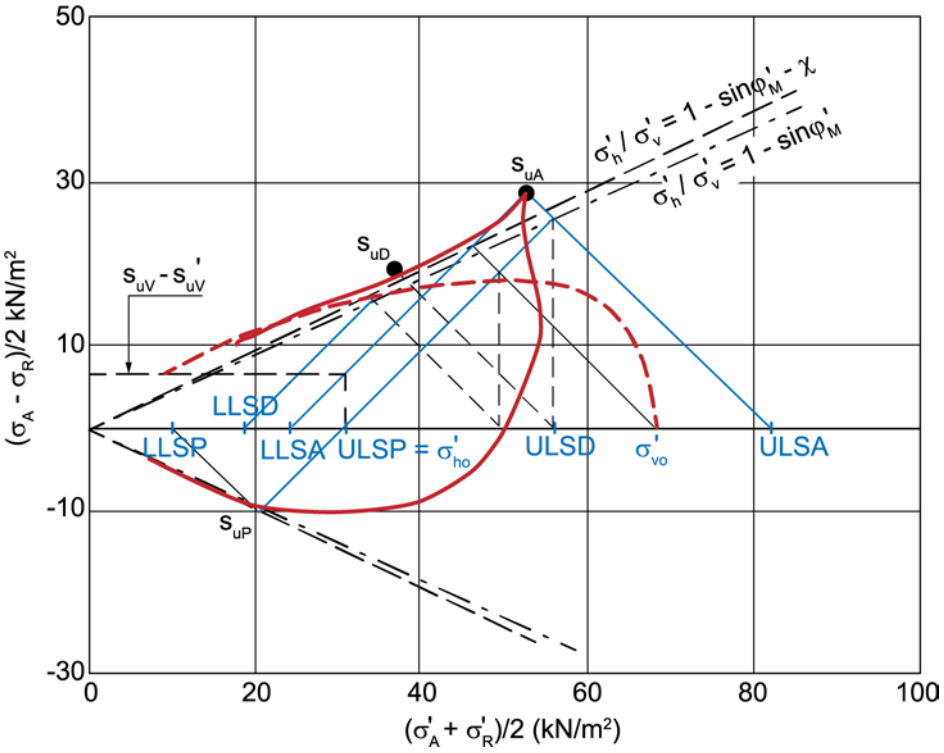

Figure 4. Determination of the consolidation stresses and effective stress strength parameters for the aged Ellingsrud quick clay at depth 8.1 m (Lacasse et al. 1985)

As the stress paths from the passive triaxial and direct simple shear tests show poorly defined maxima for this clay, the value of $\sin\varphi'_M$ had to be determined by the help of the vane test data (Aas and Lacasse, 2021). As illustrated in Figure 4, the intersection of the horizontal dotted line representing $s_{uv} - s'_{uv,}$ and the 45° line starting at s_{uA} defines the *in situ* horizontal consolidation stress, σ'_{ho}, and is equal to $(1 - \sin\varphi'_M)\cdot\sigma'_{vE}$. Points on the lines describing the ratio $\sigma'_{ho}/\sigma'_{vo} = 1 - \sin\varphi'_M$ and the "χ-line", respectively, are determined as described in Figure 2.

The tests indicate that for this aged clay the following strength parameters are the most representative: $\chi = 0.02$ and $\sin\varphi'_M = 0.62$. In addition, the tests give a value of 0.46 for the coefficient of earth pressure at rest, K_0. For the sample from a depth of 13.1 m, similar parameters were determined: $\chi = 0$, $\sin\varphi'_M = 0.62$ and $K_0 = 0.49$. It should be mentioned that these K_0-values correspond well with values measured by the self- boring pressuremeter tests at this site (Lacasse and Lunne, 1982) and with the newest statistically based correlations developed by L'Heureux *et al*., 2017.

For this very soft clay, there is a fairly good agreement between the laboratory-inferred values of LLSD values from the laboratory-measured s_{uD} and the theoretical value halfway between LLSA and LLSP on the zero shear stress line.

Calabar Clay, Kenya (NGI, 1976)

Figure 5 presents the results from undrained triaxial active and passive tests from 9.2 m depth on a soft highly plastic clay ($I_p = 88\%$). In addition, the measured field vane shear strength at the same depth is shown. Calabar clay is a weathered clay, where two distinct sets of consolidation stresses were used: the higher ones, σ'_{vE} and $\sigma'_{vE}(1 - \sin\varphi'_M)$, represent the upper limiting stresses, while the *in situ* stresses σ'_{vo} and $K_0\sigma'_{vo}$ represent the lower limiting stresses.

For this weathered clay, $K_0\sigma'_{vo}$ does not coincide with $\sigma'_{vE}\cdot(1 - \sin\varphi'_M)$, which means that the passive undrained shear strength s_{uP} has to be constructed with the help of a lower value of effective horizontal stress and using the shear vane strength, as described earlier. This highly plastic clay shows, as expected, a very high value for attraction ($\chi = 0.50$) and a correspondingly low friction angle ($\sin\varphi'_M = 0.28$). For this highly plastic clay, the field vane undrained shear strength is close to the undrained shear strength from triaxial active tests.

Haga Clay, Akershus (Christoffersen and Lacasse, 1985)

The Haga clay is a leached marine clay with salt content of 1 g/l, a plasticity index of 11 to 14% and a sensitivity of 4 to 5. The clay is highly overconsolidated at shallow depths, and the derived overconsolidation ratio OCR is about 10 at a 2 m depth.

An overconsolidated clay has undergone in its past history a loading and unloading under conditions of no lateral yield. This has led to a state of static equilibrium implying a ratio between the vertical and horizontal effective stress equal to that for the corresponding young clay, if the deformations are the same. Hence, the overconsolidated clay will behave like a young, normally consolidated clay, however taking into consideration the higher level on the upper limiting stresses.

Figure 6 presents the effective stress paths from consolidated undrained triaxial active and passive tests on a 95 mm tube sample from 2.2 m depth. Using the procedure described earlier, the Haga tests indicate the following soil parameters: $\sin\varphi'_M = 0.50$, $\chi = 0.21$, $K_0 = 2.00$.

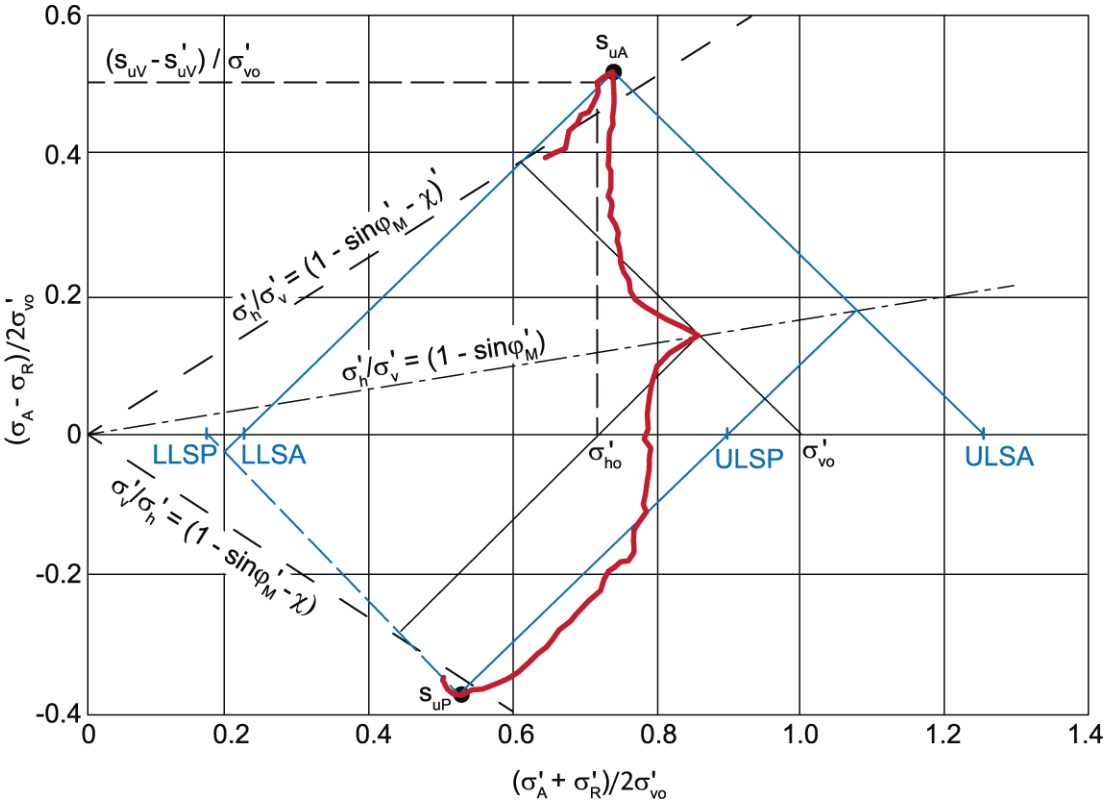

Figure 5. Determination of the consolidation stresses and effective stress parameters for soft, highly plastic Calabar clay at 9.2 m depth

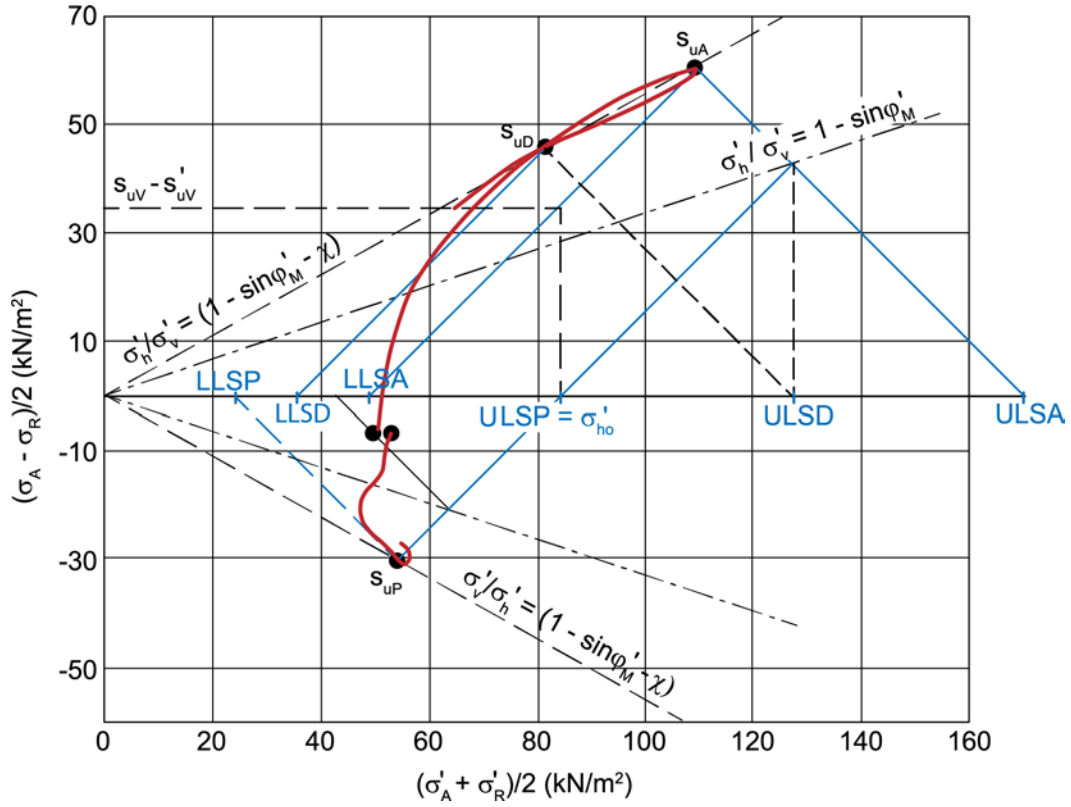

Figure 6. Determination of the consolidation stresses and effective stress strength parameters for the highly overconsolidated Haga clay at 2.2 m depth

The same value of K_0 is obtained if one combines the results of vane and triaxial data. It should also be mentioned that this K_0 value corresponds well with values recorded in self-boring pressuremeter tests at this location (Lacasse and Lunne, 1982).

Results from a direct simple shear test, K_0-consolidated in the conventional manner to the *in situ* effective vertical stress, showed an undrained shear strength reaching only about 50% of the theoretical value of the simple shear strength, s_{uD}.

A series of three additional direct simple shear tests were run on specimens from depth 2.2 m. Each specimen was first consolidated under a vertical stress substantially higher than the *in situ* value σ'_{vo}, and then unloaded to a value equal to σ'_{vo} (similar to the original SHANSEP approach (Ladd *et al.*, 1977).

The results from the three additional tests showed quite remarkably that the effect of a preloading above the preconsolidation stress and unloading in the laboratory is considerable. In the test where the OCR was 11, both the magnitude of the measured shear strength and the position of the peak shear stress on the stress path corresponded well with the theoretical values shown in Figure 6.

Such preloading procedure is believed to be necessary in a direct simple shear test to ensure a full contact between the clay specimen and the enclosing rubber membrane to ensure zero lateral strain and to reestablish the correct *in situ* stress conditions in weathered and overconsolidated clays.

Relationship between strength parameters and plasticity

Is it reasonable to assume that in a clay the material friction decreases and the attraction increases with increasing content of active clay minerals, i.e., with increasing plasticity index. However, some reservations need to be made because certain variations in mineral composition and chemistry in the clay may not have exactly the same effect on attraction and plasticity.

Mobilized friction angle and attraction

Figure 7 presents the values of $\sin\varphi'_M$ and the attraction ratio χ determined with the above procedures versus the plasticity index, I_p, for 25 sets of triaxial active and passive effective stress paths. Table 1 lists each of the clays the data in Figure 7 are based on. There is some scatter. However, even with scatter, there is a definite relationship correlation with plasticity index: $\sin\varphi'_M$ decreases from a value a little above 0.6 ($\varphi' = 37°$) in a very low plastic clay to about 0.3 ($\varphi' = 17.5°$) in a highly plastic clay. Correspondingly, the attraction χ varies from zero to about 0.5 as I_p increases from zero to about 90%. The reason for the very low attraction values for a few clays in Figure 7 is not understood at the present time.

There exist very little published data on the relationship between $\sin\varphi'_M$ and I_p. Kenney (1959) showed a decreasing friction angle with increasing plasticity. The data from Table 1 agree with Kenney's trend for low plasticity index ($I_p < 20\%$). For higher plasticity indices, the Kenney $\sin\varphi'$-values gradually diverge with the friction angle values deduced from the effective stress paths from triaxial tests. The difference is believed to be due to the following: even though the triaxial clay sample has lost some of its undrained shear strength when maximum obliquity is reached (when σ'_v/σ'_h is maximum, which forms the basis for determining the friction angle),

there still exists attractive forces between the clay particles and there is attraction in the clay. In a standard undrained triaxial test, a residual attraction will act to give an apparently friction angle that is too high, with the discrepancy increasing with higher plasticity and attraction.

Undrained shear strength

A closer look at the two diagrams in Figure 7 reveals that the sum of $\chi + \sin\varphi'_M$ varies little with increasing plasticity. The sum $\sin\varphi'_M + \chi$ for the clays in Table 1 has a mean value of 0.76. This means that a normally consolidated clay ($\sigma'_{vE}/\sigma'_{vo} = 1$) according to Eq. 4 would have an active, undrained shear strength equal to about $0.38\sigma'_{vo}$, independently of I_p.

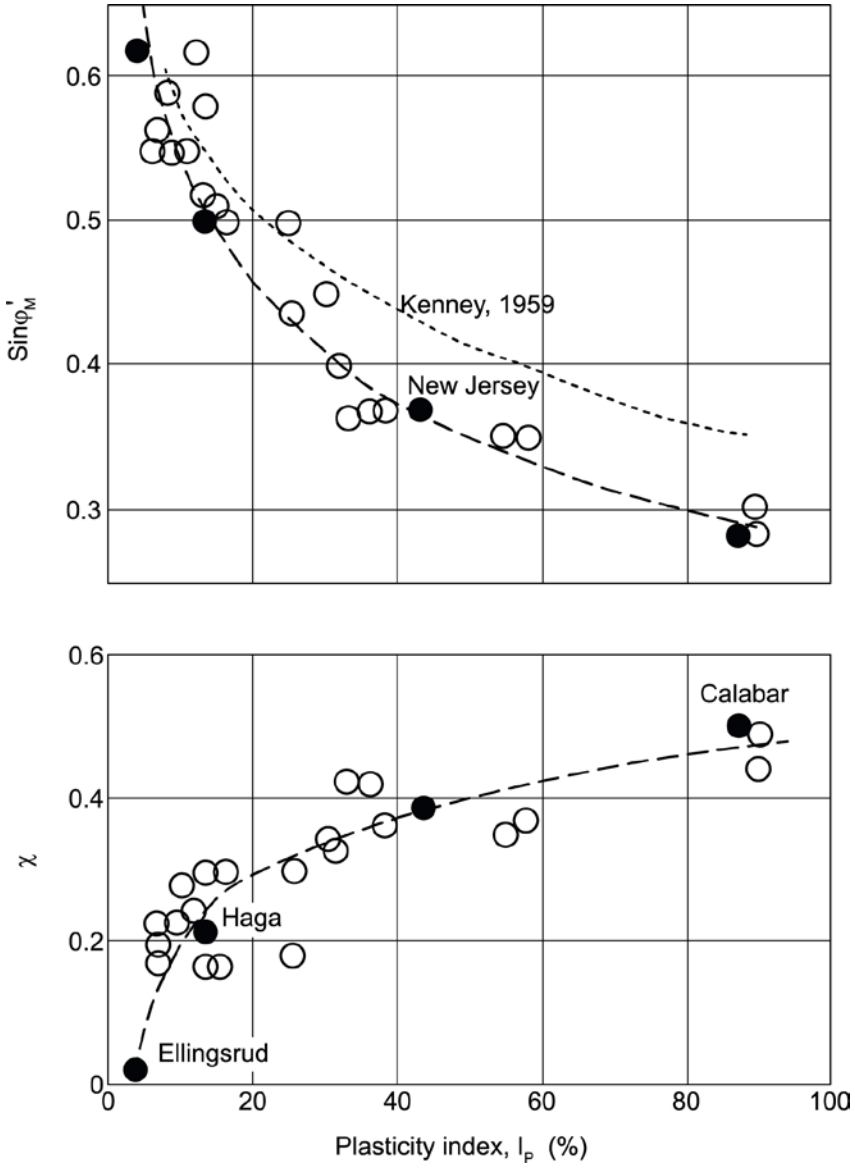

Figure 7. Relationship between friction angel and attraction parameters and plasticity

The same clay would theoretically (Eqs 5 and 6) show the following values in passive and direct simple shear: $(1 - \sin\varphi'_M)\ s_{uA}/\sigma'_{vo}$ and $(1 - {}^1/_2 \cdot \sin\varphi'_M)\ s_{uA}/\sigma'_{vo}$, respectively. Combining the two expressions with the deduced ratio between I_p and $\sin\varphi'_M$ in Figure 7, one obtains the results in Table 2 for normally consolidated clay.

Table 1. Values of $\sin\varphi'_M$ and χ vs plasticity index from triaxial active and passive tests for 25 clays

Site	Depth (m)	I_p (%)	$\sin\varphi'_M$	χ	$\sin\varphi'_M + \chi$	Clay category
Ellingsrud, Norway	8.1	4	0.62	0.02	0.64	Aged
Emmerstad, Norway	5.9	7	0.55	0.23	0.78	OC
Emmerstad, Norway	7.8	7	0.55	0.20	0.75	OC
Olga, Canada	3.9	36	0.37	0.42	0.79	Weathered
Olga, Canada	5.0	33	0.36	0.42	0.78	Weathered
Olga, Canada	6.9	25	0.44	0.30	0.77	Weathered
Olga, Canada	7.1	30	0.45	0.35	0.80	Weathered
Rupert, Canada	5.3	14	0.58	0.30	0.88	OC
Rupert, Canada	9.3	7	0.56	0.19	0.77	OC
Haga, Norway	2.2	13	0.50	0.21	0.71	OC
Haga, Norway	5.3	38	0.37	0.36	0.73	OC
Arendal, Norway	7.5	10	0.55	0.28	0.83	OC
Arendal, Norway	15.3	16	0.50	0.30	0.80	OC
Åndalsnes, Norway	7.2	25	0.50	0.19	0.69	OC
Åndalsnes, Norway	21.2	13	0.52	0.16	0.68	OC
Bangkok, Thailand	5.3	90	0.30	0.49	0.79	Weathered
Bangkok. Thailand	8.5	90	0.28	0.43	0.71	Weathered
Drammen, silty, Norway	10.2	15	0.50	0.16	0.66	Aged
Lille Melløsa, Sweden	9.0	58	0.35	0.37	0.72	OC
Singapore	18.5	55	0.35	0.35	0.70	NC, young
Gøteborg, Sweden	14.0	31	0.40	0.33	0.73	NC, young
Calabar, Kenya	9.2	88	0.28	0.50	0.78	Weathered
New Jersey, USA	?	43	0.37	0.39	0.76	NC, young
Québec, B-6, Canada	12.0	9	0.59	0.22	0.81	OC
Québec, B-2, Canada	7.2	12	0.62	0.24	0.86	OC

Table 2. Effective strength parameters for I_p of 10 and 90%

I_p (%)	$\sin\varphi'_M$	s_{uA}/σ'_{vo}	s_{uP}/σ'_{vo}	s_{uD}/σ'_{vo}
10	0.55	0.38	0.17	0.27
90	0.28	0.38	0.27	0.33

Consequently, the strength anisotropy of a clay decreases with increasing plasticity as also demonstrated by for instance Ladd *et al*. (1977) (Fig. 8) and Jamiolkowski *et al*. (1985). The explanation for this is apparently that strength anisotropy is associated exclusively with the friction component of the shear strength, and of minor importance where attraction is responsible for the major part of the shear strength.

Generally, one has to run both active and passive triaxial tests as basis for a stability analysis to model the parts of the failure surface under active and passive conditions. However, a compilation of 46 different cases, including the 25 cases in Table 1, indicated the following approximate relationship (Fig. 9):

$$^1/_2\,(s_{uA} + s_{uP}) = {}^3/_4\, s_{uA} \qquad (12)$$

and therefore

$$s_{uP}/s_{uA} = ½ \qquad (13)$$

Figure 9 indicates that for the softest clays, this ratio might be lower:

$$^1/_2\,(s_{uA} + s_{uP}) = {}^2/_3\,s_{uA} \tag{14}$$

and therefore

$$s_{uP}/s_{uA} = {}^1/_3 \tag{15}$$

One can question, however, whether sample disturbance could have affected the lower values, especially in silty and sensitive clays with low plasticity.

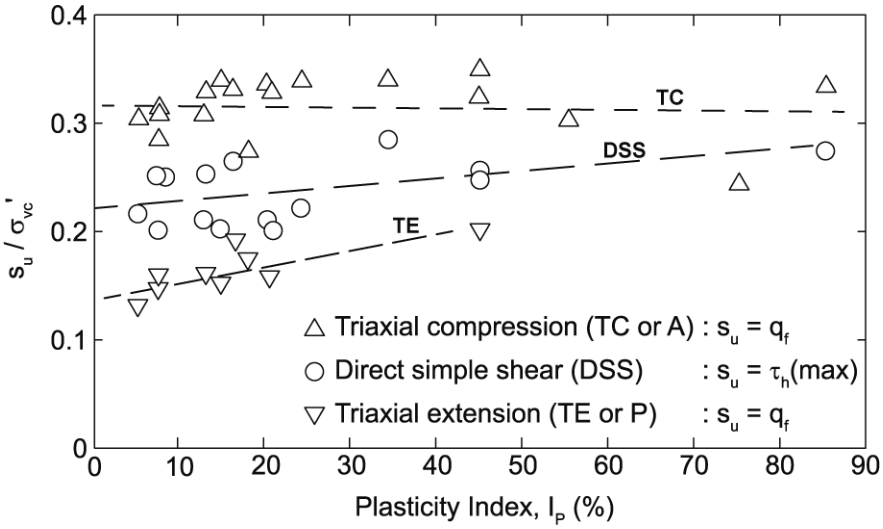

Figure 8. Anisotropy of undrained shear strength as function of plasticity (Ladd et al., 1977; Jamiolkowski et al., 1985)

Since the direct simple shear strength theoretically lies midways between the active and passive strength (Equation 7), s_{uD} can be calculated approximately on the bases of active strength and the expressions above.

Figure 9 presents the relationship between the active undrained shear strength, s_{uA}, and the s_{uLAB} for overconsolidation ratios between 1 and 3, where s_{uLAB} is the average of s_{uA} and s_{uP} (Eq. 12).

Conclusions

The study showed that the undrained shear strength of soft, contractant clays can be expressed as a function of two effective stress strength parameters, the *material friction* and the *relative material attraction*, χ. The two effective stress strength parameters are pure material constants and thus independent of stress level, stress directions and stress history. The material friction decreases and the relative attraction increases with increasing clay plasticity. These basic strength parameters can be determined from sets of effective stress path tests from active and passive triaxial tests and direct simple shear tests, and possibly, in addition, vane strength.

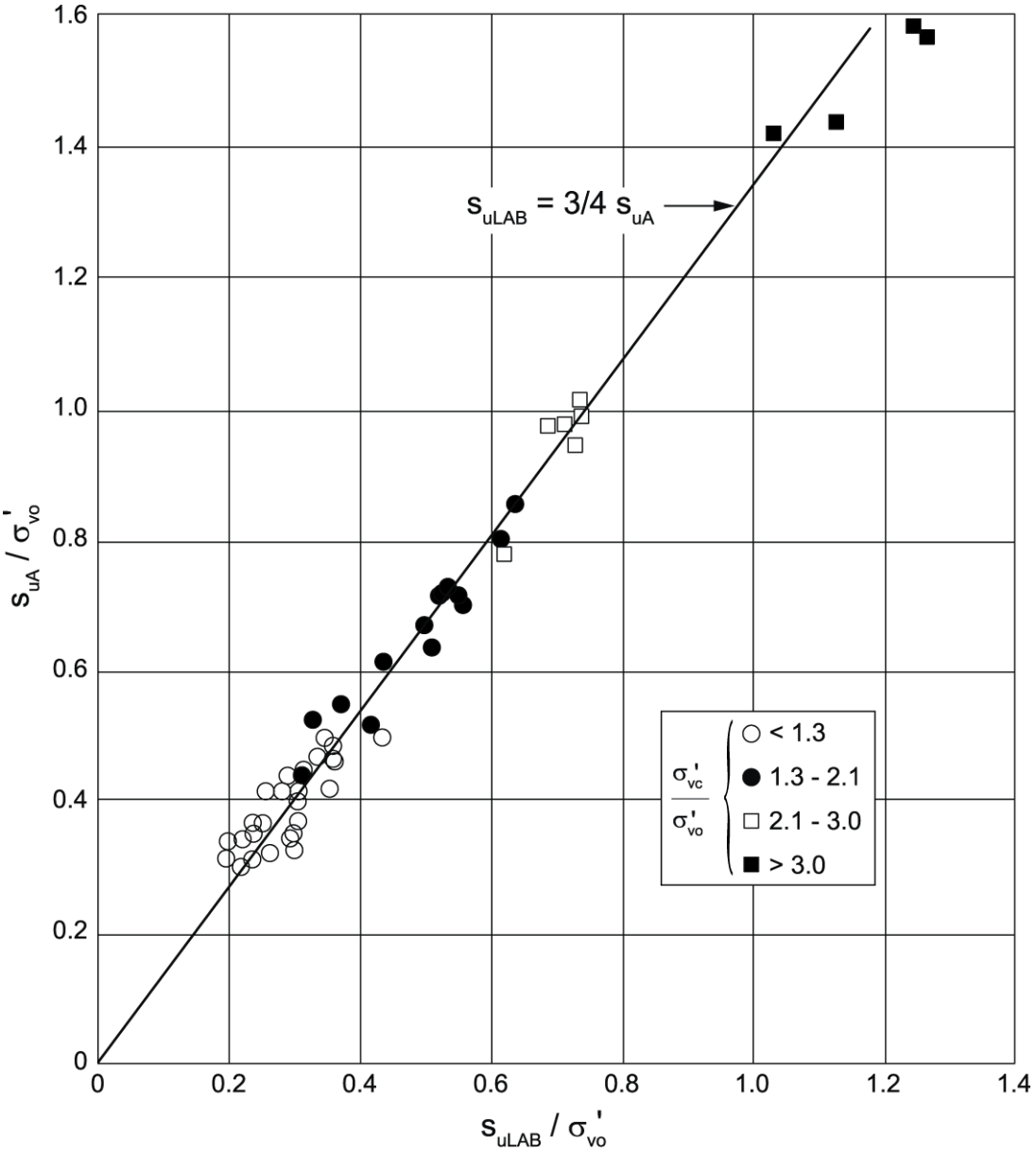

Figure 9. Relationship between normalized shear strength $s_{uLAB} = {}^1/_2 (s_{uA}+s_{uP})$ and s_{uA} for overconsolidation ratios between 1.0 and 3.0

The results show that the mobilization of the material friction and relative attraction under undrained shear is closely related to the consolidation stresses and strains, and to the nature of the deformations imposed on the clay before failure. The mobilization of the material friction constitutes physical work, resulting in a special relationship for the interaction between charging force and resulting plastic deformation (where work is force times distance). On the other hand, only a small elastic strain is necessary to activate attraction, which is also a function of consolidation stresses. The attraction acts like a tension reinforcement in the clay.

In a soft, contractant clay, the yielding conditions imply that only friction due to the vertical stress contributes to the undrained, active shear, and only friction due to the horizontal stress contributes to the undrained, passive strength. Any further loading to mobilize friction from either the horizontal stress in active shear or the vertical stress in passive shear, leads to structural collapse and failure.

The study included several different clay types from around in the world. The data, embracing from silty Norwegian clay to highly plastic Nigerian clay, support that the proposed framework applies in general to soft, contractant clays and can provide a realistic measure of stress-strain-strength behavior of soft clays under undrained shear.

The consequence of these findings is that a conventional Mohr-Coulomb failure criterion is, in reality, not valid for contractant soils such as soft, sensitive clay and loose, narrow graded sand/silt. In these soils, failure takes place as a result of a structural collapse before the full mobilization of friction, in accordance with the presuppositions for this failure criterion. Therefore, in lieu of a conventional effective stress analysis, one needs to use, for stability calculations of natural slopes, an "ADP-type" of analysis based on representative values of the undrained strengths from active (A) and passive (P) triaxial (or plane strain) tests and direct simple shear (D) tests.

The results of the above study show that if one takes into consideration the relationships between deformations and mobilization of friction and attraction, each of the different undrained shear strengths can be explained with the effective stress strength concept, based on the actual values of the effective stress strength parameters.

References

Aas, G. and Lacasse, S. (2021). Vane Shear Strength in Terms of Effective Stress. 3rd paper in this NGI publication.

Aas, G., Lacasse, S., Lunne, T. and Høeg, K. (1986). Use of in Situ Tests for Foundation Design on Clay. ASCE. Conf. in Situ ’86 Blacksburg, Virginia, USA, 1986. 1−30.

Bishop, A.W., Webb, D.L. and Skinner, A.E. (1965). Triaxial tests on soil at elevated cell pressures. International Conference on Soil Mechanics and Foundation Engineering, 6. Montréal 1965. Proceedings. **1**: 170−174.

Bishop, A.W. (1966). The strength of soils as engineering materials. 6th Rankine Lecture. *Geotechnique.* **16**(2): 91−128.

Bjerrum, L. (1973). Problems of soil mechanics and construction on soft clays. State-of-the-art report to session IV. International Conference on Soil Mechanics and Foundation Engineering, 8. Moscow 1973. Proceedings. **3**: 111−159.

Christoffersen, H.P. and Lacasse, S. (1985). Offshore site investigation techniques. Laboratory tests on Haga clay. Norwegian Geotechnical Institute, Oslo. Internal Report 40019-8.

Jaky, J. (1948). On the bearing capacity of piles. International Conference on Soil Mechanics and Foundation Engineering, 2. Rotterdam 1948. Proceedings. **1**: 100−103.

Jamiolkowski, M., Ladd, C.C, Germaine, J.T. and Lancellotta, R. (1985). New developments in field and laboratory testing of soils. State-of-the-art Paper. International Conference on Soil Mechanics and Foundation Engineering, 11. San Francisco 1985. Proceedings. **1**: 57−153.

Kenney, T.C. (1959). Discussion of "Geotechnical properties of glacial lake clays" by T.H. Wu. ASCE. *Soil Mech. and Foundations Div.*, Paper 1732. **85** (SM3): 67−79.

Koutsoftas, D.C. and Ladd, C.C. (1985). Design strengths of an offshore clay. J. *Geotech. Eng.*, ASCE, **111**(3): 337−355.

L'Heureux, J.S., Ozkul, Z., Lacasse, S., D'Ignazio, M. and Lunne, T. (2017). A revised look at the coefficient of earth pressure at rest for Norwegian Clays. Fjellsprengningsteknikk - bergmekanikk - geoteknikk. Oslo 2017. Chapter 35.

Lacasse, S. and Lunne, T. (1982). *In situ* horizontal stress from pressuremeter tests. Symp.on the Pressuremeter and its Marine Applications. Paris, Editions Technip. 187–208.

Lacasse, S., Berre, T. and Lefebvre, G. (1985). Block sampling of sensitive clays. International Conference on Soil Mechanics and Foundation Engineering, 11. San Francisco 1985. Proceedings. **2**: 887−892.

Ladd, C.C. and Edgers, L. (1972). Consolidated-Undrained Direct-Simple Shear Tests on Saturated Clays. Research Report R72–82, Dept. of Civil Engineering, MIT, Cambridge, MA. USA.

Ladd, C.C. and Foott. R. (1974). New design procedure for stability of soft clays. *J. Geotech. Eng.* ASCE. **100**(GT7): 763−786.

Ladd, C.C, Foott, R. Ishihara, K., Schlosser, F. and Poulos, H.G. (1977). Stress-deformation and strength characteristics. State-of-the-art Paper. International Conference on Soil Mechanics and Foundation Engineering, 9. Tokyo 1977. Proceedings. **2**: 421−494.

Larsson R. and Sällfors, G. (1981). Hypothetical Yield Envelope at Stress Rotation. International Conference on Soil Mechanics and Foundation Engineering, 12. Stockholm. Proceedings. Proc. **4**: 693−696.

NGI (1976). Laboratory investigations on a series of clay samples from the swampy areas. Norwegian Geotechnical Institute, Internal Report 76010-01. /G. Aas) 1976-0622. 35pp.

K_0 as a Function of Changes in Stress and Strain Conditions during Consolidation, Unloading and Reloading

Gunnar Aas[1] and Suzanne Lacasse[2]
[1] Formerly Norwegian Geotechnical Institute (NGI), [2] NGI

Abstract

There are several examples in the literature that describe empirical correlations for the coefficient of earth pressure at rest, K_0, and undrained shear strength, s_u, in normally consolidated and overconsolidated clays as a function of index properties like plasticity index, overconsolidation ratio, OCR, and friction angle. However, a physical understanding of the reason why the coefficient of earth pressure at rest varies as a function of these parameters is still lacking, which causes an uncertainty in the value of K_0 to use in geotechnical analyses and in design. This paper investigates the relationship between deformation and mobilization of friction. At the same time, it considers that the unloading process has to be looked at as a stability problem where a static, stabile equilibrium needs to be maintained, thus requiring that the mobilized shear strength equals the applied shear stress. The resulting values of coefficient of earth pressure at rest, K_0, interpreted from effective stress paths alone, give realistic results, also in agreement with recent statistical evaluations on the K_0-value in Norwegian clays. The new interpretation contributes to explain the widely used empirical correlations presented in the literature.

Introduction

It is commonly known that when a clay deposit becomes overconsolidated as a result of vertical unloading, the ratio of the horizontal to vertical effective stress increases with the overconsolidation ratio. This paper evaluates how these stress conditions are influenced by isotropic and shear stress changes during consolidation. One particular objective was to look at the difference in the behaviour of elastic and plastic strains and how they contribute to mobilize and reduce the mobilized friction resistance.

These relationships will be visualized by following a clay element in the ground from deposition through consolidation and subsequent stress relief. In addition, an attempt is made to explain what happens with the earth pressure if subsequently reloading the overconsolidated clay vertically. For simplicity, the ground surface is assumed to be horizontal, implying a state of perfect confined compression and expansion.

Model of a clay element under consolidation and drained shear

Theoretical considerations based on the study of the stress paths under uniaxial loading and unloading of a clay were used to determine the value of the coefficient of earth pressure at rest, K_0, for normally consolidated and overconsolidated clay. The analysis studied the changes in effective stresses and strains as a result of a uniaxial unloading and reloading of a clay deposit. The analysis is based on the following two basic assumptions:

Hypothesis 1. In any phase of the loading-unloading cycle, there must exist a static equilibrium, which means that shear stresses and mobilized shear strengths have to be equal.

Hypothesis 2. The mobilized frictional shear resistance is an exclusive result of the plastic deformation that has occurred. Relief of a shear stress then results in a pure elastic deformation that does not influence the mobilized shear strength.

Primary consolidation

When a clay deposit consolidates without undergoing net lateral strain, the ratio between horizontal and vertical effective stress will become equal to the coefficient of earth pressure at rest, K_0. The stress conditions for this clay represent the final stage of a yielding process, and are dictated from a simple requirement of static equilibrium mentioned in Hypothesis 1 above. This means that the shear resistance of the clay has to be fully mobilized under the actual stress-strain conditions, and thus that it is possible to calculate the value of K_0 if a correct shear strength concept is applied.

Hence, it is necessary to determine the magnitude of the shear strength mobilized on a 45° shear plane in a young consolidated soil. It is important to emphasize that the mobilization of friction is physical work which requires that the conditions of force times distance do exist. As no lateral expansion takes place, the horizontal force does not contribute to the mobilization of friction. Thus, the vertical consolidation stress alone will contribute to the build-up of a frictional resistance equal to $½\cdot\sigma'_{vo}\cdot\sin\varphi'_M$. Hence, an applied shear stress has to be equal to the mobilized frictional resistance:

$$½\cdot(\sigma'_{vo} - \sigma'_{ho}) = ½\cdot\sigma'_{vo}\cdot\sin\varphi'_M \qquad (1)$$

which gives for a normally consolidated clay:

$$\sigma'_{ho}/\sigma'_{vo} = K_o = 1 - \sin\varphi'_M \qquad (2)$$

Equation (2) is the well-known Jaky formula (Jaky, 1948) for the coefficient of earth pressure at rest for a normally consolidated soil. Here φ'_M denotes the *material friction angle* of the clay, indicating a pure material parameter, which is assumed to be independent of stress level, stress direction and stress history.

An indispensable condition for confined compression is that the clay be subjected to plastic stress increments where $\Delta\sigma'_h/\Delta\sigma'_v = (1 - \sin\varphi'_M)$. This requires that the clay undergoes at the same time an increased shear stress equal to $½\cdot\Delta\sigma'_v\cdot\sin\varphi'_M$. The top of the Mohr circle moves along the line from A to B on Figure 1 (the Mohr circle is replaced by an inscribed triangle at peak B). The line AB describes Eq. (2) or Jaky's formula.

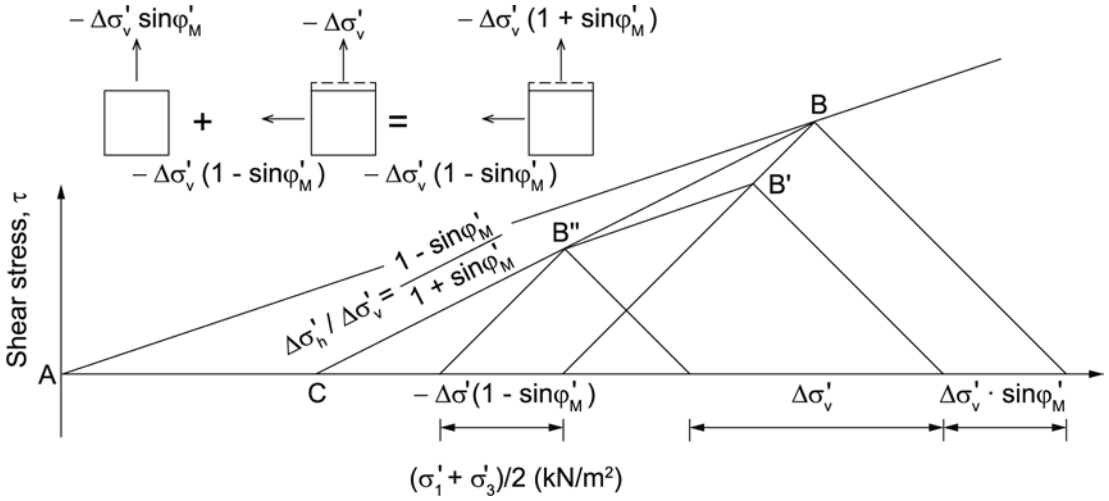

Figure 1. Changes in effective stresses and strains for a clay element during uniaxial loading under K_0-conditions and unloading resulting in an increased in K_0 from $(1 - \sin\varphi'_M)$ to 1

Unloading when $\sigma'_{ho}/\sigma'_{vo} < 1$

A reversed shear stress causes a reversed elastic shear strain, which, as opposed to a plastic strain, does not influence any change in mobilized friction. If the soil element in Figure 1 is unloaded by a reduction of the vertical effective stress equal to $\Delta\sigma'_v$, this implies a subsequent elastic shear stress reduction equal to $\frac{1}{2}\cdot\Delta\sigma'_v\cdot\sin\varphi'_M$. As illustrated in Figure 1, the unloading process is started by first removing the deviator stress $\Delta\sigma'_v \sin\varphi'_M$ (the top of the Mohr circle moves from point B to B'). For this unloading, the lateral strain remains zero. With further unloading, the stress conditions keep the same ratio between vertical and horizontal stress as for the original loading (from point B' to point B"), leading to pure confined vertical expansion.

The resulting stress change follows by the stress path indicated by B to C in Figure 1, and is described by the function:

$$\Delta\sigma'_h / \Delta\sigma_v = (1 - \sin\varphi'_M)/(1 + \sin\varphi'_M) \qquad (3)$$

By introducing the parameters preconsolidation stress, σ'_{vc}, and overconsolidation ratio, OCR expressed as $\sigma'_{vc}/\sigma'_{vo}$, the following equation describes the value of K_0 as a function of OCR:

$$K_0 = (1 + OCR\cdot\sin\varphi'_M)(1 - \sin\varphi'_M)/(1 + \sin\varphi'_M) \qquad (4)$$

The value of OCR corresponding to a K_0 of unity (point C in Fig. 1) is:

$$OCR_{K0=1} = 2/(1 - \sin\varphi'_M) \qquad (5)$$

As the change in shear stress by unloading along the B to B' line does not influence the amount of mobilized friction, the change in shear strength becomes $\frac{1}{2}\cdot\Delta\sigma'\cdot\sin\varphi'_M$ and is equal to the change in shear stress.

Unloading when $1 < \sigma'_{ho}/\sigma'_{vo} < 1/(1 - \sin\varphi'_M)$

With an unloading to stresses corresponding to point C (the isotropic line) in Figure 2, the clay element is subjected to isotropic compressive stress. Under these conditions, further vertical stress relief, equal to $\Delta\sigma'$, occurs. The stress relief does not include any shear stress removal and corresponding elastic strain. Thus, a confined unloading requires that $\Delta\sigma'_h/\Delta\sigma'_v = (1 - \sin\varphi'_M)$. Consequently, for this unloading along the stress path C to D in Figure 2, the effective stress ratio becomes:

$$\Delta\sigma'_{ho}/\Delta\sigma'_{vo} = 1/(1 - \sin\varphi'_M) \quad (6)$$

And the following relationship between K_0 and OCR can be derived:

$$K_0 = [2 + OCR\cdot(1 - \sin\varphi'_M)\sin\varphi'_M]/2(1 + \sin\varphi'_M) \quad (7)$$

The value of OCR corresponding to a K_0 equal to $1/(1 - \sin\varphi'_M)$, i.e. point D in Figure 2, is:

$$OCR_{K0=1/(1-\sin\varphi'M)} = 4/(1 - \sin\varphi'_M)^2. \quad (8)$$

In this case, the change in the applied passive shear stress is $\frac{1}{2}\cdot\Delta\sigma'\cdot\sin\varphi'_M$, and is equal to the mobilized passive shear strength.

Unloading when $\sigma'_{ho}/\sigma'_{vo} > 1/(1 - \sin\varphi'_M)$

As for the unloading under active shear in Figure 1, an unloading $\Delta\sigma'_v$ leads to a reduction of the passive shear stress equal to $\frac{1}{2}\cdot\Delta\sigma'_v\cdot\sin\varphi'_M$, resulting in a pure elastic strain. Again, the conditions of zero lateral strain require an effective stress ratio $\Delta\sigma'_h/\Delta\sigma'_v$ equal to $(1 - \sin\varphi'_M)$. The ratio of the stress change corresponding to the stress path D to E in Figure 3 can be described by:

$$\Delta\sigma'_h/\Delta\sigma'_v = 1 \quad (9)$$

The following relationship for the coefficient of earth pressure at rest K_0 can be derived:

$$K_0 = 1 + OCR\,(1 - \sin\varphi'_M)\sin\varphi'_M/4 \quad (10)$$

The maximum value of K_0, corresponding to a passive failure, i.e. point E in Figure 3, is:

$$K_0 = (1 + \sin\varphi'_M)/(1 - \sin\varphi'_M) \quad (11)$$

The value of OCR corresponding to a value of K_0 equal to $(1 + \sin\varphi'_M)/(1 - \sin\varphi'_M)$, i.e. point E in Figure 3, is:

$$OCR_{K0} = (1 + \sin\varphi'_M)/(1 - \sin\varphi'_M) = 8/(1 - \sin\varphi'_M)^2 \quad (12)$$

In this last phase, the change in shear stress and shear strength are both equal to zero.

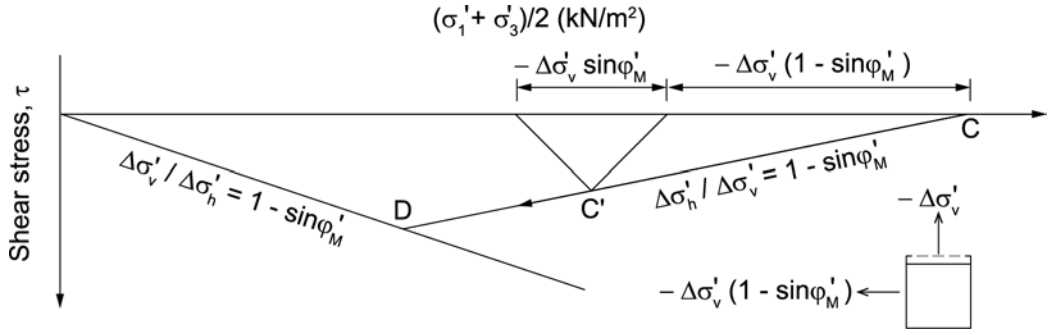

Figure 2. Changes in effective stresses and strains for a clay element during uniaxial unloading resulting in an increase in K_0 from 1 to $1/(1 - \sin\varphi'_M)$

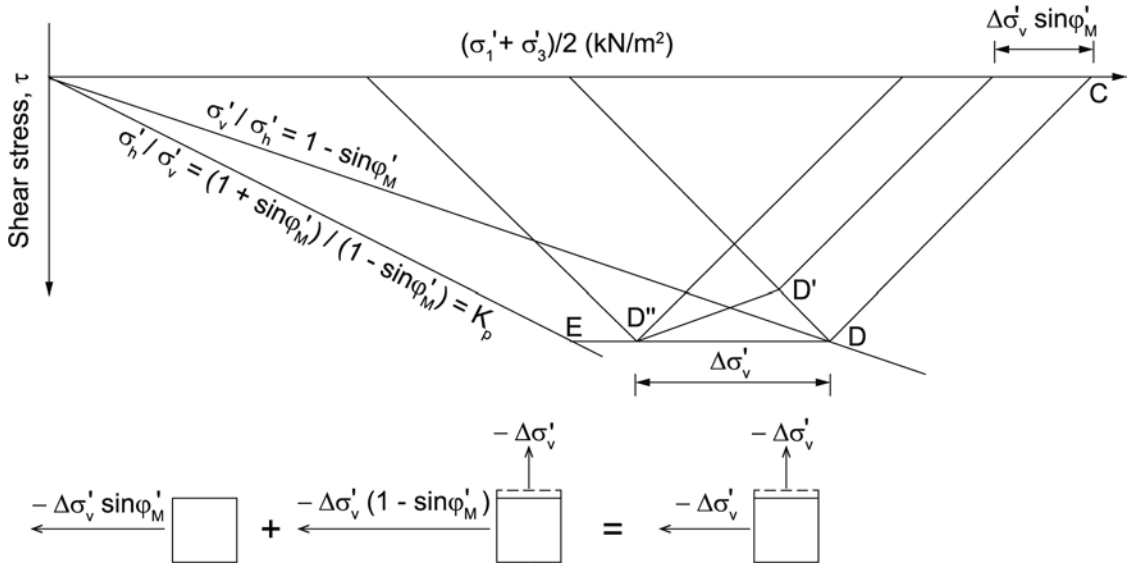

Figure 3. Changes in effective stresses and strains for a clay element during uniaxial unloading for $K_0 > 1/(1 - \sin\varphi'_M)$

Coefficient of earth pressure at rest, K_0

The coefficient of earth pressure K_0 is an important parameter for the design of, e.g., retaining walls, basement walls, pile foundations, pipelines and tunnels. It is also used for generating initial stresses when using advanced numerical methods to solve complex geo-engineering problems. The results of several laboratory tests also strongly depend on the estimate of K_0 (e.g. small strain shear modulus, G_{max}, from resonant column tests, strength and moduli from static and cyclic triaxial tests). Although K_0 can have a significant impact on inputs and calculation results, the reliability in the estimates of K_0 in the laboratory or *in situ* is still uncertain.

Examples of relationships and charts for the evaluation of K_0 include those of Jaky (1944), Kenney (1959), Brooker and Ireland (1965), Massarsch (1979) and Mayne and Kulhawy (1990), and more recently L'Heureux et al. (2017). Except for the most recent paper, most of these relationships were developed for clay types and soil history which are not necessarily representative of Norwegian conditions.

Jaky (1944) established a theoretical solution where K_0 was presented as a function of the effective friction angle (φ') of the soil:

$$K_0 = 1 - sin\varphi' \left(\frac{1 + \frac{2}{3} sin\varphi'}{1 + sin\varphi'} \right) \quad (13)$$

The simplified Eq. [2] was also presented by Jaky (1944):

$$K_0 = 1 - sin\varphi' \quad (2)$$

The difference between Eq. (13) and (2) is about 8% at low friction angles and 16% at high friction angles. However, considering the difficulty of making an appropriate choice for the friction angle φ' for a given soil, this approximation was suggested as sufficiently accurate for most engineering purposes (Wroth, 1972).

Brooker and Ireland (1965) performed a comprehensive series of laboratory K_0-tests on five clay soils with well-documented properties. In their study, all soils were air-dried and passed through a number 40 sieve before testing on specimens reconstituted at a water content corresponding to a liquidity index of about 0.5. In the oedometer cell, loads were thereafter applied to the sample in increments up to a maximum pressure of 15 MPa. The Brooker and Ireland (1965) plasticity chart for estimating K_0 has been extensively used over the years and is still one of the main reference for the evaluation of K_0 in practice.

$$K_0 = 0.95 - sin\varphi' \quad (14)$$

The results obtained by Brooker and Ireland (1965) also showed that K_0 in clay soils was strongly dependent on the overconsolidation ratio (OCR) and the plasticity index (I_p).

L'Heureux *et al*. (2017) presented the results of a review of a database for K_0-measurements during first unloading in the oedometer cell, including the results for eight Norwegian clays. A series of multivariate regression analyses were done on the Brooker and Ireland data and the data in the K_0 database to establish guidelines for a reliable estimation of K_0 in Norwegian clays in the absence of site-specific K_0-data. The resulting regression equation for the combined K_0-triaxial tests and K_0-oedometer tests, for OCR between 1 and 8 was:

$$K_0 = 0.48\, I_p^{0.03}\, OCR^{0.47} \quad (15)$$

where the regression coefficient (R^2) was 0.98. The exponent on the plasticity index, I_p, is very close to zero, indicating little influence of the plasticity index on the K_0-value.

The regression analyses for eight Norwegian clays showed even less influence of plasticity index, I_P, on K_0. For all practical purposes, the exponent in I_p from the regression analyses was zero. Regression analyses were also performed on the Norwegian clay database between K_0 and OCR only. The best fit was given by the following equation:

$$K_0 = 0.53 OCR^{0.47} \quad (16)$$

The results of this regression analysis showed that all of the K_0-laboratory data on the eight Norwegian clays fell within ±5% of Eq. (16). A similar analysis was performed on the Brooker and Ireland (1965) data and the results were:

$$K_0 = 0.57OCR^{0.39} \quad (17)$$

In this case the difference in measured K_0 and the K_0 from multivariate regression analysis were larger than for the Norwegian clays and fell within a ±15% interval.

In the following. stress path-based analysis of K_0, both the original relationship by Brooker and Ireland (1965) and the L'Heureux *et al.* (2017) relationship will be used.

Relationship between K_0 and φ'_M for normally consolidated clays

Figure 4 shows the relationship between the coefficient of earth pressure at rest K_0 and plasticity index I_p for 5 different clays and one sand (I_p = 0) after uniaxial consolidation of remoulded material in the laboratory (Brooker and Ireland, 1965). The curve in Figure 4 is for normally consolidated material.

Using the above stress-path considerations on a clay element, the values of K_o determined in this way should come close to the value of $1 - \sin\varphi'_M$. This curve, denoted $1 - \sin\varphi'_M$, is shown on Figure 4. The curve is based on a relationship between friction angle and plasticity index (Aas, 1986). Except for the London Clay, the experimental data by Brooker and Ireland (1965) (and Hendron, 1963) fit exceptionally well to the stress-path based values.

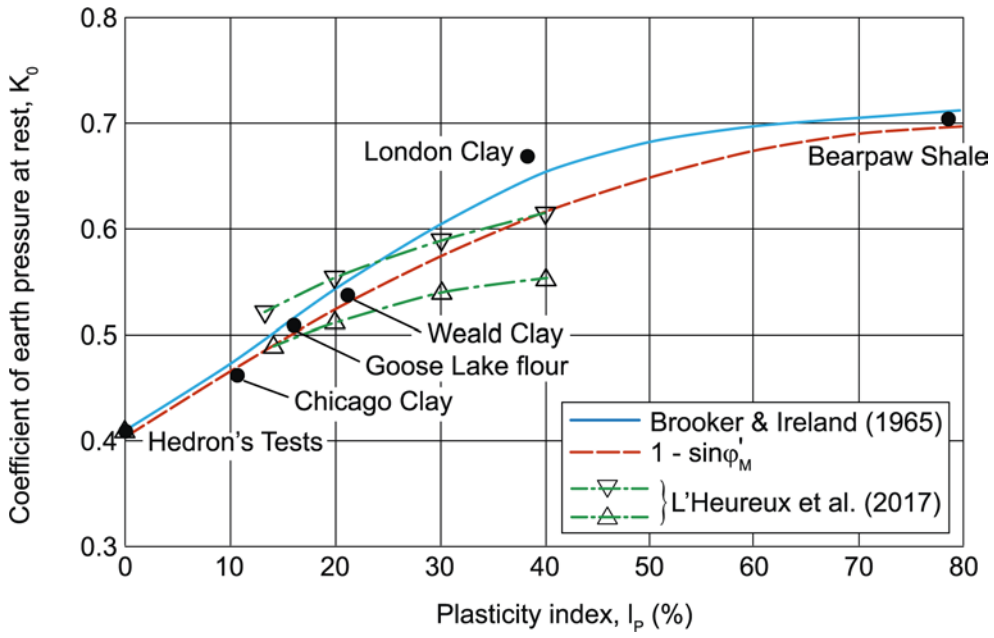

Figure 4. Measured (Brooker and Ireland, 1965; L'Heureux et al, 2017) and stress-path-based values of K_0 as a function of plasticity index I_p for normally consolidated clays

Relationship between K_0 and OCR

These "theoretical" values in Figure 4 are compared in Figure 5 with the Brooker and Ireland (1965) experimental data. The upper diagram in Figure 5 makes the comparison for $1 - \sin\varphi'_M$ equal to 0.5 (ϕ = 30°). A plasticity index I_p of 16% and a normally consolidated K_0-value of 0.5 was used. The I_p is based on Figure 4, where an I_p of 16% corresponds to a value of $(1 - \sin\varphi'_M)$ of 0.5 and $K_0 = 1 - \sin\varphi'_M = 0.5$.

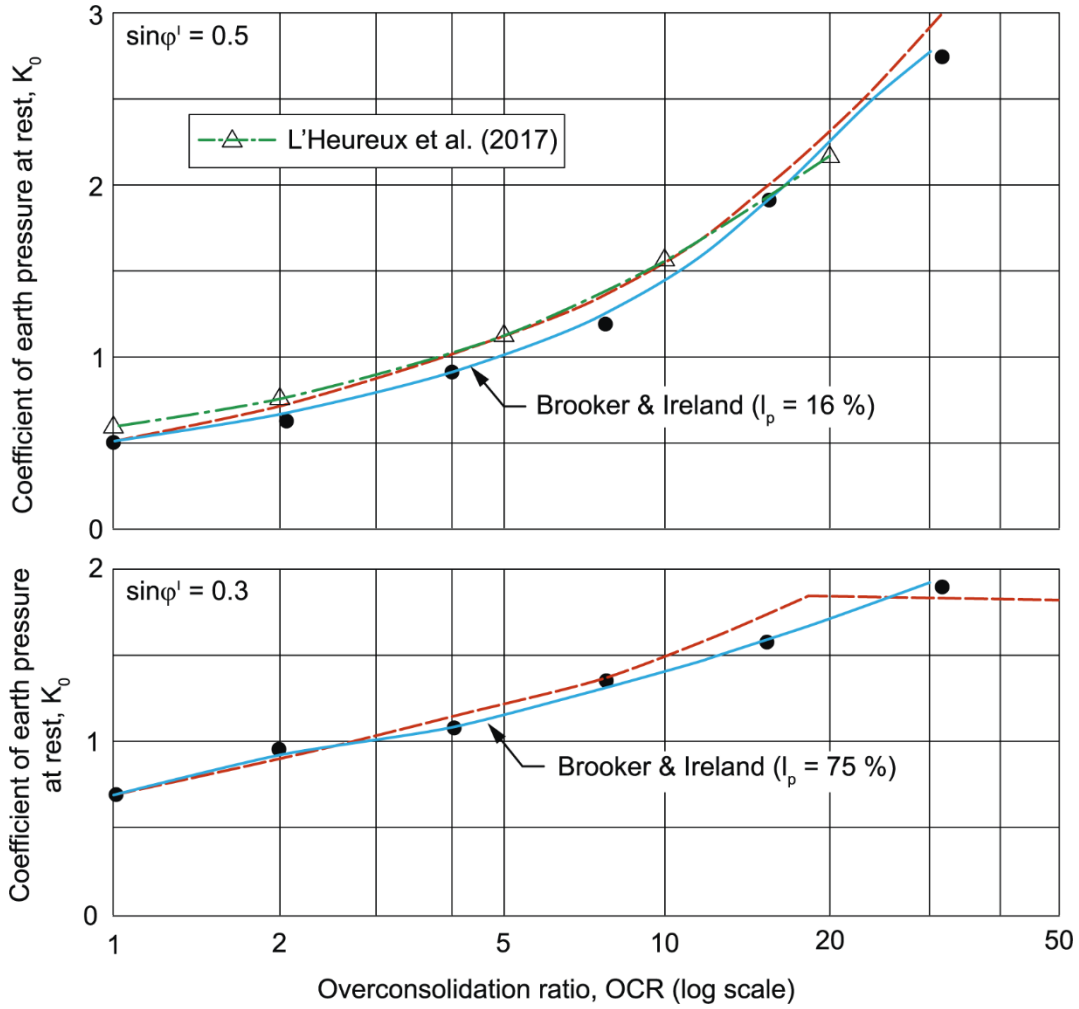

Figure 5. Measured (Brooker and Ireland, 1965) and stress-path-based values of K_0 as a function of overconsolidation ratio for clays 4

Brooker and Ireland (1965) also studied a clay with an I_p of 78% (Bearpaw Shale) and normally consolidated K_0 value of 0.7. Figure 4 indicated that an I_p of 78% corresponds to a value of $1 - \sin\varphi'_M = 0.7$, which in turn confirms the reported value of $K_0 = 1 - \sin\varphi'_M = 0.7$. The lower diagram in Figure 5 compares the Brooker and Ireland data with the stress path-predicted values for a clay with $\sin\varphi'_M = 0.3$. There is a reasonably good agreement between the stress path-calculated values of K_0 and the measured Brooker and Ireland values for both clays.

The three comparisons show that the Brooker and Ireland data support the theoretical explanation given above on effective stress and strain conditions in uniaxial loading of overconsolidated clays.

Schmidt (1966) presented an empirical equation between the overconsolidated and normally consolidated coefficient of earth pressure at rest, $K_{0\,OC}$ and $K_{0\,NC}$, valid for uniaxial unloading of a clay:

$$K_{0\,OC}/K_{0\,NC} = OCR^m \tag{18}$$

and proposed the value of $1.2 \cdot \sin\varphi'$ for the exponent m.

The theoretical considerations described above make it possible to determine the value of exponent *m* for different values of $\sin\varphi'$, and gives the following relation:

$$m = 0.34 + 0.73 \cdot (\sin\varphi'_M - 0.3) \quad (19)$$

Table 1 compares the *m*-values for friction angles between 19 and 30°, as proposed by Schmidt and as derived from the stress path-based framework.

Table 1. Comparisons of exponent m for K_0 for overconsolidated clay

Friction angle, φ' (°)	sin φ'	*m* (Schmidt), Eq. 18	*m* (Stress paths), Eq. 19
19	0.33	0.39	0.36
20	0.35	0.41	0.37
23	0.40	0.47	0.41
25	0.42	0.51	0.43
28	0.47	0.56	0.45
30	0.50	0.60	0.49

K_0 in an overconsolidated clay under reloading

Figure 6 illustrates the loading-unloading sequence A-B-C-D-E from Figures 1 to 3. In addition, the figure shows what is considered to be the result of a reloading of this overconsolidated clay (Path EFG).

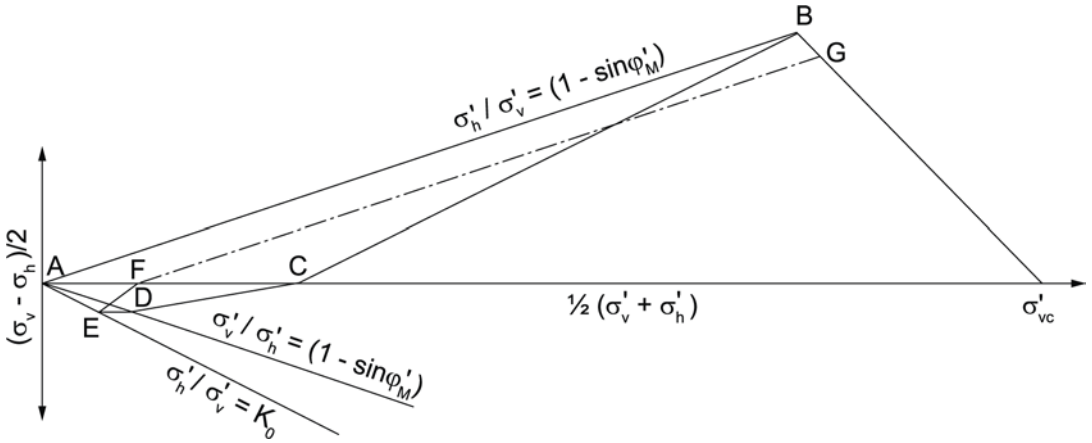

Figure 6. Loading, unloading and reloading of overconsolidated clay

At stage E, the clay is subjected to the largest possible passive shear stress, and is close to yielding. If the deviator stress is removed by increasing the vertical stress, the clay undergoes elastic deformation, and reaches a situation of isotropic consolidation (point F), comparable with that at point A at the start of the first loading.

Under these conditions, a further isotropic stress increase $\Delta\sigma'$, combined with a decrease in horizontal stress equal to $\Delta\sigma' \cdot \sin\varphi'_M$, contributes to maintain zero net lateral strain. As illustrated in Figure 6, the resulting effective stress path follows the F to G line, parallel to the path of the first loading A to B:

$$\Delta\sigma'_h / \Delta\sigma'_v = 1 - \sin\varphi'_M \quad (20)$$

Figure 7 shows the relationship between K_0 and OCR for a clay with $\sin\varphi'_M = 0.5$, as calculated with the stress path model. Curve A describes unloading from OCR = 1 to 30 (the same curve as shown in the upper diagram in Fig. 5), Curve B reloading from OCR = 10 to 1, and Curve C reloading from OCR = 30 to 1.

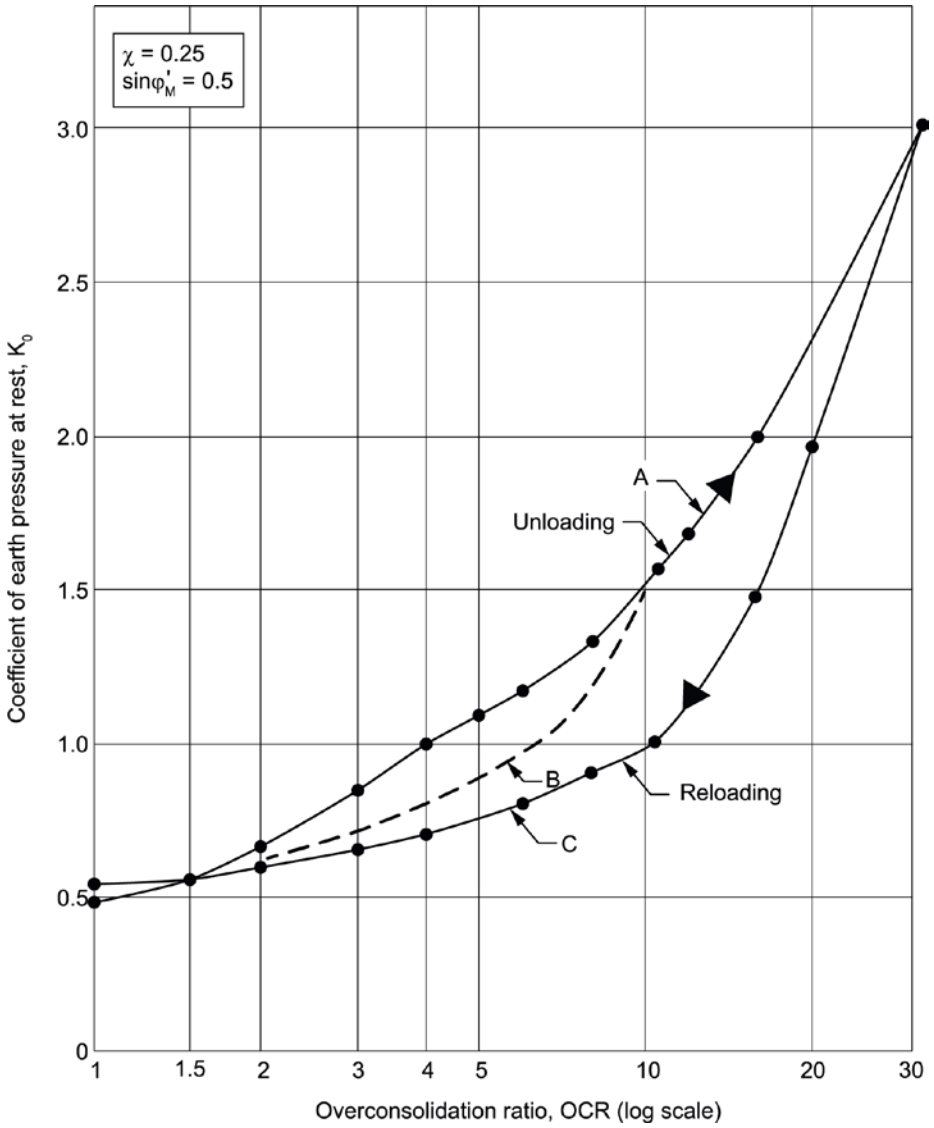

Fig. 7: Relationship between K_0 and OCR during first loading, unloading and reloading

Without implying the general validity of expression

$$K_{0\,OC}/K_{0\,NC} = \mathrm{OCR}^m \qquad (21)$$

the value of *m* that gives the best fit to the curve A is about 0.5. Introducing a value of K_{oNC} of 0.5 in Eq. 21 gives *m* = 0.486, while Schmidt's equation yields 0.6. The multi-regression statistical analysis by L'Heureux *et al.* (2017) suggested an *m*-value of 0.47 for a K_{oNC} of 0.53, based on laboratory measurements on eight Norwegian clays with OCR between 1 and 8 and plasticity index between 10 and 40%.

It is important to realize that the value of K_0 for a given overconsolidation ratio OCR depends significantly on whether the clay has been subjected to a first loading, unloading or reloading.

Limited evidence so far (NGI database and in L'Heureux *et al.*, 2017) indicates the K_0-value under unloading and second unloading are very similar. In practice, it is therefore important to consider whether a soil is subjected to an increased vertical stress due to subsequent construction activities, such as embankments or buildings.

Figure 8 gives the result of an actual measurement of the relationship between K_o and OCR during unloading and subsequent reloading for a soft sensitive clay in an instrumented oedometer in the laboratory (Campanella and Vaid, 1972). The K_0-values for this clay agree well with the stress path derived K_0-values: it shows a value of K_0 of about 0.55 at OCR = 1, and a reloading curve very similar to that shown in Figure 7.

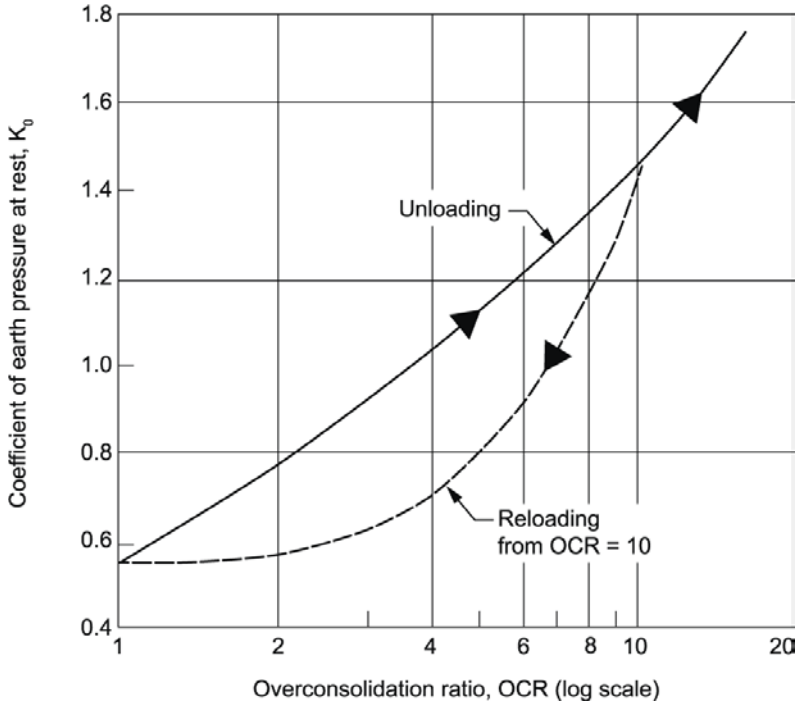

Figure 8. K_0 as a function of OCR for Haney sensitive clay (Campanella and Vaid, 1972).

Concluding remarks

Theoretical considerations based on the study of the stress paths under uniaxial loading and unloading of a clay were used to determine the value of the coefficient of earth pressure at rest, K_0, for normally consolidated and overconsolidated clay. The analysis studied the changes in effective stresses and strains as a result of a uniaxial unloading and reloading of a clay deposit. The analysis is based on the following two basic assumptions:

- In any phase of the loading-unloading cycle, there must exist a static equilibrium, which means that shear stresses and mobilized shear strengths have to be equal.
- The mobilized frictional shear resistance is an exclusive result of the plastic deformation that have occurred. Relief of a shear stress results in a pure elastic deformation that does not influence the mobilized shear strength.

The paper provides an explanation for the values of K_0 through an interpretation of the effective stress paths during uniaxial loading. One particular consideration was looking at the difference

in the behaviour of elastic and plastic strains and how they contribute to mobilize and reduce the friction resistance.

The analysis led to relationships between the coefficient of earth pressure at rest K_0 and $\sin\varphi'_M$ (the mobilized friction angle) and between K_0 and overconsolidation ratio OCR for unloading. The stress path-derived values of K_0 agreed closely with the well-known results presented by Brooker and Ireland (1965) and with recent statistical analyses of laboratory-measured K_0 data on eight Norwegian clays presented by L'Heureux *et al*. (2017).

The reloading phase with the stress path model was found to give lower values of K_0 for the same OCR than the unloading phase. This was reported by Ladd *et al*. (1977), where they presented a loading-reloading curve (OCR = 1−10) for a sensitive clay with a normally consolidated value of K_0 equal to 0.55. The stress-path derived values of K_0 during reloading also agreed well with the measured data presented by Campanella and Vaid (1972).

In general, the calculated curves with the stress path model, across a range of OCR-values, harmonized well with the measured values presented in the literature.

References

Aas, G. (1986). In situ investigation techniques and interpretation for offshore practice. Recommended interpretation of vane tests. Final report. Norwegian Geotechnical Institute, Oslo. Report 40019-24. 1986-09-08.

Brooker, E.W. and Ireland, H.O. (1965), Earth pressures at rest related to stress history. *Canadian Geotechnical Journal*. **2**(1): 1−15.

Campanella, R.G. and Vaid, Y.P. (1972). A Simple K_o-Triaxial Cell. *Canadian Geotechnical Journal*. **9** (3): 249−260.

Hendron, A.J. (1963). The behaviour in sand in one-dimensional compression. PhD Thesis. Dept of Civil engineering, University of Illinois.

Jaky, J. (1944). The Coefficient of Earth Pressure at Rest (in Hungarian), *Journal Society of Hungarian Architects and Engineers.* Budapest, Hungary. 355−358.

Jaky, J. (1948). On the bearing capacity of piles. 2nd Int. Conf. Soil Mechanics and Foundation Engineering, Rotterdam. Proceedings. **1**: 100−103.

Kenney, T.C. (1959). Discussion of "Geotechnical properties of glacial lake clays" by T.H. Wu. *Soil Mech. and Foundations Div.,* ASCE, 85(3), 67−79.

L'Heureux, J.S., Ozkul, Z., Lacasse, S., D'Ignazio, M. and Lunne, T. (2017). A revised look at the coefficient of earth pressure at rest for Norwegian Clays. Fjellsprengningsteknikk - bergmekanikk - geoteknikk. Oslo 2017. Ch. 35.

Ladd, C.C., Foott, R., Ishihara, K., Schlosser, F. and Poulos, H.G. (1977). Stress-deformation and strength characteristics: State of the art report. 9th Int. Conf. Soil Mechanics and Foundation Engineering, Tokyo. Proceedings. **2**: 421−494.

Massarsch, K.R. (1979). Lateral earth pressure in normally consolidated clay. In Design parameters in geotechnical engineering. Proc., 7th European Conference on Soil Mechanics and Foundation Engineering, Brighton, UK. **2**: 245−249.

Mayne, P. W. and F.H. Kulhawy (1990). "Direct and indirect determinations of in situ K_0 in clays". *Transportation Research Record.* (1278).

Schmidt, B. (1966). Discussion of "Earth Pressure at Rest Related to Stress History". *Canadian Geotechnical Journal*. **3**(4): 239−242.

Wroth, C.P. (1972). General theories of earth pressure and deformation. Proc. 5th European Conf. on Soil Mechanics and Foundation Engineering, Madrid, **1**: 33−52.

Vane Shear Strength in Terms of Effective Stresses

Gunnar Aas[1] and Suzanne Lacasse[2]
[1]formerly Norwegian Geotechnical Institute (NGI); [2]NGI

Abstract

Experience with the shear strength determined with the field vane has shown that the measured values of the strength, normalized with the effective overburden stress, s_{uv}/σ'_{vo}, are often lower than 0.1 for normally consolidated quick clays of low plasticity. This undrained shear strength ratio is less than one third of the corresponding undrained strength measured in a triaxial active test in the laboratory. For more plastic clays and overconsolidated clays, however, the difference between field vane and triaxial active shear strength is found to be less. The ratio of the two strengths might even be close to unity in some cases. The explanation for this phenomenon is not that the insertion of the field vane causes disturbance and remoulding in soft, sensitive clays. With a revised failure criterion for soft, contractant clays, it is possible to express the vane strength in terms of effective stresses, and thus to explain the differences in the shear strengths measured by the vane and in the laboratory. It is concluded that the directly measured vane shear strength values do not constitute, in most cases, a representative strength for stability analysis, for instance for embankments and excavations. A method for correcting the vane shear strength for stability analysis in practice is proposed.

Introduction

The main objective of the study is to express the shear strength obtained with the field vane test in terms of effective stresses, and to develop a deeper understanding of the factors that control the undrained shear strength measured by the field vane. The study collected an extensive series of data from field vane and laboratory shear tests and compared the values of undrained shear strengths from each of the different methods of testing. An important part of the study was to make an interpretation of the vane test in light of a recently extended failure criterion for contractant clays (Aas, 1986; Aas and Lacasse 2021a). Once the new understanding was established, the aim of the work was to establish a modified correction factor to apply to the measured vane shear strength for design.

A method was also developed to derive the coefficient of earth pressure at rest in situ, K_0, by combining the measured values of field vane and triaxial active strengths.

Shear strength obtained from the field vane

If one assumes equal values and simultaneous mobilization of shear strength on the cylindrical and the two horizontal end failure surfaces in a vane shear test, the "average" vane shear strength, s_{uV}, for square-ended vanes is given by the expression:

$$s_{uV} = T/(^1/_2 \pi D^2 H + {}^1/_6 \pi D^3) \quad (1)$$

where T denotes the maximum applied torque and D and H are the vane diameter and height, respectively. If one assumes that the shear strength on the horizontal end surfaces, s_h, differs from the shear strength on the vertical cylindrical surface, s_v, Eq. (1) may be re-written:

$$s_{uV} = (s_v + {}^1/_3 D/H \cdot s_h)/(1 + {}^1/_3 D/H) \quad (2)$$

In particular, for a vane with height to diameter ratio, H/D, of 2, the expression for the field vane strength, s_{uV}, becomes:

$$s_{uV} = {}^6/_7 s_v + {}^1/_7 s_h \quad (3)$$

For values of s_h/s_v between 1.5 and 2.0, the difference between s_{uV} and s_V is between 7 to 14% only.

In the rest of the paper, the term "vane shear strength" will, for simplicity, be used for the vertical shear strength s_V. The influence of strength anisotropy will be discussed later in the paper. A detailed description of the correct procedures for performing vane tests in Norway is given by Aas *et al*. (1986) and in different standards, including ASTM (2009).

Stress conditions around the vane

Insertion of vane and stresses around the vane

On the basis of pore pressure measurements in connection with vane-triaxial tests, the insertion of the vane creates a substantial increase in pore pressure in the surrounding clay (Kimura and Saitoh, 1983). It is reasonable to believe that, in a saturated clay, this rise in pore pressure should correspond closely to the increase in total horizontal stress, and hence, cause no changes in effective stresses in the clay. Reported measurements of effective stresses in a triaxial specimen before and after the vane insertion (Matsui and Abe, 1981) appear to support this assumption.

Any subsequent dissipation of excess pore pressure will have to be accompanied by a decrease in the total horizontal stress, because the clay, as a result of the specific boundary in situ conditions, cannot undergo any volume changes. Consequently, one should expect rather limited changes in the effective stresses in the clay even in tests where there is a considerable delay between insertion and rotation of the vane (consolidated tests).

Application of torque and zone of shear distortion

Fundamental to any interpretation of the vane test are the assumptions made regarding the interaction, or mode of transfer of stresses, between the vane and the clay when rotating the vane to failure. As a consequence of the axisymmetric geometric conditions of the vane, all four blades have to be deflected and rotate in exactly the same manner. Hence, soil distortion in the sectors between adjacent blades will not contribute to the resisting torque. Matsui and Abe (1981) investigated experimentally and analytically the shear mechanism of the vane shear test in soft clays, and concluded that the normal effective stress in front of and behind the blades remained essentially constant. This means that the point of application of the reaction forces between clay and vane are located at the blade edges, thus causing a concentration of shear distortion in a limited zone circumscribing the vane. Such a concentration of reaction forces at the edges of the vane blades has been confirmed in an *in situ* test with an instrumented vane in

London clay (Menzies and Merryfield, 1980). In addition, the presence of a narrow ring of strained clay next to the edges of the vane blades has also been observed in the laboratory with the help of X-ray photographs (Kimura and Saitoh, 1983).

Failure mechanism in field vane test

Based on the stress conditions and observed distortion around the vane, the failure mechanism in a vane test appears to be very similar to that in a simple shear test, implying uniformly distributed shear stress and strain all over the cylindrical shear zone circumscribing the vane.

Undrained shear strength concept for contractant clays

A method is proposed using new ideas concerning the assumption of a fundamental failure criterion valid for undrained loading of soft, contractant clays exposed to a brittle failure. The method can be explained with a triaxial active test on a specimen consolidated under in situ stresses, i.e. σ'_{vo} and $K_0 \cdot \sigma'_{vo}$, where K_0 is the coefficient of earth pressure at rest.

If a saturated clay specimen is loaded undrained to failure in the triaxial compression (active) mode, the effective stress path is independent of the applied total stress changes. This means that not only the maximum shear stress and the corresponding effective normal stress, but also each of the two effective principal stresses at failure, σ'_{1f} and σ'_{3f}, are entirely defined by the consolidation stresses and stress history.

If such a clay has been subjected to creep due to ageing, weathering or overconsolidation, it can withstand an increase in the effective vertical stress from σ'_{vo} to a higher value σ'_{vE} without undergoing plastic strain. This clay, which will have a higher effective horizontal stress, $K_0 \cdot \sigma'_{vo}$, compared to the original young clay, does not undergo plastic deformations and is able to reduce σ'_h back to the value for the young clay, $\sigma'_{vo} \cdot (1 - \sin\phi'_M)$, where ϕ'_M is the mobilized friction angle (Aas and Lacasse, 2021a).

In addition, the effective horizontal stress may be further reduced, as a result of the mobilization of attraction. Attraction is assumed to be due to net attractive forces acting across the water-films constituting the contact points between clay particles. Attraction acts like a tension reinforcement in the clay. It requires practically no deformations to be activated. In a given clay, the attraction will increase with decreasing distance between clay particles, and is therefore a function of the existing consolidation stress, σ'_{vo}. Consequently, the principal stresses (σ'_1 and σ'_3) at failure in the triaxial specimen become σ'_{vE} and $\sigma'_{vo} \cdot (1 - \sin\phi'_M - \chi)$, respectively. The parameter χ denotes the relative material attraction and σ'_{vo} represents the effective stress normal to the attractive force. The two principal, or limiting, stresses result in the following expression for the active undrained shear strength, s_{uA}:

$$s_{uA} = {}^1\!/_2(\sigma'_{1f} - \sigma'_{3f}) = {}^1\!/_2\sigma'_{vo}(\chi + \sin\phi'_M + \sigma'_{vE}/\sigma'_{vo} - 1) \qquad (4)$$

where
- σ'_{1f} = Major effective principal stress at failure
- σ'_{3f} = Minor effective principal stress at failure
- σ'_{vo} = In situ effective overburden stress
- χ = Relative material attraction
- ϕ'_M = Mobilized friction angle
- σ'_{vE} = Mobilized effective vertical stress

Standard field vane test

A very important condition for the interpretation of the field vane test, as indicated above, is that there cannot be any volume change and, hence, no change in the width of the cylindrical shear zone around the vane. As a consequence, the effective radial stress remains constant during a field vane test. Considering a clay that has undergone confined consolidation, this radial effective stress will be equal to $K_0 \cdot \sigma'_{vo}$. This means that an element in the cylindrical shear zone has effective stresses comparable to that of a specimen in an active triaxial test. If the clay element had been consolidated under a vertical stress σ'_{vo}, the lowest possible effective horizontal stress it can sustain without undergoing active failure, is equal to the lower limiting stress (minor principal stress) in active shear, σ'_{3f}. When this limiting value is reached, the clay starts to yield, initiating a structural break-down which rapidly leads to failure along the vertical cylindrical surface circumscribing the vane.

In a quick clay, no adhesion (between the clay and the blades) can be mobilized, irrespective of a possible relative movement between clay and vane blades. This means that the horizontal stresses coincide in directions with the horizontal principal stresses. As a result, because of the conditions of no change in radial effective stress, the intermediate and major principal stress under field vane testing, σ'_{2fV} and σ'_{3fV}, can be expressed as:

$$\sigma'_{2fV} = K_0 \sigma'_{vo} + s_V \quad (5)$$

$$\sigma'_{3fV} = K_0 \sigma'_{vo} - s_V \quad (6)$$

As the values of σ'_{3f} for the clay element in the shearing zone around the vane and in the triaxial specimen have to be equal, one obtains:

$$\sigma'_{3fV} = \sigma'_{vo}(1 - \sin\phi'_M - \chi) \quad (7)$$

and hence

$$s_V = \sigma'_{vo}[K_0 - (1 - \chi - \sin\phi'_M)] \quad (8)$$

In the case of a young, normally consolidated quick clay where the coefficient of earth pressure at rest K_0 is equal to $1 - \sin\phi'_M$, the shear strength on the vertical cylindrical surface, s_v, becomes:

$$s_v = \chi \sigma'_{vo} \quad (9)$$

If the clay next to the vane is not completely liquefied, a shear stress equal to the remoulded vane strength, s_v', may be mobilized along the blades of the vane at failure. The radial strain necessary to mobilize this adhesion occurs as a result of a simultaneous contraction and stress relief in the failure zone at the start of yield. The contraction is caused by inward drainage under the high pore pressure gradients in the failure zone. The mobilization of radial adhesion along the vane blade results in a rotation of the horizontal principal stresses and to changes in the principal stresses by approximately $-s_v'$ and $+s_v'$ compared to the above equations. This leads to an approximate expression for the shear strength tangential to the cylindrical plane, s_v:

$$s_v = \sigma'_{vo}[K_o - (1 - \chi - \sin\phi'_M)] + s_v' \quad (10)$$

Most soft clays exhibit anisotropy and sensitivity. With these characteristics, it can be implied that one may, without much error, extend the expression to also be valid for the average vane strength ($s_{uV} = s_v$ and $s_{uV}' = s_v'$):

$$s_{uV} = \sigma'_{vo}[K_0 - (1 - \chi - \sin\phi'_M)] + s_{uV}' \quad (11)$$

Anisotropy in undrained shear strength from field vane tests

By combining Eq. (4) and (11) and replacing $\sigma'_{vE}/\sigma'_{vo}$ with $K_0/(1 - \sin\phi'_M)$ for aged clays (Aas and Lacasse, 2021a), one obtains an expression describing the ratio between the triaxial active and field vane strengths and how this ratio varies with K_0, mobilized friction angle and χ. For simplicity, the term s_{uV}/σ'_{vo} in Equation (12) was given the value $0.1 \cdot s_{uV}/\sigma'_{vo}$, corresponding to a clay sensitivity equal to 10 (with sensitivity with the field vane or the fall cone). The notation is defined under Eq. (4) and K_0 is the coefficient of earth pressure at rest.

$$s_{uA}/s_{uV} = {}^1/_2[K_0/(1 - \sin\phi'_M) - (1 - \chi - \sin\phi'_M]/\ 0.9[K_0 - (1 - \chi - \sin\phi'_M)] \qquad (12)$$

Figure 1 illustrates the relationship between the ratio s_{uA}/s_{uV} and the normalized vane strength s_{uV}/σ'_{vo} for 43 sets of data from 20 different locations. The clay deposits included in this data set have experienced secondary compression, resulting in a value of $\sigma'_{vE}/\sigma'_{vo}$ between 1.05 and 1.30. To understand the large range of variation in s_{uA}/s_{uV} between 1 and 3.2 for s_{uV}/σ'_{vo} between 0.1 and 0.5, one needs to consider the values of $\sigma'_{vE}/\sigma'_{vo}$, χ and $\sin\phi'_M$ (Aas, 1986).

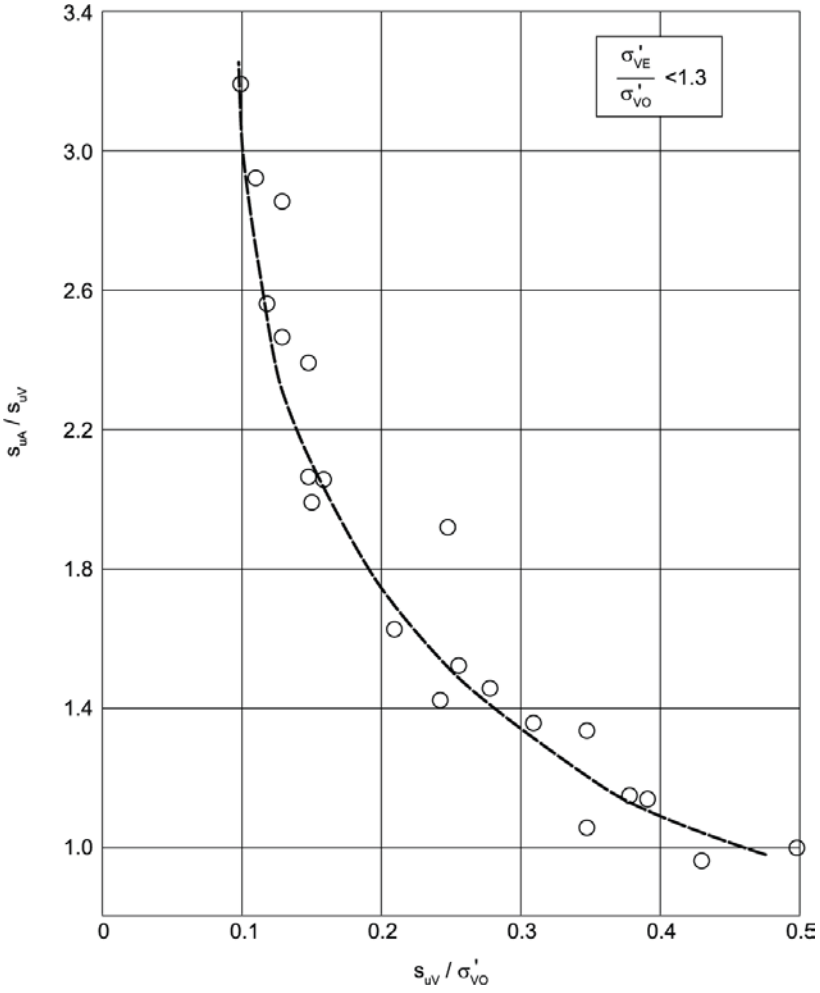

Figure 1. Relationship between the undrained shear strengths obtained from field vane and triaxial actives tests on normally consolidated aged clays (OCR = 1.05 – 1.30)

A value of s_{uV}/σ'_{vo} equal to 0.10 corresponds to a silty, low plasticity clay, exhibiting a high friction angle, a low attraction and a modest effect of ageing (small creep deformations). If one uses values of $\sin\phi'_M = 0.55$, $\chi = 0.10$ and $\sigma'_{vE}/\sigma'_{vo} = 1.05$ in Eq. (12), the resulting ratio s_{uA}/s_{uV}

is 3.2. Correspondingly, for a plastic clay exhibiting a value of s_{uV}/σ'_{vo} equal to 0.4, reasonable values of $\sin\phi'_M$, χ and $\sigma'_{vE}/\sigma'_{vo}$ could be 0.40, 0.30 and 1.30, giving a ratio s_{uA}/s_{uV} of 1.16.

Aas (1965; 1967) measured the ratio of horizontal and vertical shear strength, s_h/s_v,, determined by the field vane. To do this, series of tests were run with different shapes of vanes. Table 1 compiles the ratio of horizontal to vertical vane strengths s_h/s_{uV} for a broad variety of soft clays.

Table 1. Ratio between horizontal and vertical shear strength determined by the field vane.

Clay site	Depth (m)	Plasticity index I_p (%)	Sensitivity S_t	Strength ratio s_u/σ'_{vo}	Field vane strength ratio	
					s_h/s_v	s_h/s_{uV}
Tønsberg	2 – 8	13	30 – 80	0.48	1.0	1.00
Manglerud	4 – 16	8	40 – 70	0.11	1.5	1.40
Lierstranda	4 – 20	6	50 – 150	0.19	2.0	1.75
Fredrikstad	2 – 12	28	7 – 10	0.38	1.0	1.00
Drammen	4 – 14	14	4 – 9	0.17	1.5	1.40
Kelsås	3 – 10	6	20 – 100	0.12	1.8	1.62
Mastemyr	3 – 12	6	10 – 100	0.24	1.5	1.40
Strømsø	3 – 11	30	10	0.33	1.0	1.00
	12 – 15	--	2	0.16	1.2	1.17
Bragernes	5 – 11	--	30 (?)	0.28	1.2	1.17
	11 – 15	--	20 (?)	0.12	1.3	1.25
Skå Edeby	3 – 11	40	11 – 27	0.30	0.7	0.73
Bangkok	3 – 10	85	70	0.57	0.7	0.80

Values of s_h/s_v between 1.5 and 2.0 were reported for lean (I_p < 15%), normally consolidated Norwegian sensitive and quick clays, and a value of 1.0 for the overconsolidated, quick Tønsberg clay. The table also contains earlier unpublished data from a number of other Norwegian locations. Eide and Holmberg (1972) and Wiesel (1973) reported anisotropy ratios equal to 0.77 for Bangkok clay and about 0.7 for Skå-Edeby clay. The upper diagram in Figure 2 shows the ratio of horizontal to vertical shear strength from the field vane (s_h/s_{uV}) versus the normalized vertical vane shear strength (s_{uV}/σ'_{vo}).

Although there are uncertainties about the simultaneous mobilization of shear resistance on the two horizontal vane end surfaces, it appears reasonable to assume that the derived horizontal vane shear strength is close to the direct simple shear strength s_{uD}. To verify this assumption indirectly, the ratio of the direct simple shear strength to the field vane strength from the same database (s_{uD}/s_{uV}) is plotted versus the normalized vane strength (s_{uV}/σ'_{vo}) in the lower diagram in Figure 2. As illustrated in Figure 2, there is a reasonably good agreement between the two diagrams, thus verifying empirically the validity of the assumption, and supporting the method of determining horizontal and vertical shear strength from vane borings.

Determination of in situ value of K_0 from field vane test

Equation (8) can be rewritten in the following way:

$$K_0 = [\sigma'_{3f} + (s_{uV} - s_{uV}')]/\sigma'_{vo} \qquad (13)$$

where σ'_{3f} is the minor principal stress at failure in a triaxial active test. This means that the field vane strength can be used in combination with the triaxial test to determine the coefficient of earth pressure at rest K_0. As indicated above, use of the field vane shear strengths s_{uV} and s_{uV}' instead of the actual "vertical" strengths s_v and s'_v in Eq. (13) leads to a maximum error of only a few percent.

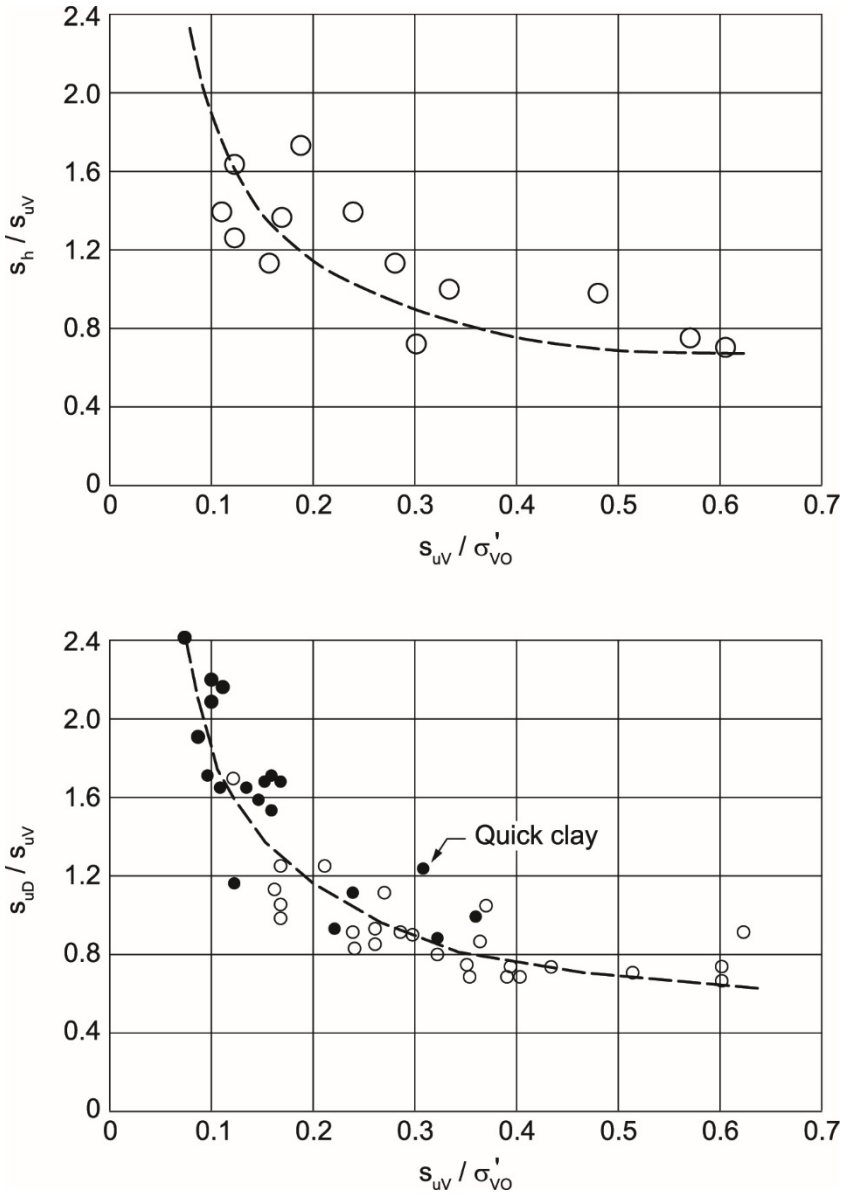

Figure 2. Comparison of horizontal shear strengths derived field vane tests and shear strength from direct simple shear tests.

Figure 3 demonstrates the graphical determination of K_0 on the basis of $s_{uV} - s_{uV}'$ and the effective stress path from an anisotropic consolidated undrained triaxial active test with vertical consolidation stress equal to σ'_{vo}. The two tests shown are for a nearly normally consolidated Ellingsrud quick clay with vane shear strength s_{uV} equal to 6 kPa, and the highly overconsolidated Haga clay with s_{uV} = 41 kPa and s_{uV}'= 9 kPa. The K_0-values for the two clays obtained from the field vane (see also Aas and Lacasse 2021b) were 0.45 and 1.92, respectively. The K_0-values of 0.60 for Ellingsrud and 1.40 for Haga shown on Figure 3, were used to consolidate the specimens in the laboratory, but they were based on an early estimate of K_0 before testing and are not representative of the *in situ* values.

For Ellingsrud clay, three K_0-triaxial tests in the laboratory were run to determine the in situ K_0 and suggested values of 0.45, 0.45 and 0.42 (Aas, 1986), which is very close to the K_0-values obtained with the field vane interpretation in Figure 3.

For the Haga clay, the comparison is more complex because the specimen came from a depth of only 2.2 m. The material was from a desiccated, fissured crust. The *in situ* clay at such shallow depth had also been subjected to many heat/cold, freeze-thaw cycles over the years. The K_0-value of 1.9 obtained from the field vane interpretation agrees well with the result of hydraulic fracturing at the depth of 2 m at the Haga site (Bandis and Lacasse, 1986). On the basis of the correlations by L'Heureux *et al.* (2017) for Norwegian clay, a K_0-value of 1.92 suggests a clay with overconsolidation ratio of 8. The stress history presented by Bandis and Lacasse (1986) gives an overconsolidation ratio of 8 at depth 2 m, based on laboratory tests on Haga clay.

It can be concluded that there is excellent agreement between the field vane-predicted K_0-value and laboratory and *in situ* derived values at both the Ellingsrud and Haga sites.

K_0-values determined as from the filed vane test have been compared with field values based on other *in situ* testing methods at other sites, i.e. hydraulic fracturing (Bjerrum and Andersen, 1972) and self-boring pressuremeter and dilatometer tests (Lacasse and Lunne, 1982a; 1982b; 1982c). The earlier comparisons also show (see Aas *et al*., 1986) that the field vane approach to determine the K_0-value *in situ* gives a good match with hydraulic fracturing and self-boring pressuremeter, whereas the dilatometer test seemed to overpredict the K_0-values.

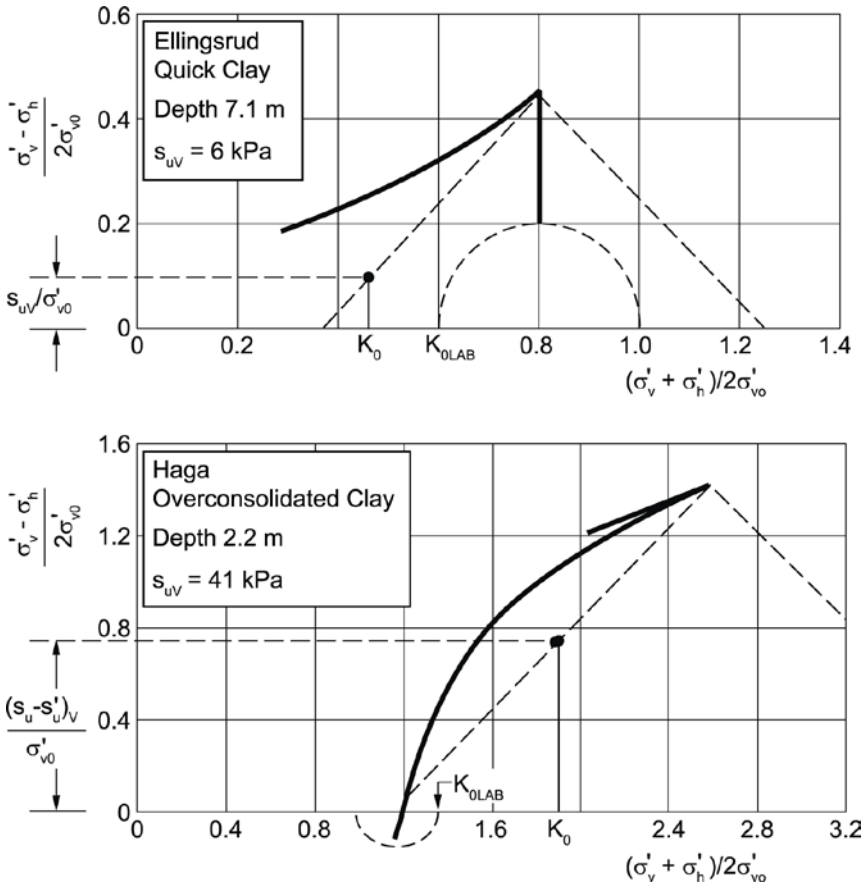

Figure 3. Graphical determination of the in situ value of K_0 from field vane strengths and effective stress paths from undrained triaxial active tests

Correction of vane strength for design analyses

Aas (1979) found that back-calculated factors of safety, based on field vane strength for a number of failed embankments and excavations, increased nearly linearly with the average value of the ratio s_{uV}/σ'_{vo} on the sliding surface. The (uncorrected) calculated factor of safety (FS) was 1.0 for cases where the s_{uV}/σ'_{vo} ratio was equal to about 0.22. The (uncorrected) factor of safety increased to about 2.0 for s_{uV}/σ'_{vo} equal to 0.6, and decreased to 0.6 for s_{uV}/σ'_{vo} of about 0.1. There was therefore need for a correction factor to ensure that the field vane strength gave a safety factor of unity for the failed embankments and excavations.

Aas (1979) also investigated the ratio between field vane strength and the "average laboratory strength", determined as the average of the triaxial active, direct simple shear and triaxial passive strengths, measured on specimen consolidated to the *in situ* stresses. Plotting the ratio s_{uV}/s_{uLAB} against s_{uV}/σ'_{vo}, the points grouped nicely along the same straight line which was fitted through the points in Aas(1979).

The average laboratory shear strength thus calculated might constitute a representative mean value for field strength along a potential failure surface in connection with excavations (base failures), embankments and shallow foundations (Bjerrum, 1972). Hence, Aas *et al.* (1986) presented a diagram where the measured ratio s_{uLAB}/s_{uV} was plotted against s_{uV}/σ'_{vo} for a large number of clays (Fig. 4). Two curves were suggested, one for "normally consolidated", and one for overconsolidated clays. The suggested ratio represented at the time the correction factor by which the measured field vane strength should be multiplied, in order to give the best estimate of average field shear strength to use for design.

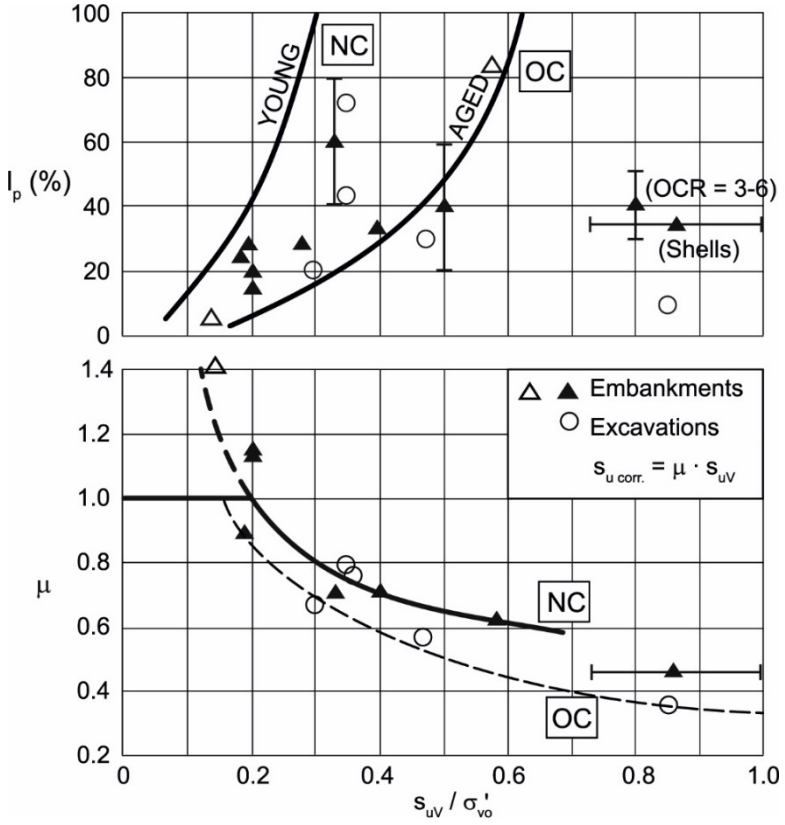

Figure 4. Correction factor for the field vane strength s_{uLAB}/s_{uV} as a function of the normalized field vane strength and the "overconsolidation ratio" (Aas et al. 1986).

Later experience with practical design showed that these relationships were essentially valid for low plasticity clays exhibiting a ratio s_{uV}/σ'_{vo} lower than 0.6. However, the relationship for overconsolidated clays has proven to be incomplete and probably valid only for loading times of considerable duration in fissured or dry crust clays.

Figure 5 collates the result of a new study of the relationship s_{uLAB}/s_{uV}, including contractant clays from several locations in Norway and abroad, each exhibiting different degree of ageing or overconsolidation (denoted $\sigma'_{vE}/\sigma'_{vo}$). In Figure 5, the clays are separated into categories with the ratio $\sigma'_{vE}/\sigma'_{vo}$, where σ'_{vE} equals the ultimate vertical failure stress, σ'_{3f}, in an active triaxial test.

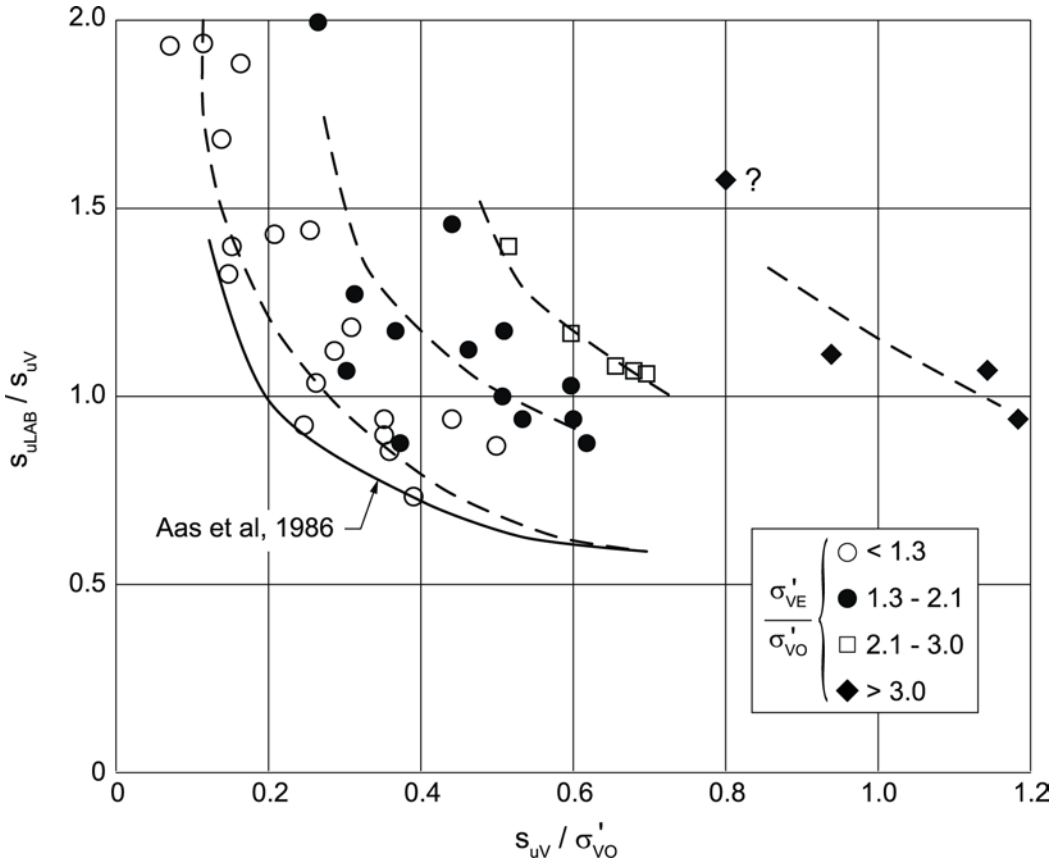

Figure 5. Field vane correction factor s_{uLAB}/s_{uV} as a function of the normalized field vane strength and the overconsolidation ratio.

The curve representing the clays exhibiting $\sigma'_{vE}/\sigma'_{vo} \leq 1.3$ and $s_{uV}/\sigma'_{vo} \leq 0.6$ appears relatively similar to the earlier curve (Aas *et al*, 1986) for normally consolidated clay. However, the diagram in Figure 5 indicates that when the values of $\sigma'_{vE}/\sigma'_{vo}$ increase, higher correction factor s_{uLAB}/s_{uV} are required for clays with the same value of s_{uV}/σ'_{vo}. It is interesting to observe that for clays with an "overconsolidation" ratio exceeding 3, the vane strength seems to be representative for the actual strength to use in design.

Because experience indicates that the direct simple shear strength often lies halfway between the triaxial active and passive strengths, and the simple shear strength may give questionable values in stiffer clays, s_{uLAB} was chosen, in the latest study as $^1/_2\,(s_{uA} + s_{uP})$.

The majority of the correction factors on the shear strength from the field vane test presented in the literature are a function of the plasticity index (e.g., Ladd *et al*. 1977), and in the case of ASTM (2009) and Chandler (1988), as a function of time to failure (mainly for embankments). No account is taken of overconsolidation ratio. Based on Figure 5, this leads to a conservative design in overconsolidated clays.

Summary and conclusions

The interpretation of the field vane test, in the light of a revised failure criterion for contractant clays, makes it possible to explain and understand the values of undrained shear strength measured in this type of test. Deduced theoretical expressions for vane strength and triaxial active strength explain why the ratio between those two shear strengths can vary from less than 0.1 in silty, low plasticity, quick clays to about 1.0 in plastic, aged or weathered clays. In the same way, the study with additional data supports earlier published data for the measured ratio between horizontal and vertical vane strength.

The study has led to a method to determine the value of the coefficient of earth pressure at rest by combining the results of field vane and triaxial active tests. Theoretically derived values have been found to agree fairly well with recorded values in situ with the self-boring pressuremeter and hydraulic fracturing tests.

An additional study included contractant clays from several locations in Norway and abroad, each exhibiting different degree of ageing or overconsolidation ratio up to about 1.3. The result confirm earlier findings that for soft clays with field vane strength ratio of $s_{uV}/\sigma'_{vo} \leq 0.6$, the ratio s_{uLAB}/s_{uV} gives a representative measure for the correction factor by which the measured field vane shear strength should be multiplied to give a representative field strength for stability analysis. So, for normally consolidated clays, the same correction factor as earlier published applies. A new correction factor is suggested for clays with apparent overconsolidation higher than 1.3.

References

Aas, G. (1965). A study of the effect of vane shape and rate of strain on the measured values of in situ shear strength of clays. ICSMFE. 6, Montreal, **1**: 141–145.

Aas, G. (1967). Vane tests for investigation of anisotropy of undrained shear strength of clays. Geotechnical Conference on Shear Strength Properties of Natural Soils and Rocks. Oslo 1967. Proc. **1**: 3–8.

Aas, G. (1979). "Vurdering av korttidsstabilitet i leire på basis av udrenert skjærfasthet". NGM-79, Helsingborg, pp. 585 – 596. (in Norwegian).

Aas, G. (1986). In situ site investigation techniques and interpretation for offshore practice. Recommended interpretation of vane tests. NGI Report 40019-24. Oslo 1986-09-08. 87 pp.

Aas, G. and Lacasse, S. (2021a). Shear Strength of Soft Clay in Terms of Effective Stresses. 1st paper in this NGI publication.

Aas, G. and Lacasse, S. (2021b). K_0 as a function of changes in stress and strain conditions during consolidation, unloading and reloading. 2nd paper in this NGI publication.

Aas, G., Lacasse, S., Lunne, T. and Høeg, K. (1986). Use of in Situ Tests for Foundation Design on Clay. ASCE Conf. in Situ ’86, Blacksburg, Virginia, USA. pp. 1–30.

ASTM (2009). STP 1014 on Vane Shear Strength Testing in Soils. *Annual Book of ASTM Standards,* 04.09.

Bandis, C. and Lacasse, S. (1986). In situ site investigation techniques and interpretation for offshore practice. Interpretation of self-boring and push-in pressuremeter tests in Haga clay. NGI Report 40019-09. Oslo 1986-09-08. 109 pp.

Bjerrum, L. (1972). Embankments on soft ground, SOA Report. ASCE. Spec. Conf. Performance of Earth and Earth-Supported Structures. Lafayette, IN, USA. **2**: 1–54.

Bjerrum, L. and Andersen, K.H. (1972). In situ measurements of lateral pressures in clay. Proc. 5th International Conference on Soil Mechanics and Foundation Engineering, Tokyo. **1**: 11–20.

Chandler, R.J. (1988). The in-situ measurement of the undrained shear strength of clays using the field vane: SOA paper. Vane Shear Strength Testing in Soils: Field and Laboratory Studies, ASTM, 1014, 13–44.

Eide, O. and Holmberg, S. (1972). Test fills to failure on the soft Bangkok clay. ASCE. Spec. Conf. Performance of Earth and Earth-Supported Structures. Lafayette, IN, USA. **1**: 159–180.

Kimura, T. and Saitoh, K. (1983). The influence of strain rate on pore pressures in consolidated undrained triaxial tests on cohesive soils. *Soils and Foundations.* **23**(1): 80 – 90.

L'Heureux, J.S., Ozkul, Z., Lacasse, S., D'Ignazio, M. and Lunne, T. (2017). A revised look at the coefficient of earth pressure at rest for Norwegian Clays. Fjellsprengningsteknikk - bergmekanikk - geoteknikk. Oslo 2017. Ch. 35.

Lacasse, S. and Lunne, T. (1982a). In situ horizontal stress from pressuremeter tests. Proc. Symp. Pressuremeter and its Marine Applications, Paris. 187–208.

Lacasse, S. and Lunne. T. (1982b). Penetration tests in two Norwegian clays. ESOPT II, Amsterdam. 661–669.

Lacasse, S. and Lunne, T. (1982c). Dilatometer tests in two soft marine clays. ASCE. Conf. Updating Subsurface Sampling of Soils and Rocks and In Situ Testing, Santa Barbara, CA. 369–379.

Ladd, C.C., Foott, R., Ishihara, K., Schlosser, F. and Poulos, H.G. (1977). Stress-deformation and strength characteristics. SOA Report. Proc. 9th International Conference on Soil Mechanics and Foundation Engineering, Tokyo. **2**: 421-94.

Matsui, T. and Abe, N. (1981). Shear mechanisms of vane test in soft clays. *Soils and Foundations*. **21**(4): 69–80.

Menzies, B.K. and Merrifield, C.M. (1980). Measurements of shear stress distribution on the edges of a shear vane blade. *Geotechnique*. **30:** (314–318).

Wiesel, C (1973). Some factors influencing in situ vane test results. Proc. 8th International Conference on Soil Mechanics and Foundation Engineering. Moscow, **1**: (475–478).

Undrained Shear Strength of Overconsolidated Clay

Gunnar Aas[1] and Suzanne Lacasse[2]
[1]formerly Norwegian Geotechnical Institute (NGI); [2]NGI

Abstract

It has been known for a long time now that in soft and sensitive clays undrained failure occurs apparently before the full friction angle has been mobilized. The main object of this paper is to clarify the importance of *deformations* in the process of mobilizing undrained shear strength. This has resulted in an improved understanding of the failure process, and made it possible to express undrained shear strength for this type of clays in terms of effective stresses and a set of effective shear strength parameters, friction and attraction. The study made it possible to determine the relationship between the coefficient of earth pressure at rest K_0, the undrained shear strength s_u and the overconsolidation ratio OCR during cycles of consolidation, unloading and reloading. The determinations, done both analytically and graphically, were done for a typical low plasticity clay, and the results compared with published data. For comparison, laboratory test results for a somewhat stiffer and dilating offshore clay are also included in this paper.

Introduction

When a soft, sensitive clay mobilizes the full friction under the major principal stress, and thereafter is stressed and mobilizes the contribution to friction from the minor principal stress, this causes a structural collapse, high pore pressures and decreasing strength. This second shearing stage implies an important change compared with the first one, as the direction of axial strain is reversed compared to the friction supporting stress component. These conditions are believed to be responsible for a structural collapse in the soil that is responsible for softening and failure in a loose (contractant) soil or strengthening in a low sensitive (dilatant) clay.

In cases involving rotation of principal stresses, it is the direction of the principal stresses at the end of the first stage that counts. In this first stage, active shear involves a reloading and only small elastic strains. During shear of the soil under other stress conditions, for instance passive shear, the process includes both elastic and plastic deformations.

Assumptions

The results in this paper are based on the following four assumptions:

1) Mobilisation of friction requires a simultaneous development of a plastic deformation in the clay. Elastic deformations do not, in the same way, contribute to build up friction

resistance.

2) Attraction is believed to be due to net attractive forces acting across the water-films constituting the contact points between clay particles. Attraction acts like a tension reinforcement in the clay and requires practically no deformation to be activated.
3) If a clay has been consolidated, thereafter unloaded and then reloaded, at all times without undergoing lateral strain, the active, frictional shear resistance will be a function of the existing vertical stress alone.
4) An attempt to force a brittle (contractant) overconsolidated clay to mobilize a contribution to friction from also the horizontal stress, leads to a structural collapse and decreasing shear strength.

It is important to realize that even though the process involves yielding, the requirement of static equilibrium must always apply.

Undrained, active shear strength

The general expression for undrained, active shear strength, s_{uA}, of a brittle, pure frictional soil is:

$$s_{uA} = ½ (\sigma'_v - \sigma'_h) = ½ \sigma'_v \sin\phi'_M \quad (1)$$

which gives:

$$\sigma'_h/\sigma'_v = K_0 = 1 - \sin\phi'_M \quad (2)$$

where σ'_v is the effective vertical stress
σ'_h is the effective horizontal stress
ϕ'_M is the material friction angle
K_0 is the coefficient of earth pressure at rest

Equation (2) is the well-known Jacky formula (Jacky, 1948), expressing the coefficient of earth pressure at rest for a normally consolidated soil.

For a clay exhibiting attraction, this will lead to an increase in strength comparable to the effect of reducing σ'_h by a stress equal to the attractive force. Hence, the expression for undrained, active shear strength becomes:

$$s_{uA} = ½ \sigma'_v (\chi + \sin\phi'_M) \quad (3)$$

where χ is the relative attraction parameter (Aas and Lacasse, 2021).

As long as one is dealing with exclusively clays exposed to a state of perfect confined compression or expansion, σ'_v may be exchanged by $K_0 \sigma'_v /(1 - \sin\phi'_M)$, which gives:

$$s_{uA} = ½\, K_0\, \sigma'_v\, (\chi + \sin\phi'_M) / (1 - \sin\phi'_M) \quad (4)$$

Equation (4) defines a proportionality between s_{uA} and K_0,and makes it possible to determine how s_{uA} is related to the overconsolidation ratio, OCR.

Figure 1 shows the values of χ and $\sin\phi'_M$ as a function of plasticity index for 25 sets of undrained triaxial tests on a variety of soft clays. As shown on the figure, χ increases and $\sin\phi'_M$ decreases with increasing plasticity. However, the increase and decrease are in a such a way that the sum of the two parameters (χ and $\sin\phi'_M$) is an almost constant value for most clays and equal to a value between 0.7 and 0.8 (Aas and Lacasse, 2021).

In the next two sections, values of χ equal to 0.25 and $\sin\phi'_M$ equal to 0.50 were selected and the approximate values of K_0 and s_{uA} for an idealized low plastic, soft clay was calculated for overconsolidated (OC) clays during unloading and reloading.

Relationship between K_0, OCR and s_{uA} for unloaded OC clays

The following section derives the relationship between s_{uA} and K_0 for a clay subjected to uniaxial unloading, and thus having an OCR greater than 1. To demonstrate this, the discussion follows the behavior of a clay from start at the conditions of earth pressures at rest (K_0-conditions) at a given preconsolidation stress, σ'_{vc}, and up to a state of passive failure.

The conditions for mobilizing friction under confined compression involves a ratio between χ and $\Delta\sigma'_3$ equal to $1/(1 - \sin\phi'_M)$.This means that the clay has been subjected to a combination of an isotropic stress $\Delta\sigma'_1$ and a shear stress equal to $-½\Delta\sigma'_1 \sin\phi'_M$, causing plastic deformations.

Unloading when $\sigma'_h/\sigma'_v < 1$

The above loading process involves a combination of an isotropic stress, σ'_v, and a horizontal deviator stress, $-\sigma'_v \cdot \sin\phi'_M$, causing plastic deformations and contributing to building up frictional resistance. If one applies an unloading involving an isotropic stress $-\sigma'_v$ and a horizontal deviator stress $\sigma'_v \sin\phi'_M$, this does not, however, lead to a reversed confined condition. This is due to the fact that the reduction in shear stress causes elastic strains only, which do not influence the mobilized friction. To produce a uniaxial deformation, the clay needs to be exposed to also a horizontal deviator stress $-\sigma'_v \cdot \sin\phi'_M$, so that the combination of stresses causing plastic strains becomes $-\sigma'_v$, and $-\sigma'_v \cdot \sin\phi'_M$. However, the value of K_0 reflects also the contribution from elastic stress, and becomes for this case:

$$K_0 = (1 - \sin\phi'_M) / (1 + \sin\phi'_M) \quad (5)$$

By introducing the preconsolidation stress, σ'_{vc}, and the overconsolidation ratio OCR $= \sigma'_{vc} / \sigma'_v$, the following relationship between K_0 and OCR can be derived:

$$K_0 = (1+OCR\cdot\sin\phi'_M)\,(1-\sin\phi'_M)/\,(1+\sin\phi'_M) \quad (6)$$

The particular values of OCR and σ'_v that correspond to a value of K_0 equal to unity are:

$$OCR_{Ko=1} = 2/(1-\sin\phi'_M) \quad (7)$$

$$\sigma'_{vc\ Ko=1} = \tfrac{1}{2}\,\sigma'_{vc}\,(1-\sin\phi'_M) \quad (8)$$

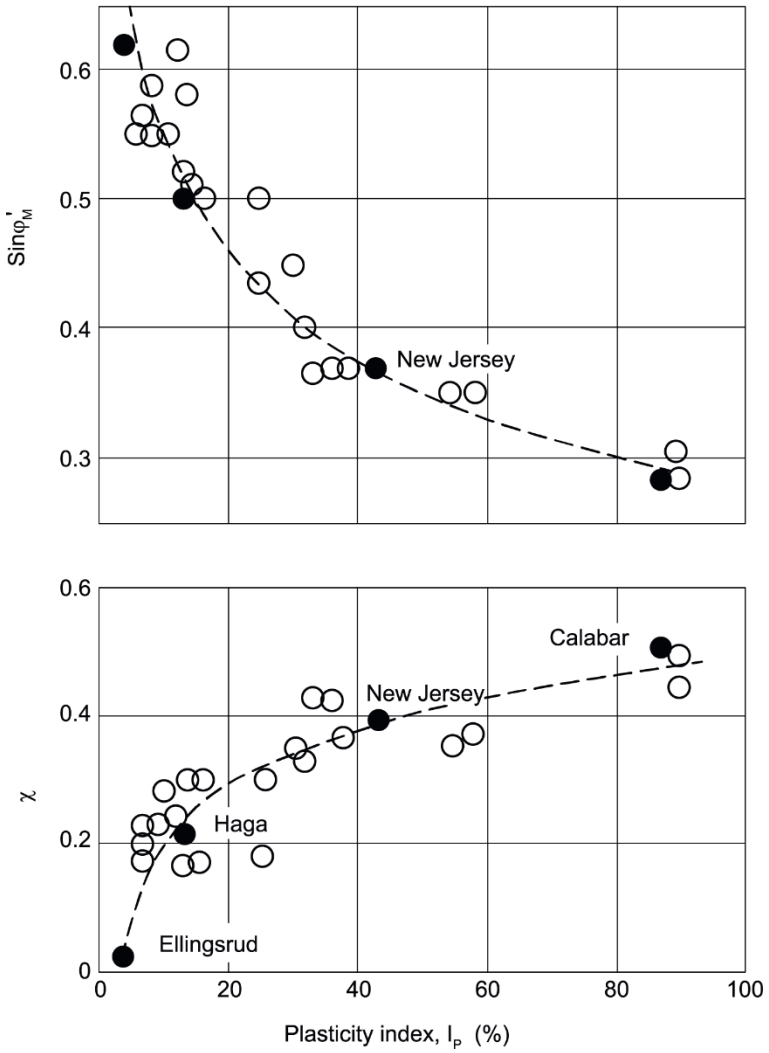

Figure 1. Relationships between shear strength parameters χ and $\sin\phi'_M$ and plasticity for 25 sets of undrained triaxial active tests.

Unloading when $1 < \sigma'_h/\sigma'_v < 1/(1-\sin\phi'_M)$

After having been unloaded to stresses corresponding to the OCR value above, the clay is subjected to a condition involving isotropic compressive stresses. Under these conditions, a

further vertical stress relief equal to $\Delta\sigma'$ does not include any shear stress removal nor corresponding elastic strain. Thus, a confined unloading has to follow the simple imposed stresses of $\Delta\sigma'_h = \Delta\sigma'_v \cdot (1 - \sin\phi'_M)$. Consequently, for this unloading stage, one gets:

$$K_0 = (1 - \sin\phi'_M) \quad (2)$$

The following relationship between K_0 and OCR can be derived:

$$K_0 = [2 + OCR\,(1 - \sin\phi'_M)\cdot\sin\phi'_M]/2\,(1 + \sin\phi'_M) \quad (9)$$

The value of OCR which corresponds to a value of K_0 equal to $1/(1 - \sin\phi'_M)$ is:

$$OCR_{Ko=\,1/(1-\sin\phi'M)} = 4/(1 - \sin\phi'_M)^2 \quad (10)$$

In the same way, the OCR corresponding to passive failure, $K_0 = (1 + \sin\phi'_M)/(1 - \sin\phi'_M)$ is:

$$OCR_{Ko=\,(1+\sin\phi'M)/(1-\sin\phi'M)} = 8/(1 - \sin\phi'_M)^2 \quad (11)$$

Combining Eq. (4) and the above values of K_0, one gets a relationship between and s_{uA} and OCR:

$\sigma'_h/\sigma'_v < 1$ $\quad s_{uA}/\sigma'_v = \frac{1}{2}\,(1+\frac{1}{2}OCR\,\sin\phi'_M(\chi + \sin\phi'_M))/2(1 + \sin\phi'_M)$ (12)

$1<\sigma'_h/\sigma'_v<1/(1-\sin\phi'_M)$ $\quad s_{uA}/\sigma'_v = (1+\frac{1}{2}OCR(1-\sin\phi'_M)\sin\phi'_M\,(\chi+\sin\phi'_M))2/(1-\sin\phi'_M)$ (13)

For the case where σ'_h/σ'_v equals $(1+\sin\phi'_M)/(1-\sin\phi'_M)$, passive failure occurs.

Figure 2 presents a graphical representation of the variation in K_0 as a clay is unloaded from an OCR of 1 to 32. The line labeled $\sigma'_h/\sigma'_v = (1 - \sin\phi'_M)$ is the original consolidation process resulting in an initially constant K_0 equal to $1 - \sin\phi'_M$. The red curve below this line shows the value of K_0 increasing from $1 - \sin\phi'_M$ to $(1 + \sin\phi'_M)/(1 - \sin\phi'_M)$ when OCR increases from 1 to 32. The latter data point is the passive failure. The dashed lines, normal to each other, demonstrate how one, on the basis of a K_0-value, gets to the failure line described by $\sigma'_h/\sigma'_v = (1 - \chi - \sin\phi'_M)$. The inset in Figure 2 gives more details for OCRs of 16 and 32 and negative shear stresses.

Relationship between K_0, OCR and s_{uA} for Reloaded OC clays.

Figure 3 shows how K_0 and s_{uA}/σ'_v may be determined from a similar graphical construction for the case where the overconsolidated clay is reloaded to its original preconsolidation stress, σ'_{vc}. The first part of the reloading process (illustrated in the inset) involves the transition of the clay from passive to active stress conditions. This occurs as an elastic recovery to an isotropic stress condition, σ'_0. The elastic rebound of passive shear stress in this phase does not imply any change in mobilized friction. As the effective vertical stress increases, however, the

ratio s_{uA}/σ'_v decreases proportionally with the increasing vertical stress. Thereafter, with further reloading of the clay bringing the clay to a condition of isotropic consolidation, the clay behaves in the same manner as a young clay, implying a stress ratio of:

$$K_0 = (\sigma'_h - \sigma'_0)/(\sigma'_v - \sigma'_0) = (1 - \sin\phi'_M) \qquad (14)$$

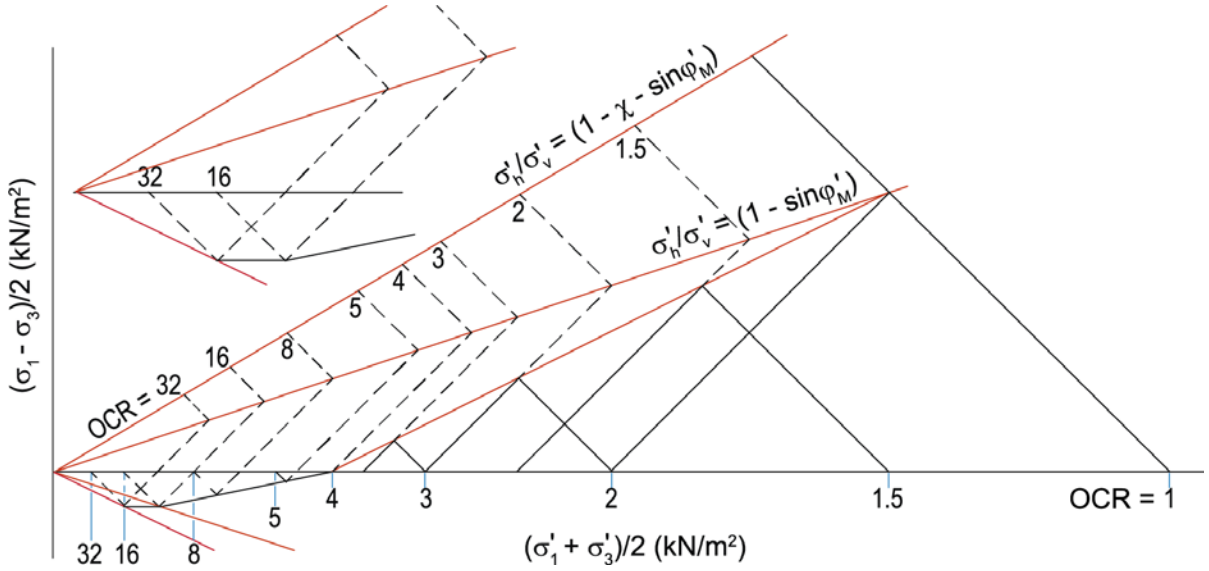

Figure 2. Graphical construction of K_0 and s_{uA}/σ'_v as a function of OCR for soft clays.

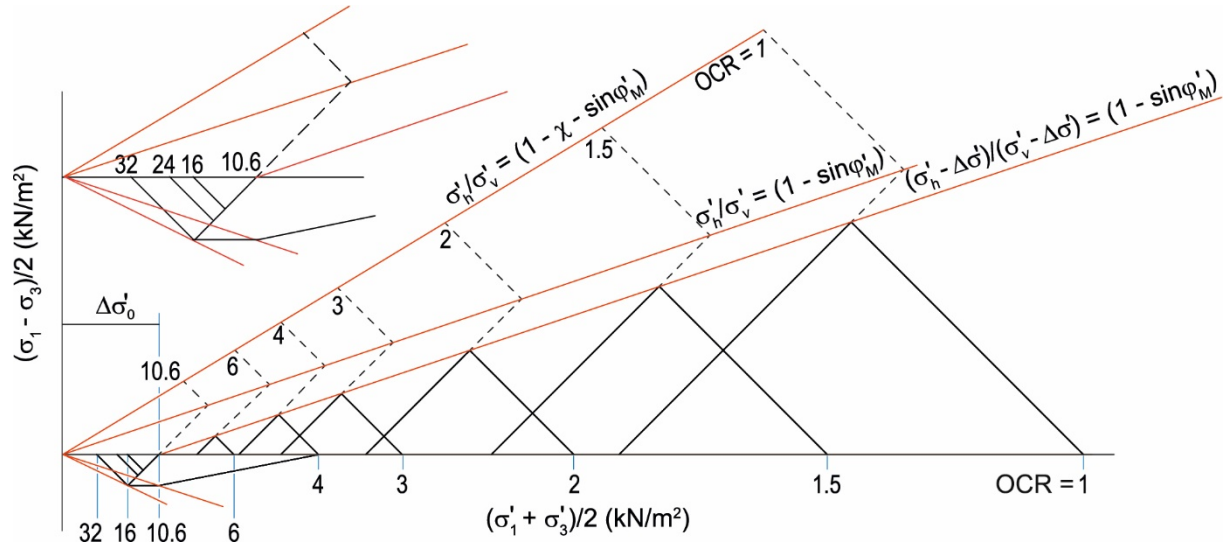

Figure 3. Theoretical values of K_0 and s_{uA}/σ'_v during reloading of an overconsolidated clay.

The expression for K_0 may be determined on the basis of Eqns. (11) and (13):

$$K_0 = 1+1/8\ OCR\ (1 - \sin\phi'_M)\ \sin\phi'_M \cdot (1 + \sin\phi'_M) \qquad (15)$$

Figures 4 and 5 show numerical values of K_0 and s_{uA}/σ'_v based on the processes in Figures 2 and 3 for unloading and reloading of a clay. Values of χ of 0.25 and $\sin\phi'_M$ of 0.50 were used.

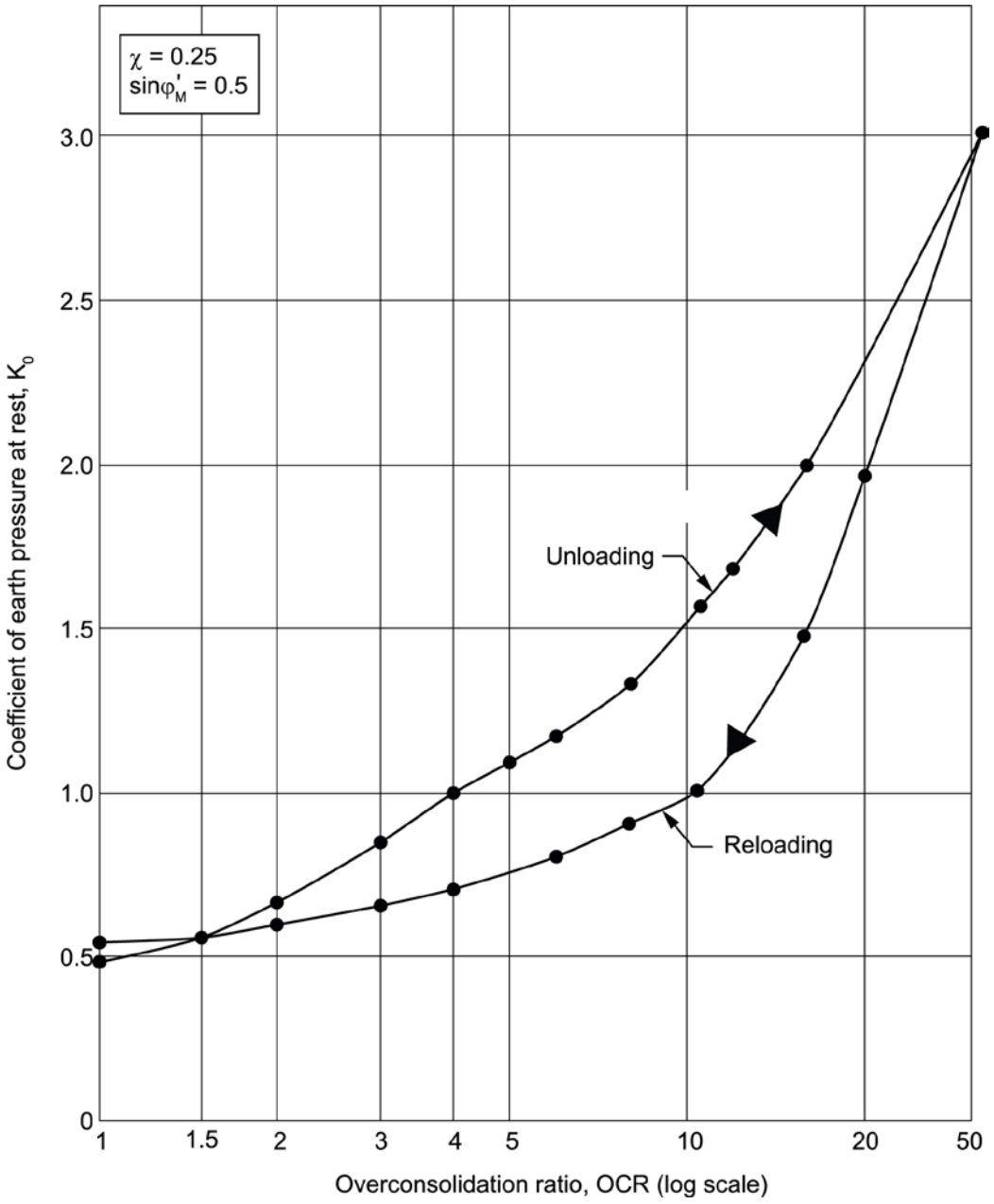

Figure 4. Change in K_0 of a clay as a result of unloading and reloading, based on Figures 2 and 3.

The resulting unloading curves describe very closely the following two well-known expressions introduced by Ladd and Foott (1974) and Ladd *et al.* (1977):

$$K_{0\,OC} = K_{0\,NC} \cdot \mathrm{OCR}^{m} \tag{16}$$

$$s_{uA\,OC}/\sigma'_{vc} = s_{uA\,NC}/\sigma'_{vc} \cdot \mathrm{OCR}^{m} \tag{17}$$

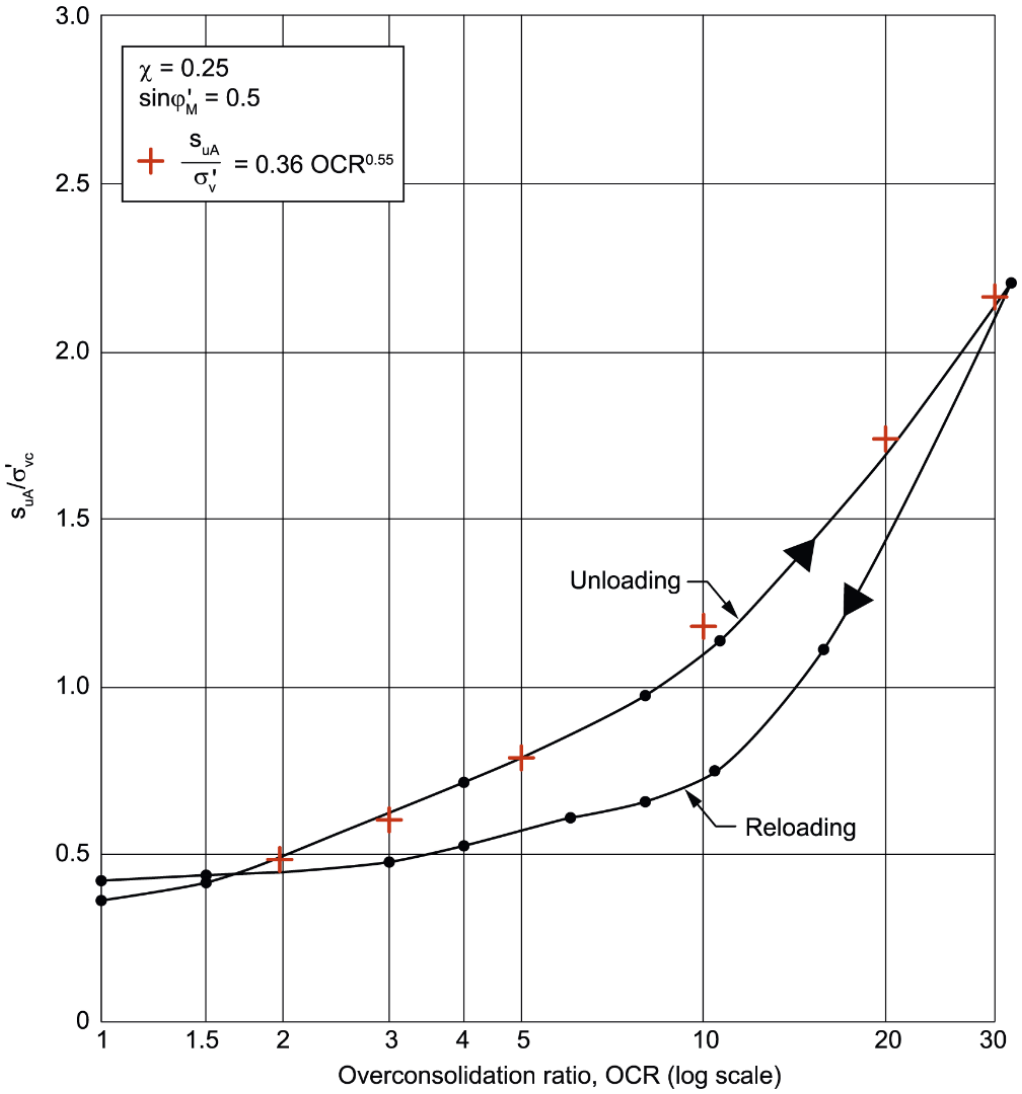

Figure 5. s_{uA}/σ'_{v} of a clay as a function of OCR during unloading and reloading, based on Figs 2 and 3.

Examination of coefficient of earth pressure at rest, K_0

The coefficient of earth pressure at rest K_0 can thus be obtained theoretically from Eq. (18), based on the analyses on an idealized clay in Figures 2 and 3. The coefficient in front of the OCR-parameter refers to the K_0-value for the normally consolidated clay, as noted in Eq. (16).

$$K_0 = \quad 0.50\ \mathrm{OCR}^{\,0.55} \tag{18}$$

It is important to realize that the K_0-value depends on whether a clay has never been reloaded or been exposed to an increased in vertical stress (or virgin consolidation) after unloading and reloading, due to, for instance, the addition of fill or construction of a heavy building.

Figure 6 shows the results of measurements of K_0 in triaxial tests during unloading and subsequent reloading of the soft sensitive Haney Clay (Campanella and Vaid, 1972). The K_0-values do not deviate much from the values for the theoretical clay in Figure 4, with a value of K_0 of about 0.55 at an OCR of 1. The laboratory data support the theoretical model in Figure 4.

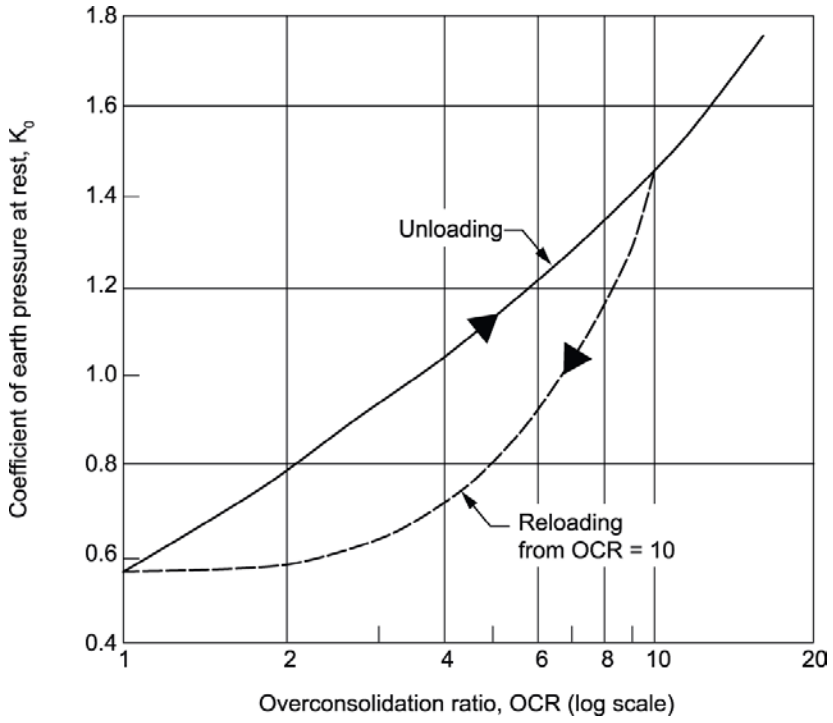

Figure 6. K_0 as a function of OCR as measured in the laboratory on Haney sensitive clay

The multi-regression statistical analyses by L'Heureux *et al.* (2017) suggested the relationship in Eq. (20), based on laboratory measurements of K_0 on eight Norwegian clays with OCR between 1 and 8 and plasticity index between 10 and 40%. The relationship in Eq. (20) is very close to the theoretically derived relationship in Eq. (18).

$$K_{0\,OC} = 0.53\,\mathrm{OCR}^{0.47} \tag{20}$$

Examination of normalized undrained shear strength ratio s_{uA}/σ'_v

The normalized undrained shear strength ratio s_{uA}/σ'_v can also be thus obtained theoretically from Eq. (19), based on the analyses on an idealized clay in Figures 2 and 3. The red crosses in Figure 5 represent the theoretical relationship from Eq. (19). The coefficient in front of the OCR-parameter refer to the normalized undrained shear strength for the normally consolidated clay, as noted in Eq. (17).

$$s_{uA}/\sigma'_{vc} = \quad 0.36 \text{ OCR}^{\,0.55} \tag{19}$$

Figure 7 presents the theoretically derived relationship in Eq. (19) with the measured data from undrained triaxial active tests on Norwegian soft clays from Karlsrud (1995).

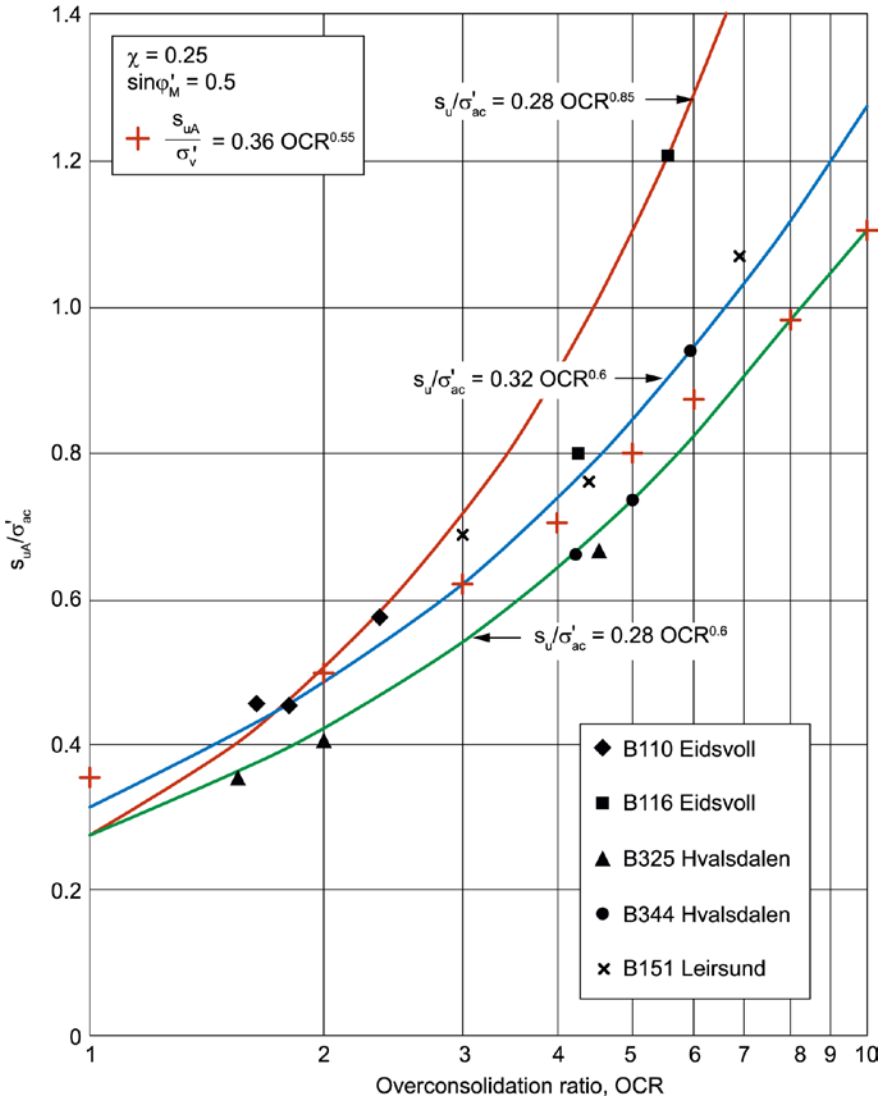

Figure 7. Theoretical shear strength ratio s_{uA}/σ'_v compared to measurement in the laboratory, with χ of 0.25 and $\sin\phi'_M$ of 0.50 (data from Karlsrud, 1995). (Note: σ'_{ac} stands for effective axial consolidation stress in the triaxial test, which in situ corresponds to σ'_{v0} (effective vertical overburden stress).

Figure 7 also compares the theoretically-derived values with the relationships proposed by Karlsrud *et al.* (2005) based on to Eq. (16):

$$s_{uA}/\sigma'_{v0} = \alpha\,\mathrm{OCR}^{m} \tag{20}$$

Karlsrud *et al.* (2005) recommended a range of α-values between 0.28 and 0.32 and exponent *m* between 0.60 and 0.90 (green and blue curves in Fig. 7). The red crosses are again the theoretically-derived values, with for $s_{uA}/\sigma'_{vc} = 0.36\ \mathrm{OCR}^{0.55}$. Figure 7 also shows the relationship $s_{uA}/\sigma'_{vc} = 0.28\ \mathrm{OCR}^{0.85}$, which includes the highest data measured on Eidsvoll clay.

Figure 8 presents the results from triaxial active tests on Norwegian clays. On the upper figure, the data accumulated by Karlsrud and Hernandez-Martinez (2013) are represented by three curves described with the following relationship:

$$s_{uA}/\sigma'_{v0} = \alpha\,\mathrm{OCR}^{m} \tag{21}$$

where the α–value represents the ratio s_{uA}/σ'_{v0} ·for normally consolidated clay noted in Eq. (17). In the upper Figure 8, α varies from 0.25 to 0.35 and exponent *m* from 0.65 to 0.75. The upper bound data are from the Emmerstad and Nybakk-Slomarka sites, two of the clays with lowest plasticity index. The lower bound data are mostly from the Kløfta-Nybakk, Klett, Tiller and Stjørdal sites.

Paniagua *et al*. (2018; 2019) updated the correlations for Norwegian clays, considering only the clays where block samples were taken and thus reduced the effect of sample disturbance to a maximum. Paniagua *et al*. also did rigorous multi-regression analyses, including water content of the tested specimens as one of the regression variables. The results are illustrated in the lower diagram in Figure 8, and compared with the estimated curves by Karlsrud *et al.* (2005) earlier, which had suggested α-values between 0.28 and 0.32 and exponent *m* between 0.60 and 0.90.

The updated Paniagua *et al*. functions for $s_{uA}/\sigma'_{v0} = \alpha\,\mathrm{OCR}^{m}$ (Eq. 21) are also a function of water content. There is an observable trend as a function of the water content. These more recent experimental correlations for s_{uA}/σ'_{v0} have an α-value of 0.32 for all water contents *w*. The exponent *m* is equal to (0.20 + 1.17*w*), with *w* expressed as a percentage between 0 and 1. The correlations in Figure 8 mean that exponent *m* increases from 0.55 to 1 for water contents between 30 and 70%.

D'Ignazio *et al*. (2017) studied 6 clay sites in Finland Statistical analysis of the normally consolidated shear strength ratio and the exponent *m* was done. The ratio s_{uA}/σ'_{v0} varied between 0.30 to 0.48 and the exponent *m* could vary between 0.5 and 1.0.

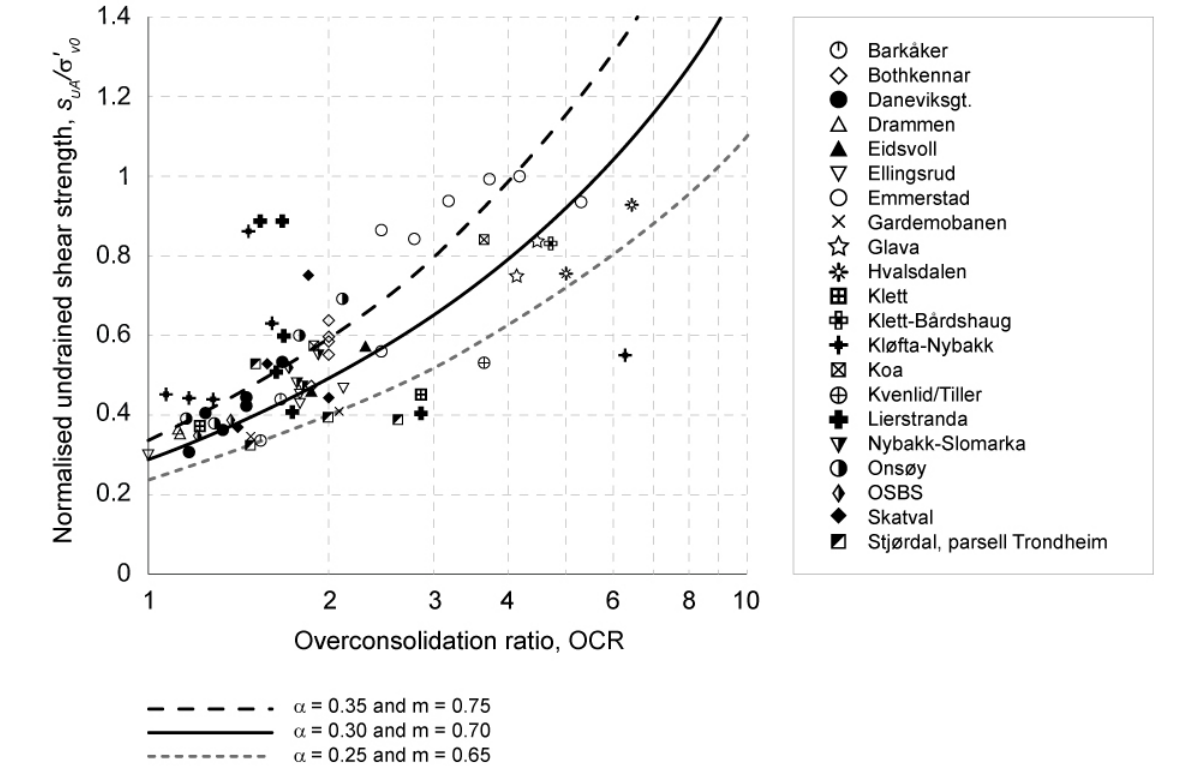

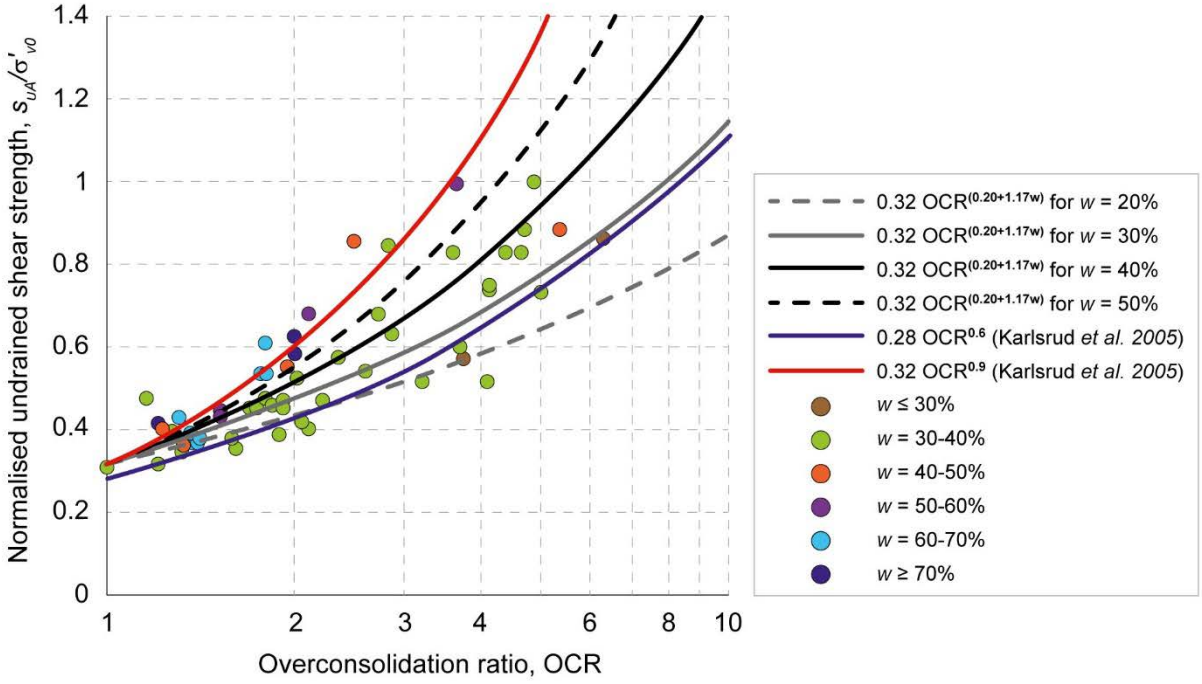

Figure 8. Undrained shear strength ratio s_{uA}/σ'_{v0} from triaxial compression tests, with relationships $s_{uA}/\sigma'_{v0}=\alpha\ OCR^m$: Top: 21 Norwegian clays (Karlsrud and Hernandez-Martinez, 2013); Bottom: exclusively block sample data, and as a function of water content w (Paniagua et al., 2019).

There is naturally scatter in the laboratory data, and the parameters may depend on other clay characteristics such as, for example, clay mineralogy and/or sensitivity, although Paniagua et al. (2019) concluded that the main significant factor was water content The laboratory values may also be affected by sample disturbance, even if the samples are taken by block samplers.

Nevertheless, in spite of the scatter in the laboratory results, the theoretically-derived model in this paper (shown as crosses in Fig. 7) provide a good picture of the relationship between normalized active undrained shear strength and overconsolidation ratio for low plasticity soft clays. The experimental exponent *m* may be somewhat higher than the theoretical value, but this may be a reflection of the water content, as exponent m seems to increase with increasing water contents.

Behaviour of North Sea dilatant clays

Triaxial tests on clay from the offshore Sleipner field in the North Sea were included in the present study. The reason for including a dilatant clay was to demonstrate that a contractant and a dilatant clay behave similarly up to a critical point. Once this critical point is reached, the contractant clay starts building up pore pressures and loosing strength, whereas the dilatant clay generates negative pore pressures and increases in strength.

The three series of active and passive triaxial tests examined herein were run on samples taken from depths of 3.35, 5.6 and 8.0 m below seabed. Each sample was reconsolidated to the *in situ* effective stresses and sheared under undrained conditions. As illustrated in Figures 9, 10 and 11, the three series of test showed remarkably consistent behavior.

The behavior of the dilatant clay can be described as follows: the clay from the three depths showed a "material" friction ($sin\phi'_M$) varying from 0.55 to 0.59, based on the highest value of σ'_h/σ'_v in active shear and σ'_v/σ'_h in passive shear. Both active and passive tests showed a small (elastic) strain of about 0.5%. At this point, large deformations started to develop suddenly.

By drawing straight lines from the origin and through these critical points, the lines should, based on the experience with the soft clays, correspond to:

$$\sigma'_h/\sigma'_v = 1 - sin\phi'_M \text{ in active shear} \quad (22)$$

$$\sigma'_v/\sigma'_h = 1 - sin\phi'_M \text{ in passive shear} \quad (23)$$

The values of $sin\phi'_M$, determined from these lines lie between 0.55 and 0.57, and support the theoretical model developed for the idealized soft clay in the precious sections. The data show that dilatant and contractant clays behave similarly up to a stress level where only σ'_v contributes to the mobilized active strength and only σ'_h contributes to the passive strength.

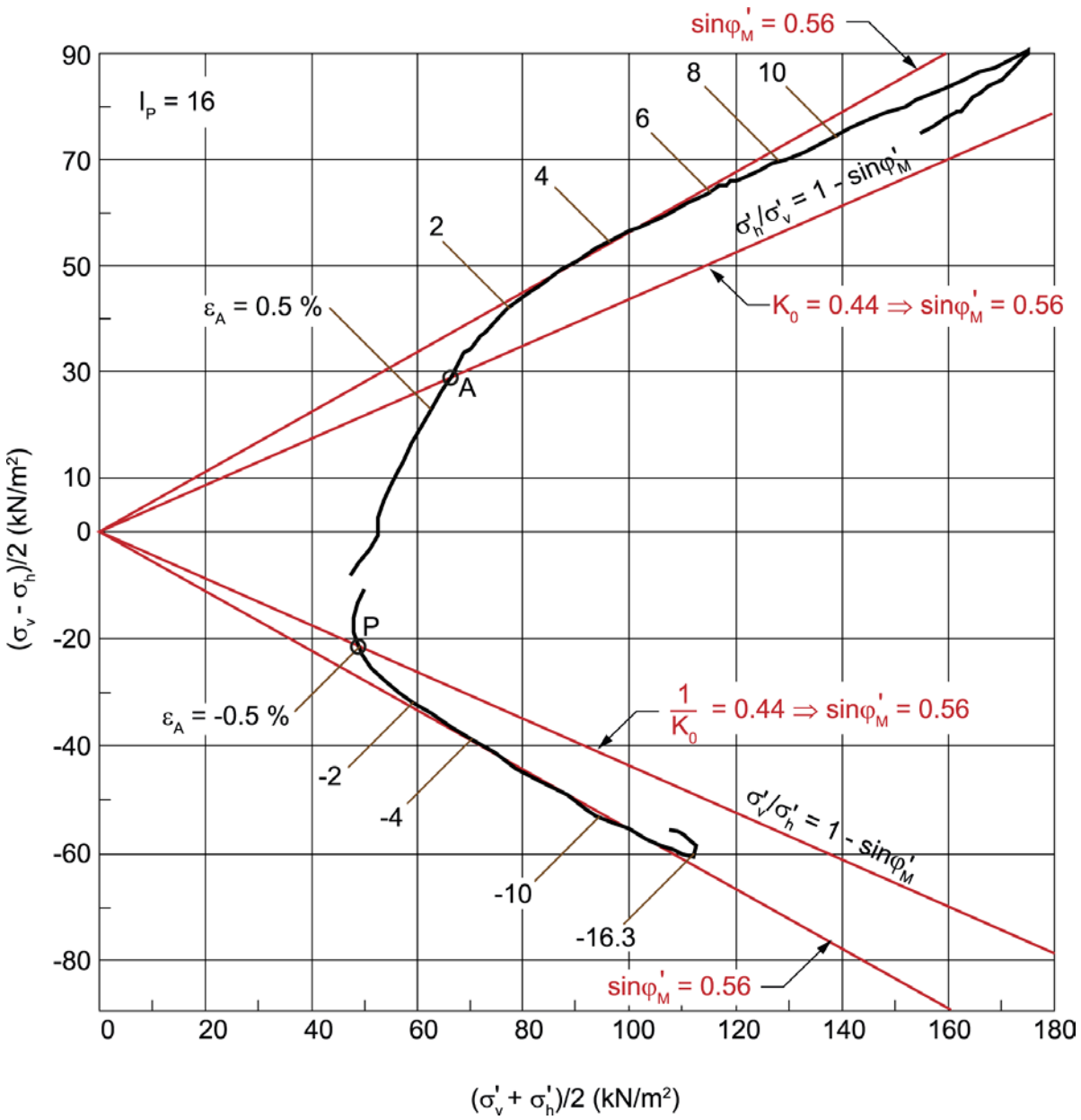

Figure 9. Effective stress path for active and passive triaxial tests on dilatant Sleipner clay from 3.35 m depth.

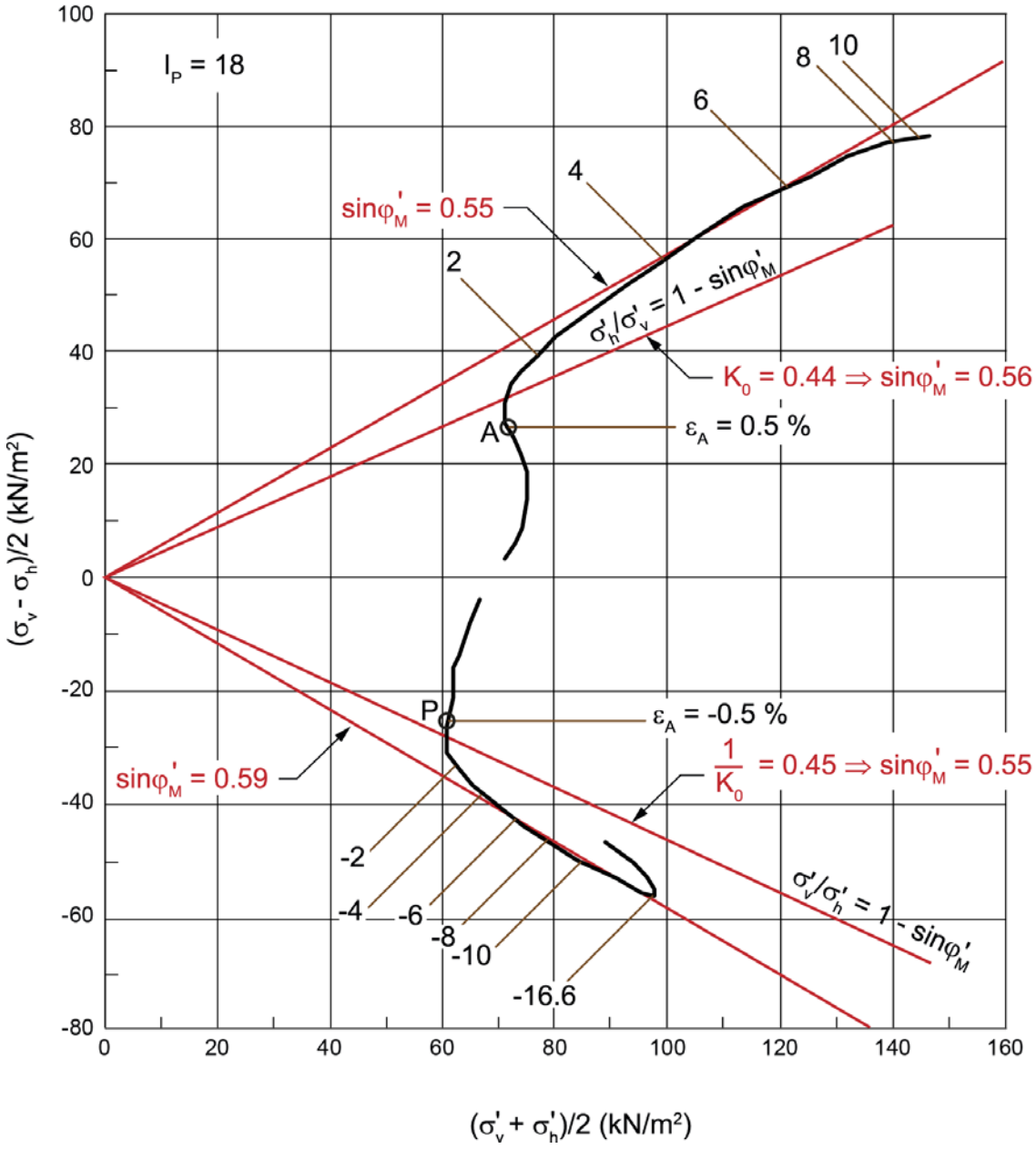

Figure 10. Effective stress path for active and passive triaxial tests on dilatant Sleipner clay from 5.6 m depth.

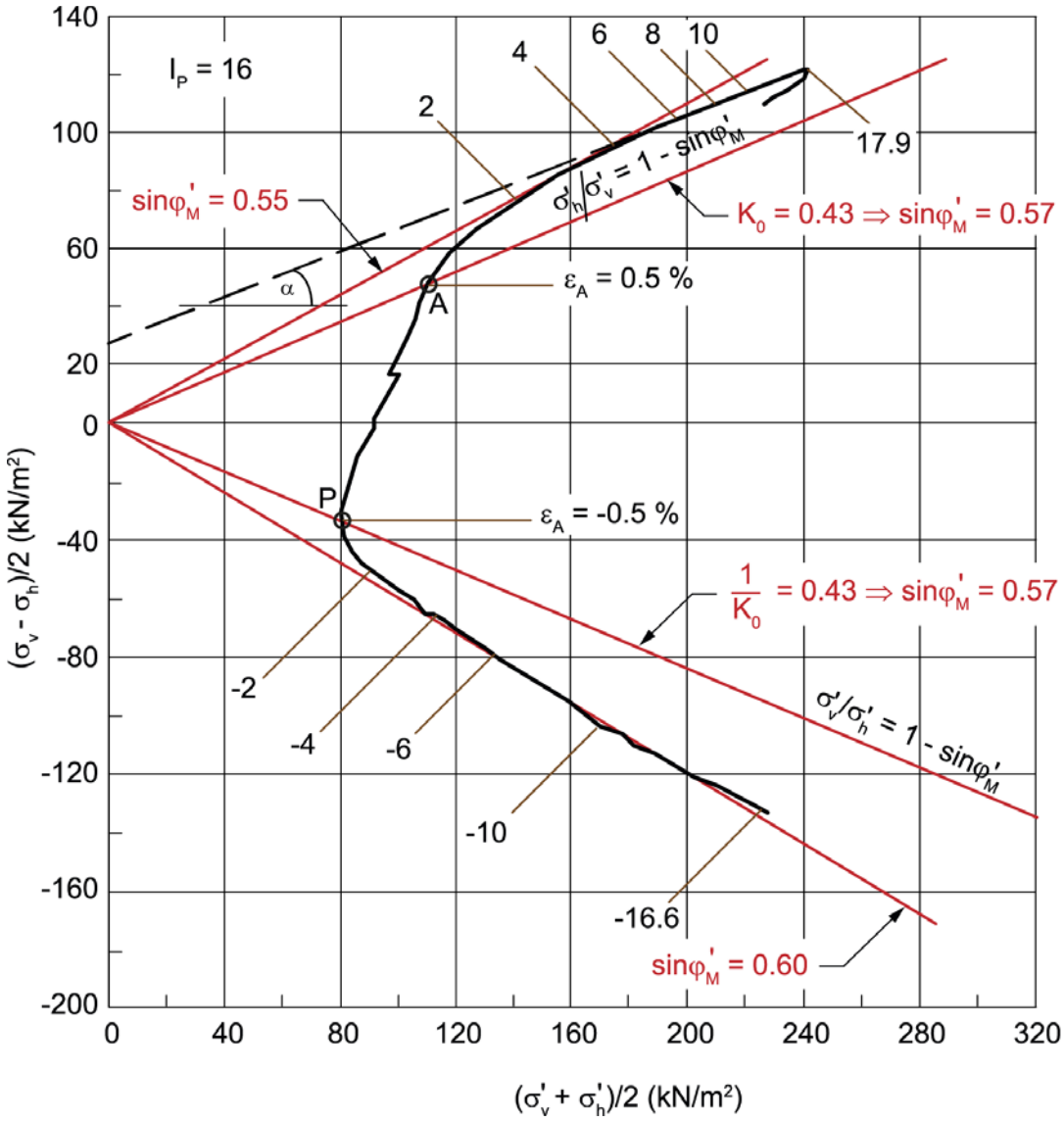

Figure 11. Effective stress path for active and passive triaxial tests on dilatant Sleipner clay from 8.0 m depth.

CONCLUSIONS

When consolidating under confined compression, a soft clay is subjected to a combination of an isotropic stress and a shear stress, causing plastic deformations and responsible for mobilizing friction resistance. Since no lateral strain takes place, the change in vertical stress only is responsible for mobilizing friction. The requirement for static equilibrium then defines a generally valid ratio between the principal stresses equal to $1/(1 - sin\phi'_M)$, where $sin\phi'_M$ is the ("material ") friction angle of the clay.

If unloading occurs, this clay will now be subjected to a reduction of both an isotropic stress and a shear stress. In this case, however; the reversion of shear stress results in an elastic strain

only, which has no influence on the mobilized friction. The contribution to friction from plastic strains which fulfils the condition of no lateral strain, then has to be based on the "general" principal stress ratio for virgin consolidation.

These principles have made it possible to calculate, both analytically and graphically, how K_0 varies as a function of overconsolidation ratio (OCR) as a low plastic clay is unloaded from a condition of earth pressure at rest (K_0) to passive failure, and then reloaded back to the initial stresses. In confined compression, there exist a constant ratio between K_0 and normalized shear strength ratio s_{uA}/σ'_{vc}, and where the effective stress strength parameters, x and $sin\phi'_M$ are two defining parameters. The paper compares theoretical-derived values of K_0 and normalized shear strength ratio s_{uA}/σ'_{vc} with the values measured in the laboratory for a large number of Norwegian clays. The agreement is good and the theoretical approach can be used when there is a lack of experimental data.

Laboratory test results from a dilatant offshore clay show that the dilatant clay behaves exactly as a contractant clay up to a certain critical stress level, where a soft and sensitive clay will continue to failure, whereas a dilatant clay increases in strength, and until failure following a conventional Mohr Coulomb failure.

REFERENCES

Aas, G. and Lacasse, S. (2021). Shear Strength of Soft Clay in Terms of Effective Stresses. 1st paper in this NGI publication.

Campanella, R.G. and Vaid, Y.P. (1972). A Simple K_0-Triaxial Cell. *Canadian Geotechnical Journal*. **9** (3): 249−20.

D'Ignazio, M., Kok-Kwang, P., Ann Tan, S., Länsivaara, T. and Lacasse, S. (2017). Reply to the discussion by Mesri and Wang on "Correlations for undrained shear strength of Finnish soft clays".*Canadian Geotechnical Journal*. **53** (5). https://doi.org/10.1139/cgj-2016-0686.

Jaky, J. (1948). On the bearing capacity of piles. 2nd Int. Conf. Soil Mechanics and Foundation Engineering, Rotterdam. Proceedings. **1**: 100−103.

Karlsrud, K. (1995). Blokkprøvetaking i kombinasjon med CPTU gir nye muligheter (Block sampling in combination with CPTU gives new possibilities). Fjellsprengningsteknikk - bergmekanikk - geoteknikk. Oslo. Ch. 38.1−38.18 (NGI Report 521674-1). In Norwegian.

Karlsrud, K., Lunne, T., Kort D.A. and Strandvik, S. (2005). CPTU correlations for clays. International Conference on Soil Mechanics and Geotechnical Engineering (ICSMGE) 16. Osaka, Proc. **2**: 693−702.

Karlsrud, K. and Hernandez-Martinez, F.G. (2013). Strength and deformation properties of Norwegian clays from laboratory tests on high quality block samples. *Canadian Geotechnical Journal.* **50**(12): 1273−1293. DOI: 10.1139/cgj-2013-0298 (korrigenda 2014).

L'Heureux, J.S., Ozkul, Z., Lacasse, S., D'Ignazio, M. and Lunne, T. (2017). A revised look at the coefficient of earth pressure at rest for Norwegian Clays. Fjellsprengningsteknikk - bergmekanikk - geoteknikk. Oslo 2017. Ch. 35.

Ladd C.C. and Foot R. (1974). New design procedure for stability of soft clays. J*ournal of the Geotechnical Engineering Division*. ASCE. **100**(7): 763−786.

Ladd, C.C., Foott, R., Ishihara, K, Schlosser, F. and Poulos, H.G. (1977). Stress-deformation and strength characteristics: SOA report. 9th Int. Conf. Soil Mechanics and Foundation Engineering, Tokyo. Proceedings. **2**: 421−494.

Ladd, C.C. and DeGroot, D.J. (2003). Recommended Practice for Soft Ground Site Characterization. The Arthur Casagrande Lecture, Proc. 12th Panamerican Conference on Soil Mechanics and Geotechnical Engineering, Boston, MA, **1**: 3−57.

Paniagua, P, L'Heureux, J.S., Sæthereng Gundersen, A. (2018). GEODIP's high-quality database: Clay. NGI 20150030-02-R Rev. 2. 2018-01-17. 106 pp.

Paniagua, P., D'Ignazio, M., L'Heureux, J.S., Lunne, T. and Karlsrud, K. (2019). CPTU correlations for Norwegian clays: an update. *AIMS Geosciences.* **5**(2): 82−103. doi: 10.3934/geosci.2019.2.82.

Stability of Natural Slopes in Quick Clay

Gunnar Aas[1] and Suzanne Lacasse[2]
[1]formerly Norwegian Geotechnical Institute (NGI); [2]NGI

Abstract

Norway and Sweden have been subjected to landslides for several centuries, with some of the largest landslides involving a large block sliding out as a continuous flake on a deposit of soft quick clay. Attempts to calculate the stability conditions for this type of landslides by using a conventional effective stress analysis have shown to considerably overestimate the safety factor. The introduction of the concept of limiting or yielding stresses in the course of the last 3 to 5 decades resulted in the general acceptance that stability calculations, even for natural slopes, should be based on undrained shear strength. Early in the seventies the ADP-type of analysis was proposed (Bjerrum, 1973; Ladd and Foott, 1974), based on triaxial and direct simple shear tests on tests specimens reconsolidated to *in situ* stresses, and thus simulating the stress conditions along different parts of the failure surface. The present study describes recently developed relations between undrained shear strength parameters and effective shear strength parameters, friction and attraction. The new relationships make it possible to do an effective stress analysis, and thus take existing pore pressures into consideration in a better way than in an ADP-type analyses. These effective stress-strength parameters have been determined for several Norwegian and Swedish clays, and used for a recalculation of some of the older Scandinavian flake type landslides.

Introduction

It is commonly accepted today that in soft, sensitive clays yielding and failure take place at a critical stress, occurring before the clay has been able to fully mobilize its effective stress strength parameters. This has led to the conclusion that stability calculations even for natural slopes should be carried out with an undrained (ADP-type[1]) stability analysis, based on normalized values of active and passive triaxial and direct simple shear strengths. Figure 1 shows the results from ADP-analyses of five old Norwegian quick clay flake landslides presented earlier by Aas (1981). For simplicity, the stability conditions were expressed by comparing the calculated average shear stress along the shear plane $(\tau_\beta/\sigma'_0)_{aver.}$ with the direct simple shear test results from the laboratory (s_{uD}/σ'_0), and in one case (the Furre landslide), with the shear stress ratio measured from large shear box tests *in situ*, $(\tau_{\beta\,Cr}/\sigma'_0)$.

The present paper presents the relationships between the normalized undrained shear strengths and the effective shear strength parameters, friction and attraction, thus confirming that the ADP analysis can be considered as theoretically well founded, and in accordance with the fundamental and well-established effective stress strength concept. Since the occurrence of quick clay is often tied to flowing water and artesian pore pressures, it is important to determine exact values of pore pressures and corresponding effective stresses in the clay. This also applies for an ADP-analysis.

[1] ADP-approach: A denotes Active, D Direct simple shear and P Passive, as determined, e.g. from laboratory tests, and where three different undrained shear strengths are used along the sliding surface.

Reliable values of pore pressure and effective stresses are of great importance for an alternative effective stress analysis based on the effective shear strength parameters, and for a new failure criterion for soft, sensitive clays. Aas and Lacasse (2021a) presented a reliable relationship between effective stress strength parameters and plasticity, illustrated in Figure 2.

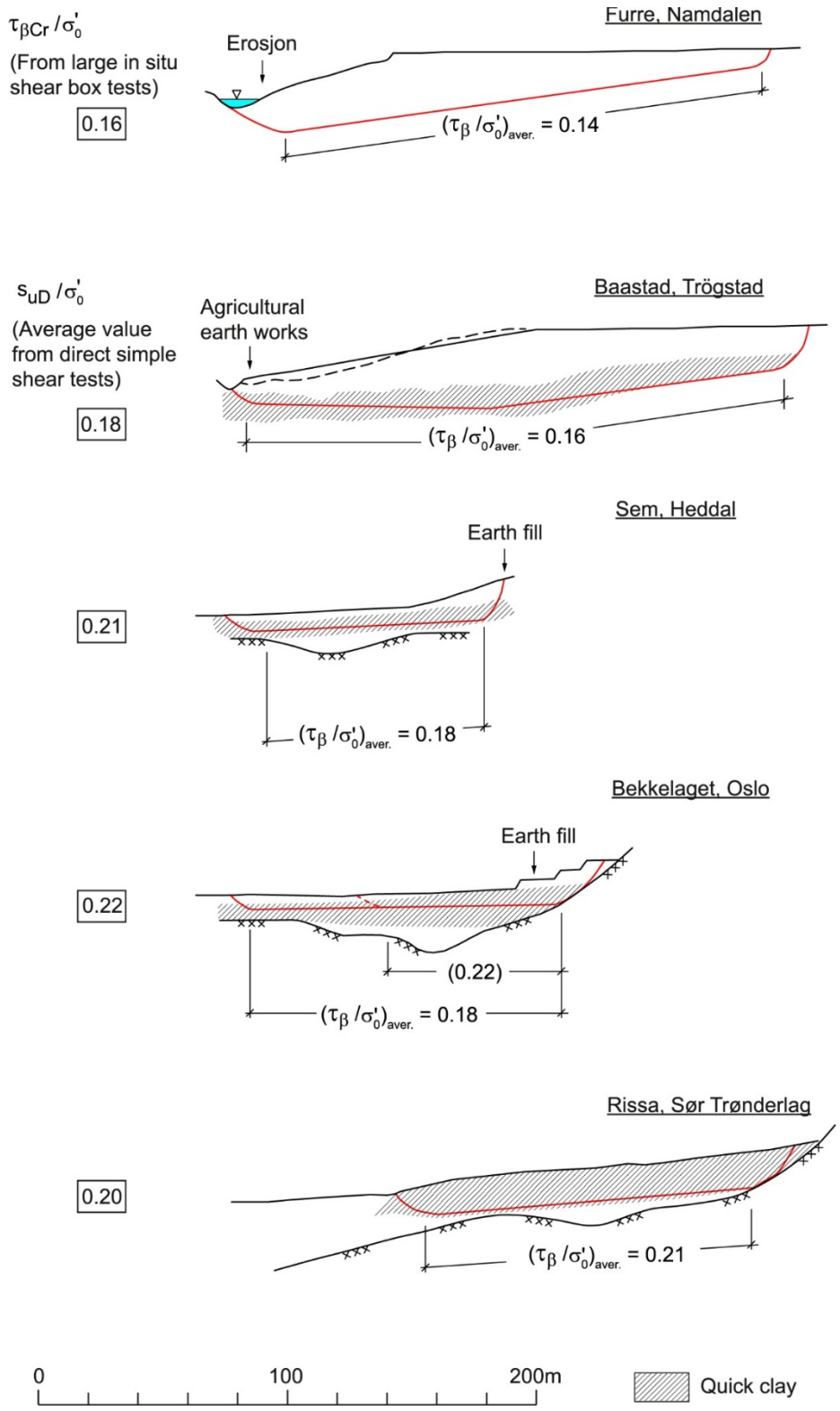

Figure 1. Comparison of calculated average shear stress acting along plane sliding surface $(\tau_\beta/\sigma'_0)_{aver.}$ and measured direct simple shear strength for five landslides in Norwegian quick clay.

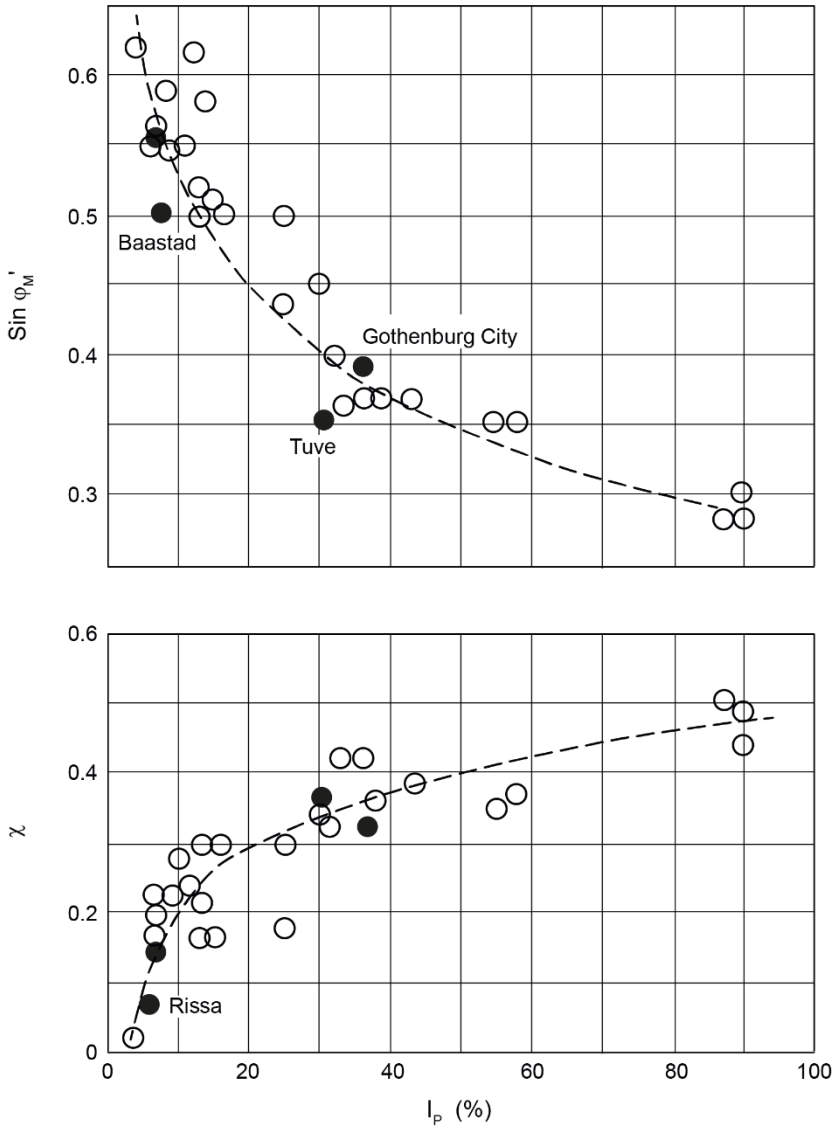

Figure 2. Relationship between effective stress strength parameters and plasticity index (Aas and Lacasse 2021a).

In this paper, an estimate was done to back-calculate the stability conditions for five older Scandinavian quick clay slides, using an effective stress analysis as mentioned above. However, a limitation of the approach is that pore pressure data are very limited or sometimes are not available. To compensate for this, one has had to investigate the relationship between calculated safety factor and assumed pore pressures, and evaluate whether the pore pressure values that lead to SF = 1.0 seem realistic. The calculations were based on effective shear strength parameters determined from the actual landslide area, or if those were missing, on data from other locations with similar clays and stresses. In the present study, information about geometric and geotechnical conditions was collected from reports and publications, and from personal communication with people with knowledge of the landslides.

Shear strength of soft, sensitive clays

In the following description, the clay considered is assumed to have been consolidated under a condition of no lateral yield. If one assumes in addition that the mobilization of friction is closely

related to the condition that plastic deformation takes place, this means that the amount of mobilized friction in the quick clay is the result of vertical stresses and strains alone. Consequently, in active shear, the mobilized friction is equal to $^1/_2\sigma'_v \cdot sin\varphi'_M$. In passive shear, decreasing vertical stress and plastic deformation make possible to mobilize friction equal to $^1/_2 K_0 \cdot \sigma'_v \cdot sin\varphi'_M$. This means full mobilization of friction due to σ'_v in active shear and in passive shear due to σ'_h (= $K_0 \cdot \sigma'_v$), using the following notation:

σ'_v	=	Effective vertical stress
φ'_M	=	Material friction angle
K_0	=	Coefficient of earth pressure at rest
σ'_h	=	Effective horizontal stress

An attempt to mobilize friction also due to the horizontal stress in active shear, or due to the vertical stress in passive shear, results in structural collapse, mobilization of high pore pressures and complete failure. For a normally consolidated clay sample reconsolidated under in situ stresses, such attempts would imply a transition from a state of uniaxial vertical strain, to a condition of large shear strains (Fig. 3), which is believed to be responsible for the structural reorganization and disturbance of the clay structure (Aas and Lacasse, 2021d).

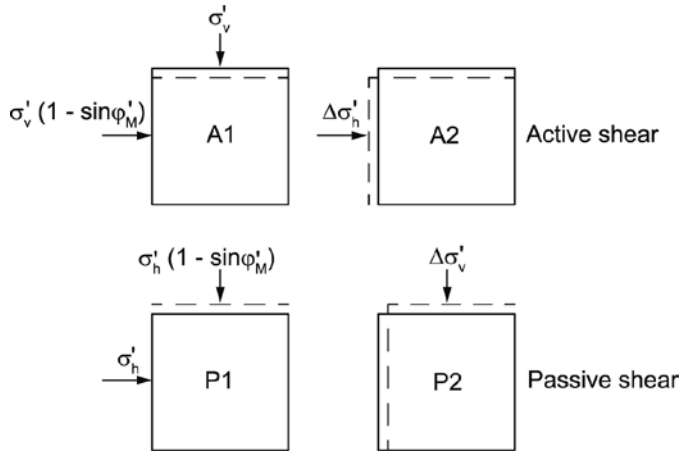

Figure 3: Transition from elastic, uniaxial strain to critical shear stress condition

Figure 4 shows examples of such dramatic failures in active undrained triaxial tests for five different clays (Aas, 1981). The clays have a plasticity index between 3 and 85% and a sensitivity between 3 and 94.
During the reloading up to failure, the increase in pore pressure equals the increase in maximal shear stress, thus confirming initially perfect elastic conditions. The major principal stresses at failure in active and passive shear equal σ'_{vE} and $\sigma'_{vE}\,(1 - sin\varphi'_M)$ respectively, where σ'_{vE} represents an equivalent effective vertical stress larger than the *in situ* stress, σ'_{vo}, and is determined by consolidation strain conditions, as for instance ageing or weathering. The minor principal stresses for a purely frictional soil is $\sigma'_{vo}(1 - sin\varphi'_M)$ and $K_0 \cdot \sigma'_{v0}(1 - sin\varphi'_M)$ in active and passive shear respectively. These values are, however, reduced with $\chi \cdot \sigma'_{v0}$ and $\chi \cdot K_0 \cdot \sigma'_{v0}$, in a clay exhibiting attraction.

The parameters φ'_M and χ denote *the material friction angle*, and the *normalized material attraction*, the term "material" indicating pure material constants, and hence are independent of

stress level, stress direction and stress history. The attraction acts like a tensile reinforcement in the clay, allowing the clay to reduce the minor principal stresses and thereby increase the shear strength prior to failure.

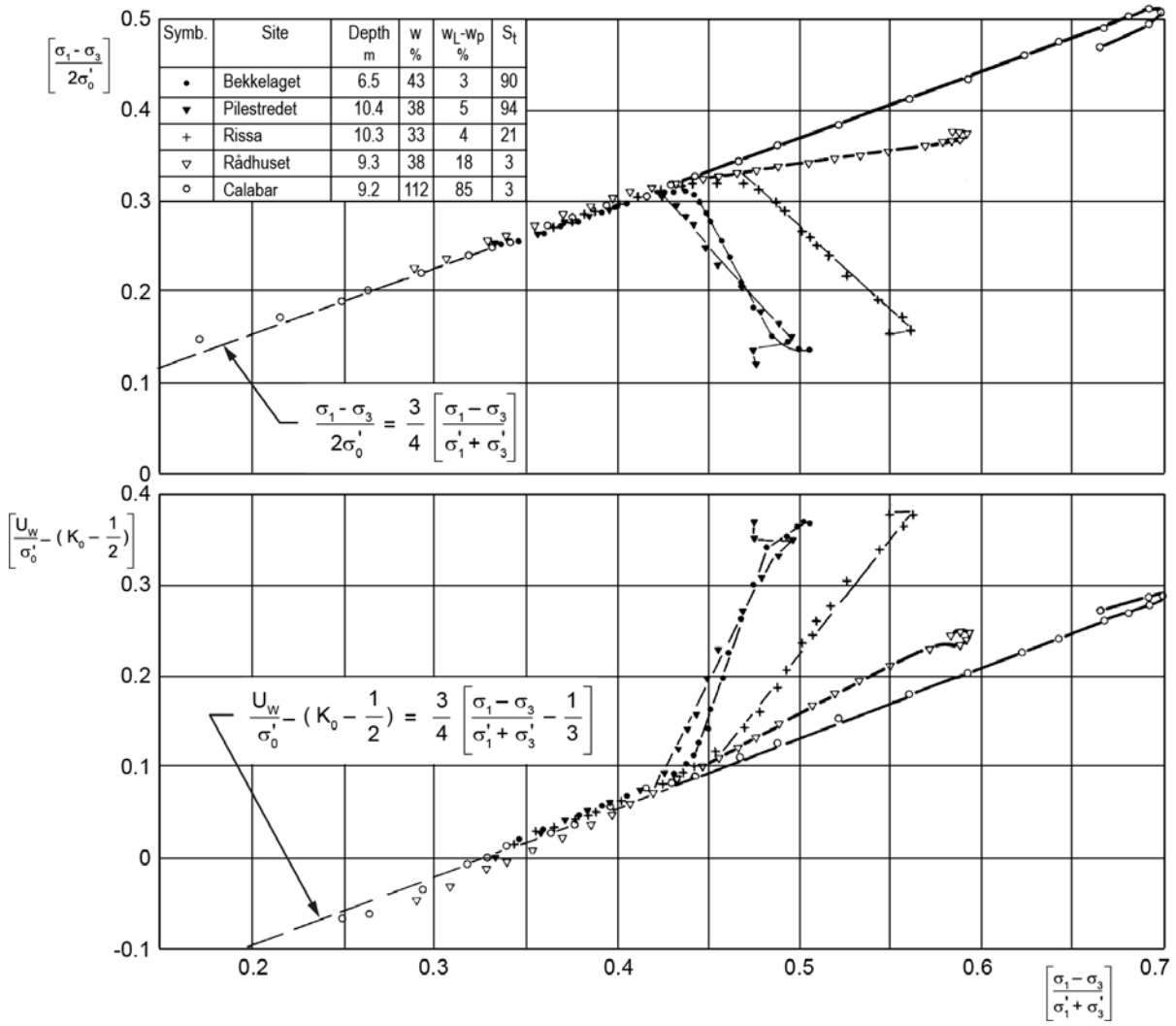

Figure 4. Results from undrained, active triaxial tests on specimens consolidated to in-situ stresses.

Combining the principal stresses outlined above leads to the following general expressions for the active, passive and direct simple shear strengths, s_{uA}, s_{uP} and s_{uD}:

$$s_{uA} = {}^1/_2\sigma'_{vo}\,[(\chi + \sin\varphi'_M) + \sigma'_{vE}/\sigma'_{vo} - 1] \quad (1)$$

$$s_{uP} = {}^1/_2\sigma'_{vo}\,[K_0\,(\chi + \sin\varphi'_M) + \sigma'_{vE}/\sigma'_{vo}\,(1 - \sin\varphi'_M) - K_0] \quad (2)$$

$$s_{uD} = {}^1/_4\sigma'_{vo}\,[(1+K_0')\,(\chi + \sin\varphi'_M) + \sigma'_{vE}/\sigma'_{vo}\,(2 - \sin\varphi'_M) - (1 + K_0] \quad (3)$$

Laboratory shear tests on quick clay close to landslide sites

Figure 5 shows the results from undrained triaxial tests on quick clay from a location close to the large Tuve landslide 1977, 10 km north of Gothenburg (NGI, 1988). Effective stress paths

from active and passive triaxial tests on specimens from 15.5 and 20 m depths made it possible to determine effective stress strength parameters of $sin\varphi'_M$ = 0.35 and χ = 0.36. Parallel tests (NGI, 1979) on a specimen in Gothenburg City gave $sin\varphi'_M$ = 0.39 and χ = 0.32 (Fig. 6). The parameters seem to vary little from one location to the other in the "Gothenburg area". For the tree Swedish clay landslides close to Gothenburg analysed below, values of $sin\varphi'_M$ of 0.36 and χ of 0.35 were used.

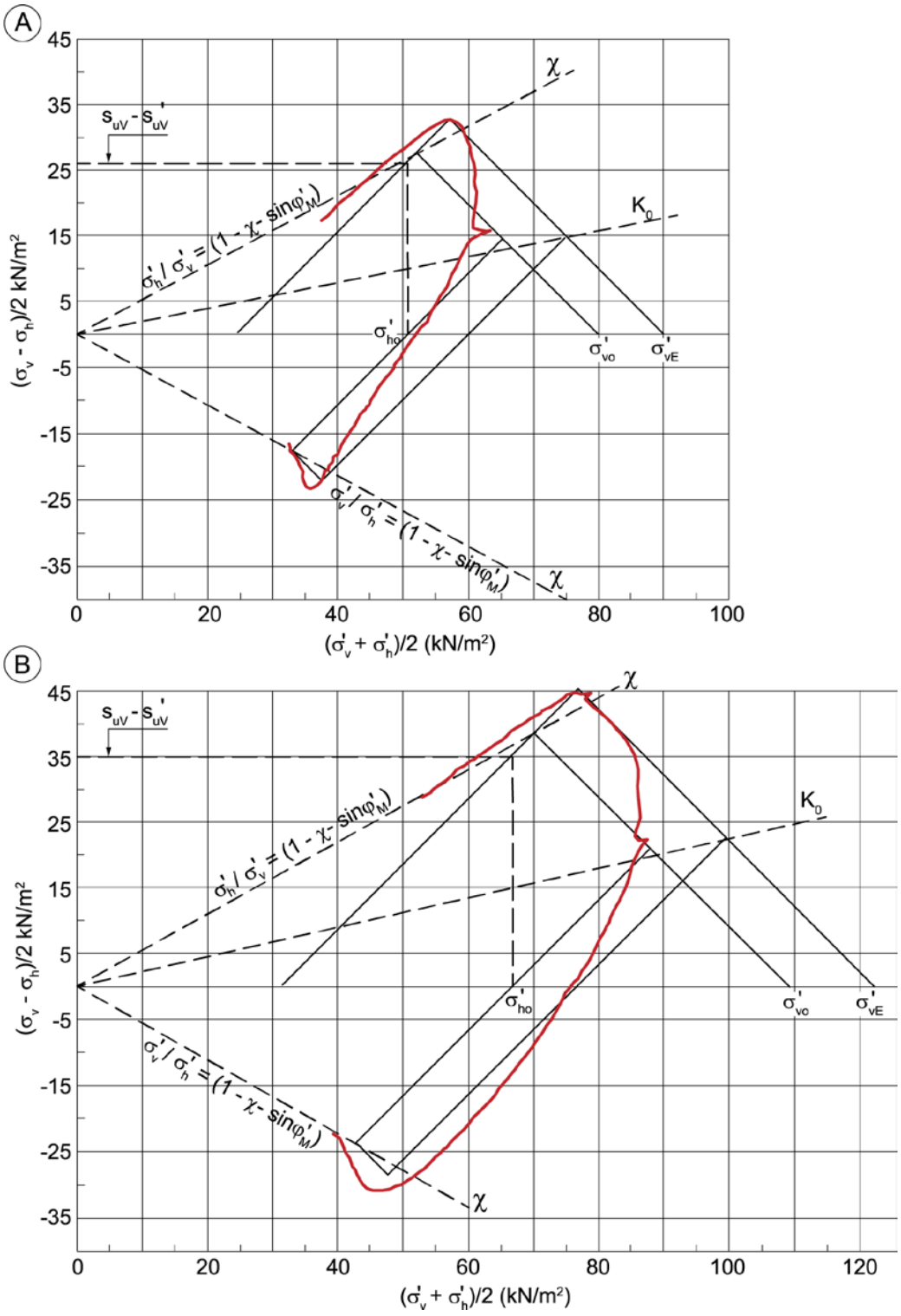

Figure 5. Results from active and passive triaxial tests on Tuve specimens from 15.5m (A) and 20m (B).

In the stress-strain diagrams, the crossing point of the two lines representing σ'_{vE} and $\sigma'_{vE}(1 - sin\varphi'_M)$ is on the "K_0-line" ($\sigma'_h/\sigma'_v = 1 - sin\varphi'_M$). This point defines the value of $sin\varphi'_M = 1 - K_0$. Similarly, the crossing point of the two lines representing σ'_{vo} and the minor principal stress in active shear is on the χ-line ($\sigma'_h/\sigma'_v = 1 - \chi - sin\varphi'_M$), thus making it possible to determine the value of χ. In the case of the Tuve clay, however, due to a certain degree of weathering, K_0 is no longer equal to $\sigma'_{vE}(1 - sin\varphi'_M)$, and has to be determined from vane shear data.

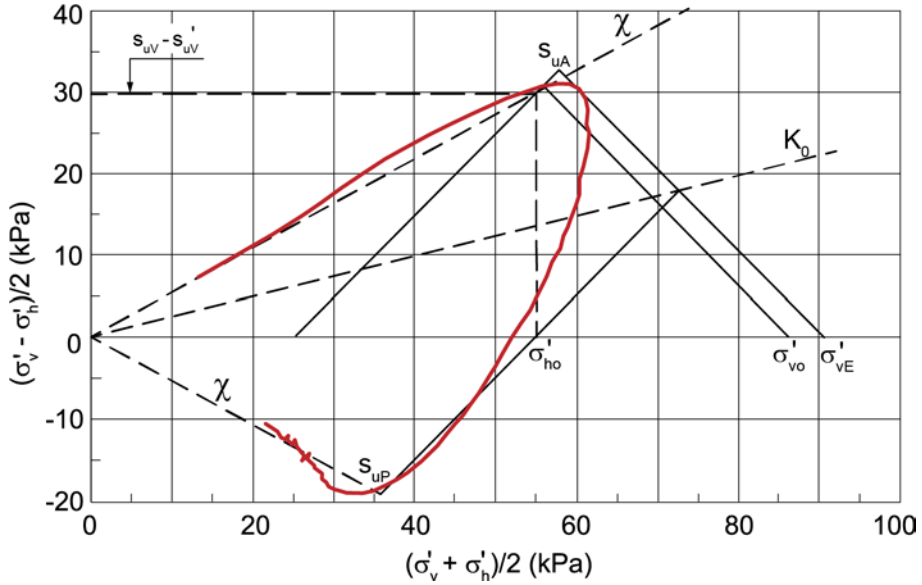

Figure 6. Results from active and passive triaxial tests on samples from 14 m depth in Gothenberg.

The same type of tests on representative clays from two older Norwegian quick clay landslides, Baastad and Rissa, suggest the values of $sin\varphi'_M = 0.50$, $\chi = 0.15$ and $sin\varphi'_M = 0.55$, $\chi = 0.06$, respectively (Figs 7 and 8).

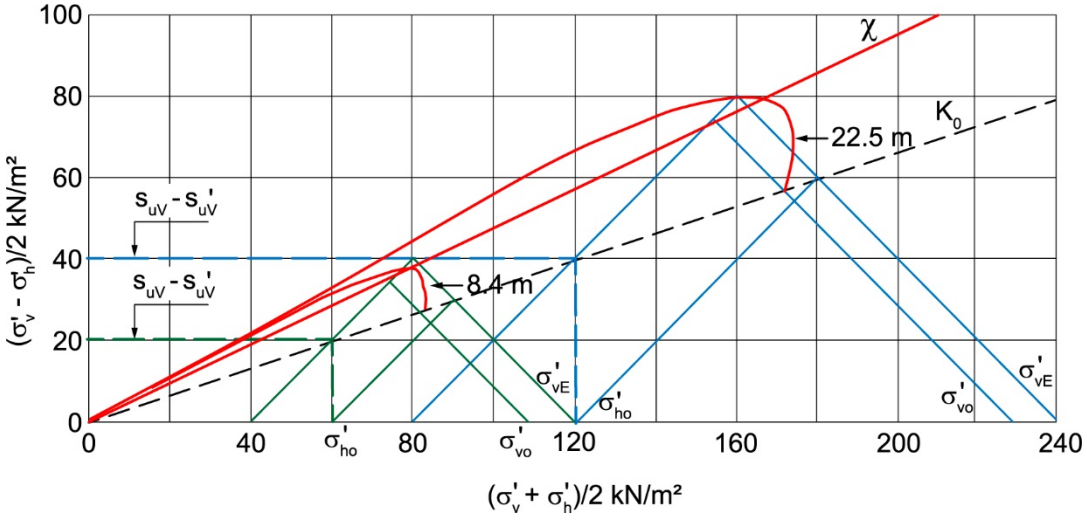

Figure 7. Results from active triaxial tests on specimens 8.4 and 22.5m depth at Baastad.

Typically for soft, quick Norwegian clays, and contrarily to Swedish clays, the effective stress path from passive tests does not give a sufficiently accurate peak value to determine K_0. Aas *et al*., 1986) demonstrated though that through a combination of in situ vane boring and active triaxial test results, one can determine the K_0-parameter with a construction as done on Figures

7 to 9. Figure 6 give examples showing that the use of both methods leads to the same result.

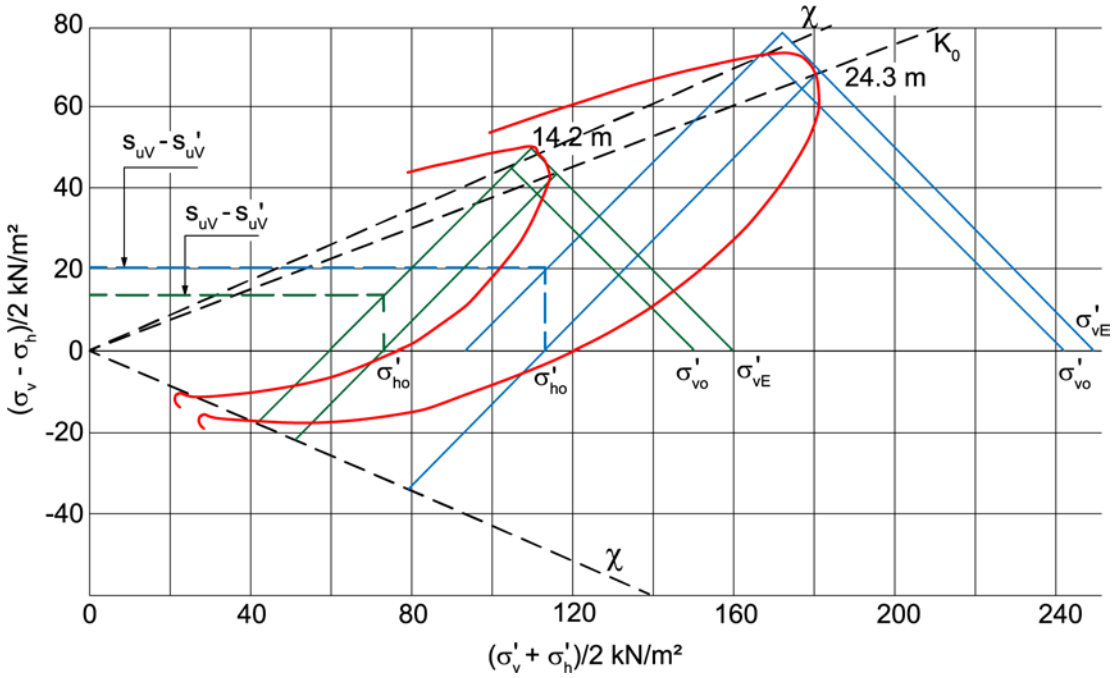

Figure 8. Results from active and passive triaxial tests on specimens from 14.2 and 24.3 m at Rissa

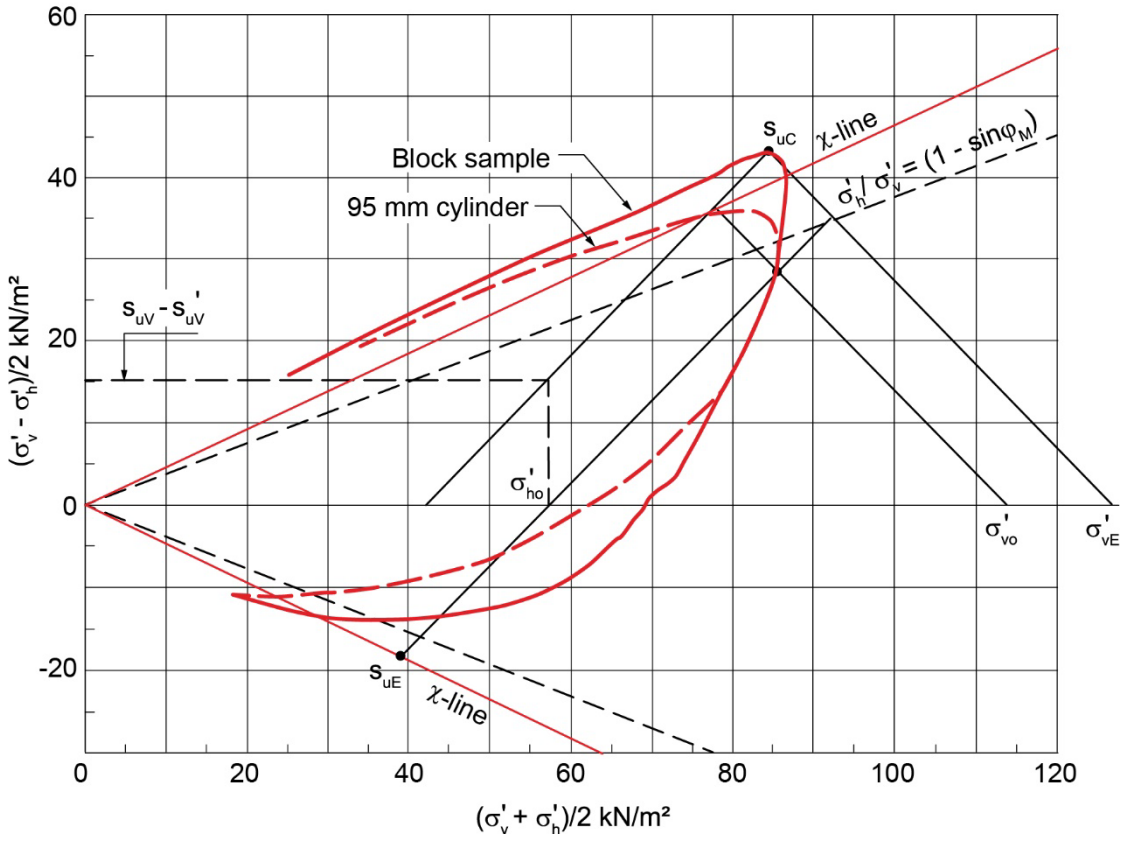

Figure 9. Results from active and passive triaxial tests on samples from 10.2m in Drammen.

The values of the parameters $sin\varphi'_M$ and χ used in the stability analysis are shown as a function of the plasticity index of each clays in Figure 1.

Figure 9 shows the test results for a quick clay sampled at 10.2m in Drammen City. The test program included both block sampling and sampling with a 95-mm piston cylinder. In Figures 5 to 9, s_{uv} and s_{uv}' denote undisturbed and remoulded field vane strength. This is due to the disturbance related to the use of piston sampler in this extremely quick clay almost nullifies the effect of ageing, appearing in the test on the block sample. This disturbance results in a reduction in $sin\varphi'_M$ (from 0.55 to 0.51) and an increase in χ (from 0.08 to 0.12). However, from a practical point of view, it is important to recognize that the sum of the two parameters (Aas and Lacasse 2021a) is almost not affected by sampling disturbance.

Stability analysis

Stability analyses were performed for two Norwegian and three Swedish flake type landslides. A simplified model was used, including an active earth pressure at the landslide rear scarp, a passive earth pressure at the front of the landslide, and a sliding body in between.

Active pressure:	$P_a = \gamma D^2/2 - 2s_{uA}/\sigma'_{vo}\,(\gamma' D - 10x)D/2$	(4)
Passive pressure:	$P_p = \gamma D^2/2 + 2s_{uP}/\sigma'_{vo}\,(\gamma' D - 10x)D/2$	
Sliding body:	$P_\beta = \gamma DL \cdot sin\beta$	
Mobilized shear strength:	$P_s = (\gamma' D - 10x)\, L\, s_{u\beta}/\sigma'_{vo}$	
Safety factor	$F = P_s/(P_a + P_\beta - P_P)$	(5)

where γ and γ' denote total and submerged unit weight, D depth down to the sliding surface, L length of the sliding body, and β the inclination of the failure surface. For the Swedish clays, a total unit weight of 16 kPa/m^3 was assumed, whereas for the Norwegian clays, a total unit weight of 19 kPa/m^3 was used at Rissa and 20 kPa/m^3 at Baastad. The term "x" in the equations expresses the piezometric elevation in meters above the ground surface in the failure plane.

Isostatic uplift and erosion have caused increasing shear stresses and increased pore pressures and water flow in the clay deposits. This has led to a washing out of salt in the pore water, making the clay "quick", and causing a strain-softening. This process is still in progress today. Therefore, it is reasonable to believe that the clay does not have significant ageing, and can be considered as "young" and almost normally consolidated. For the stability analyses, the ratio $\sigma'_{vE}/\sigma'_{vo}$ was assumed equal to 1.1 and 1.05 for the Swedish and Norwegian clays, respectively, in Eqs (1) to (3), based on the results of the triaxial tests. The shear strength on a gently dipping (β degrees) failure plane is given by the formula:

$$s_{u\beta} = s_{uA} \cdot cos^2(\beta - 45^o) + s_{uP} \cdot sin^2(\beta - 45^o) \quad (6)$$

Since s_{uA} and s_{uP} are expressed in terms of effective stresses, one in reality performs an effective stress analysis, which makes it simple to consider the effect of pore pressures in the calculations.

The formation of quick clay is often tied to percolating water through a layer of marine clay. Therefore, it is reasonable to assume that artesian pore pressures may be a primary contributing factor leading to the occurrence of quick clay slides. Pore pressures usually increase with depth,

with a value of zero at the groundwater surface and increase with depth to a maximum value in permeable soils at the bottom of the deposit or in permeable rock below. The magnitude of the pore pressures in quick clay generally increase gradually over the course of a very long period of time. They are generally only slightly affected by short periods of heavy rain. This means that the natural slopes studied in this paper may have been on the brink of failure for many years. In general, most quick clay slides are triggered by a moderate reduction in the stability of the slope due to small earth works, pile driving, erosion or similar events.

Based on this reasoning, stability calculations can be performed as an effective stress analysis using the known effective strength parameters χ and $sin\varphi'_M$ together with a failure criterion for soft contracting clays. This will give a relationship between theoretical safety factor and average artesian water pressure along the failure surface. In the quick clay landslide examples reported below, where pore pressures records are often missing, the calculations had the purpose to estimate the existing pore pressures conditions that were necessary to obtain a safety factor of 1.0, and then evaluate how realistic the pore pressures were.

Stability analyses for five landslides

The 1974 Baastad landslide, Norway

The landslide took place on 5 December 1974 and involved about 1.5 million m^3 of soil (Gregersen and Løken, 1978). The landslide area covered about 80.000 m^2 of farmland. The debris extended over another 45.000 m^2 of the downstream valley bottom. The slide terminated near the dwellings on two farms. About 10 individuals were on the farms at the time of the landslide, but fortunately no lives were lost. Nobody actually witnessed the landslide. According to the persons on the farms, the landslide occurred very fast, probably within one minute or less.

The sliding masses at Baastad consisted of a non-sensitive clay. The clay was fairly homogeneous down to 16 m, and contained layers of sand and silt at greater depths. A quick clay layer of considerable thickness (20 m or more) was found at 21 m. The water content of the quick clay was about 28%, the plastic limit, w_P, 13% and liquid limit, w_L, 20%.

Stability analyses were carried out for a profile in the centre of the landslide. The initial depths to the sliding surface, 22 m in the active zone and 12 m in the passive zone (Fig. 10) were determined with vane borings and sampling trough the slide masses. The inclination of the failure surface under the block in between, was 4.9°. The calculated safety factor was 1.22 if one assumed hydrostatic pore pressures with groundwater level at ground surface, and 1.0 if one assumed the water rising 1.2 m above the ground surface.

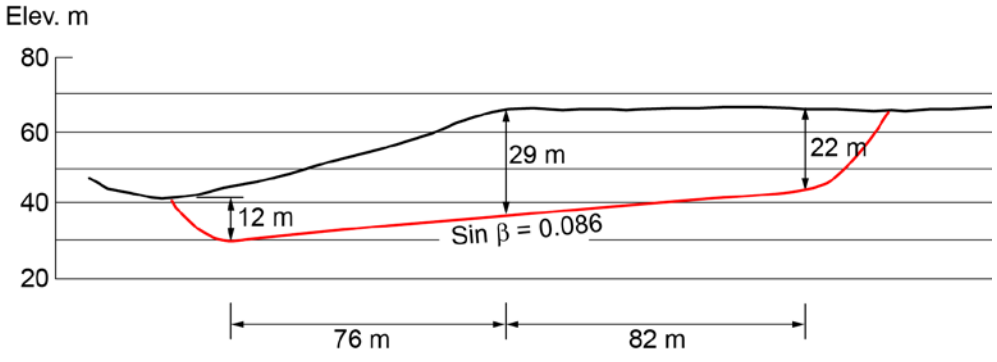

Figure 10. The Baastad landslide.

The 1978 Rissa landslide, Norway

The Rissa landslide happened on 29 April 1978 and involved an area of about 333.000 m^2 and 5 to 6 million m^3 quick clay (Gregersen, 1981). The main part of the landslide slid out in the course of 5 minutes. The sliding area damaged seven farms and five dwellings, either taken by the slide or condemned from safety reasons. About 40 persons were present in the area, and one live was lost. After initial, smaller, progressive slides, the main landslide started, resulting in an extensive disaster! An area 250 m in width (normal to the sliding direction) and 150 m long slid out as a monolithic block, downwards, into Lake Botnen. The major part of the landslide, analysed below, was assumed to have been only slightly influenced by the initial slides. The slope was considered to have been standing with a safety factor close to one prior to the landslide.

A boring just behind the slide showed quick clay down to 15 to 20 m. The clay had a natural water content of 30 to 35%, a liquid limit of about 20 to 25% and a plastic limit of 17%. New site investigations at the site in 2009 (NGI, 2009; Liu *et al*., 2021) confirmed a water content of 35%, a plasticity index less than 10% and an overconsolidation ratio of about 1.4. An artesian pore pressure of 10 kPa (1 m) was measured close to Lake Botnen, just south of the Rissa landslide. At the top of the slope, it was estimated that the porewater pressures were either hydrostatic or slightly below hydrostatic.

In front of the slide (Fig. 11), the sliding mass met stiffer clay, and ended up in a 8 m deep passive zone. Between this passive zone and the 12 m deep active zone in the back of the slide, a 127-m long block of quick clay was sliding along a shear plane dipping 5.0°. The calculated safety factor was 1.33 for groundwater at the ground surface. The factor of safety reduced 1.0 for pore pressures corresponded to the groundwater 1.9 m above ground surface.

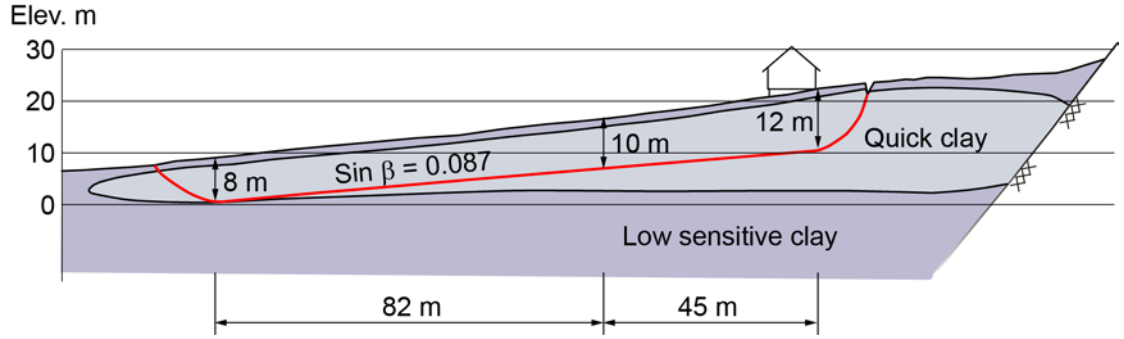

Figure 11. The Rissa landslide

The 1950 Surte landslide, Sweden

The Surte landslide that took place on 29 September 1950 was located in a village about 15 km upstream of Gothenburg (Jacobsson and Mohren, 1952). The area that slid out had a width of about 400 m, parallel to the river, a total length of about 600 m, and a volume estimated at 4 million m^3. Thirty one domestic houses and about 10 outhouses were swept 50 − 150 m down towards the Göta River. Three hundred persons became homeless, and one elderly woman died.

The river bank had practically no height, and the terrain was practically horizontal within 200 m from the river. The landslide lasted for 2-3 minutes, and during that time the clay masses

raised the bottom of the river several meters, blocking the river and impeding shipping.

The sliding masses consisted of clay containing several thinner layers of more permeable material. Samples from the back part of the slide showed a thick layer of quick clay with the following properties: sensitivity 50 – 100, a plastic limit of 25 – 30%, a liquid limit of 50 – 55%, and a natural water content of about 70%. Artesian pore pressures corresponding to a water rise above terrain of 6 – 7 m in the sliding masses and 3 – 4 m just outside the edge of the landslide were recorded.

Stability analysis were done for three cases, including a 100-m long part of the total slide, which was extending further about 300 m out to the river (Fig. 12). The most critical case gave a safety factor 2.7, if assuming pore pressures corresponding to a water rise to terrain, and 1.0, for a water rise 4.0 m above terrain. This alternative included depths in active and passive zone 12 and 14 m, leading to an sliding surface inclination of 5.7°. A five meter deeper shear surface gave corresponding values: safety factor of 2.8 and water level rise 5.2 m above terrain, respectively.

It should be emphasized that the stability analysis included a length of about only 100 m of the total slide. If the analysis included the 300 m of land extending to the river, the calculated safety factors was considerably higher. The mechanism of failure in this outer zone is discussed below.

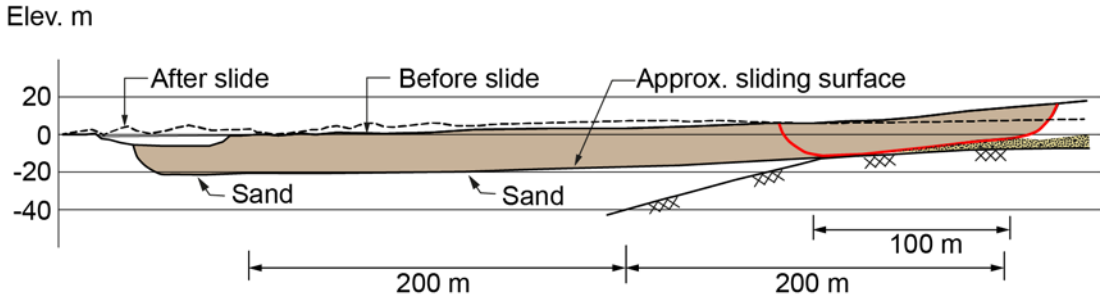

Figure 12. The Surte landslide

The 1957 Göta landslide, Sweden

The first sign of instability on 7 June 1957 was a 130-m long crack in the ground just inside the river bank, which was observed about three hours before the landslide rapidly expanded to 200 to 300 m inland from the Göta River shore (Odenstad, 1958). The river bank was displaced up to 60 − 70 m towards the river, and the ground surface sank down 7 to 8 m within the slide area. A pulp-mill, located where the slide started, was totally destroyed. Of the 200 persons working in the factory area, three lost their lives. Shipping on the Göta River was suspended for a month. Prior to the landslide, the depth of the river seemed to have been 10−12 m.

Based on borings in the upper part and upstream of the sliding area, the soil profile was sensitive and quick clay, with a plastic limit 25 to 30%, a liquid limit 50 to 60%, and a natural water content of about 75%.

Stability analyses were carried out for two profiles (Fig. 13) oriented normally to the Göta River. One profile passed through the factory area, where the slide was initiated by a local failure in the river bank. The other profile extended through an area located upstream of the factory, where

the clay seemed to have been sliding toward the river as a whole flake. The terrain at Göta River consisted of a steep river bank, followed by an almost horizontal terrace extending several hundred meters from the Göta River.

The slide that destroyed the factory, had a total length of about 280 m, a depth to the sliding surface of 5 and 10 m in the active and passive zones, a maximum depth of 22 m, and an inclination of the 266 m long sliding surface equal to 6.1°. The calculated safety factor was 2.2 for pore pressures at the sliding surface rising to terrain, and 1.0 if the pore pressures corresponded to 4.3 m above ground level.

The upstream slide had a total length of about 230 m, a depth to the sliding surface 3 and 6 m in the active and passive zone, and a maximum depth of 20 m. The inclination of the sliding surface was 6.9° in the upper 134 m and 1.2° in the lower 86 m of the sliding surface. The calculated safety factor was 2.4 for the case where pore pressures corresponded to a water rise up to ground level, and 1.0 if 4.3 m above ground level.

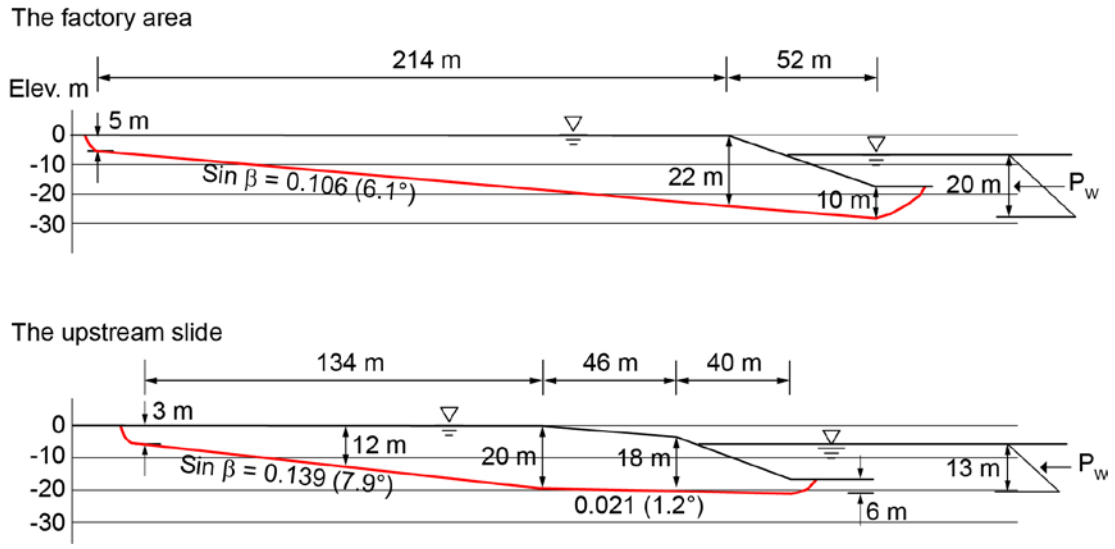

Figure 13. The Göta landslide.

The 1977 Tuve Slide, Sweden

An initial slide occurred suddenly on 30 November 1977 (Larsson and Jansson, 1982). Within about five minutes, the appearance of an area of 270.000 m^2 changed completely. As a consequence of the slide, 65 domestic houses were completely destroyed, and another 84 houses condemned for safety reasons. Nine peoples died from injuries caused by the landslide. Fortunately, most of the people who lived in the area, were absent on the afternoon when the disaster took place.

Most of the borings recorded from Swedish sources (SGI, Swedish Geotechnical Institute) were performed in the slide area, and give results with considerable variations and uncertainty. This made it difficult to choose reliable shear strength parameters from the data for a stability analysis of the landslide. However, in the spring of 1979, NGI received a series of undisturbed cylinder samples for research on the Tuve clay (NGI, 1979). The samples, from a depth interval between 15 and 20 m, were taken at a location well outside the slide area. They gave the following

approximate results with small variations: plastic limit = 35%, liquid limit = 65% , natural water content = 70%, and unit weight = 16 kN/m^3. Furthermore, active and passive triaxial tests on specimens between 15.5 and 20 m provided a set of effective stress strength parameters χ and $sin\varphi'_M$, as described above.

A few alternative stability analyses were carried out for the Tuve landslide which had a total length of approximately 220 m long. This study consisted of the 180 m segment between the active and passive zones with an inclination of 6°. The depths to the sliding surface were 11 m at the active zone and 19 m at the passive zone. The calculated factors of safety were equal to 3.2 if the pore pressures were assumed to correspond to a piezometric elevation up to ground level, and 1.0 if the piezometric elevation was 5.3 m above ground level. The calculated artesian pressures were assumed to be average values for the entire sliding surface.

As for the Surte landslide, the total slide length at Tuve also extended over a long distance, namely 120 m in front of the 180 m long part included in the stability analysis. If one combines these areas in a conventional stability calculation, this would require unreasonably high pore pressures to yield a safety factor equal to 1.0. Nevertheless, both zones took part in the slide, and there must be an explanation for the failure.

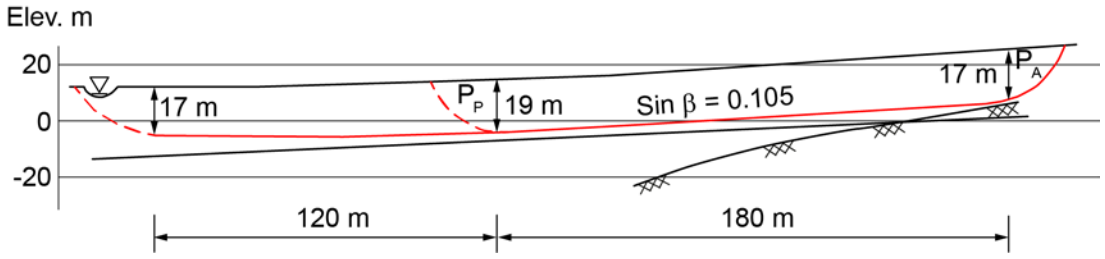

Figure 14. The Tuve landslide.

Typical for the Surte and Tuve landslides, the secondary parts of the sliding consisted of a block with almost constant height, and a constant capacity with respect to resisting a passive earth pressure. As a result of isostatic land uplift and erosion over thousands of years, this clay block had undergone a decreasing vertical effective stress under conditions of no lateral yield. This is exactly the way a clay specimen is brought to failure in a passive triaxial test, indicating that the clay in the sliding block was exposed to a pure passive shear involving no shear stress acting on the vertical and horizontal planes. Hence, the explanation for the failure might be that before the slide started, this block ensured the stability of the area behind, such that mobilization of shear strength under the block was not necessary. Under such circumstances, this lower part of the slide would act as a compression member and then fail as a house of cards at the same time as the area above.

Discussion of stability calculations

The two Norwegian slides at Baastad and Risa show safety factors of 1.0 for pore pressures corresponding to a piezometric level of 1.2 and 1.9 m above terrain, respectively. However, the reality of the calculated pore pressures is encumbered with an obvious uncertainty. As pointed out by Bjerrum et al. (1969), the downward percolation of surface water is usually negligible with respect to formation of quick clay. The leaching of salt water that transforms the clay to quick clay is, in almost all known cases, caused by an upward flow of fresh groundwater,

originating from deeper permeable layers or bedrock below. Although reliable pore pressure measurements are limited at these two locations, the magnitude of the calculated pore pressures needed to provide a safety factor of 1.0 are reasonable, if one takes into consideration the precision of the performed calculations.

The landslides at Göta show safety factors of approximately 1.0 assuming the pore pressure at failure corresponds to a water level 4.3 m above the ground surface. The most critical example at Tuve shows a safety factor of about 1.0 assuming that the pore pressure at failure corresponds to a water level 5.3 m above the ground surface. For the landslide at Surte, the calculated safety factor is 1.0 if the water level rises to 4.0 m above ground surface.

To verify the whether or not an artesian pore pressures of 40 to 53 kPa was possible in the Gothenburg valley, samples were taken in the sampling location in Gothenburg City, and artesian pressures of 50 to 70 kPa were measured at depth of about 25 m. At this location, the terrain level was 18 to 22 m above sea level. The depth to the groundwater table was about 2 m, and the observed artesian pore pressure increased steadily with depth. Persson *et al*. (2011) also reported measurements of up to 7 m artesian water pressures at locations in the southern part of the Göta River valley. At Tuve, very high artesian pressures were measured in the slide area (Berntsson and Lindt, 1981). However, the values of the pore pressures prior to the slide are uncertain. Alte *et al.* (1989) presented recorded artesian pressures of 90 to 100 kPa down to 60 m depth at a test site in Gothenburg.

Even with only these limited actual measurements, it is the authors' opinion that the measured pore pressure are reliable and that the magnitude of the pore pressures derived to obtain factors of safety of unity in the landslide case studies are realistic. One limitation in the analyses is that the expected most realistic slip surface was analysed. It may not be the absolute most critical sliding surface. Therefore, the calculated artesian pore pressures may be overestimated.

According to Swedish experts, high artesian pore pressures are believed to have played an important role in triggering the Swedish landslides. In addition, kinetic energy, due to the moving soil mass during the first part of the slide, has been assumed, for instance by Lundstrøm, (1981), to be the only possible explanation for the failure in the almost horizontal, lower part of the Surte and Tuve landslides. This explanation assumes that there must have been a certain time interval between the two main parts of the slide. However, there were no observations that could confirm this assumption.

The relation between pore pressures and calculated safety factors in the five case studies show the importance, even the necessity, of pore pressure measurements for the assessment of the stability of quick clay slopes. It is reasonable to believe that landslides like those reported in this paper occur at locations where non-hydrostatic pore pressures conditions exist. The authors consider that ignoring pore pressure measurements and doing stability calculations using hydrostatic porewater pressures from the groundwater can lead to catastrophic slope failures.

Conclusions

The paper presents the relationship between the normalized undrained shear strength parameters used in the ADP analysis and the effective stress strength parameters, friction and attraction. This makes it possible to include pore pressure in an effective stress stability analysis, as a more realistic alternative to the ADP analysis. In a quick clay, however, the failure criteria will differ from the conventional Mohr Coulomb failure criterion, because only the vertical stress

contributes to friction in active shear, and only the horizontal stress contributes in passive shear.

A good reason for applying an effective stress analysis especially for flake slides is that they often occur in clay slopes which can have existed nearly unchanged for very long periods of time, and then suddenly fail almost for no apparent reason. Consequently, the effective shear strength parameters are fully mobilized, and the magnitude of effective stresses at failure are determined by the *in situ* pore pressures. Effectively, one then performs a drained analysis, with increasing reliability as the calculated value of SF approaches 1.0.

Based on undrained triaxial tests on clay samples from two locations in the Göta River area in Sweden, the approximate representative values of $sin\varphi'_M$ and χ are both equal to 0.35. For Norwegian quick clays from two different locations $sin\varphi'_M$ and χ were found to be respectively 0.49 and 0.18 at one location 0.55 and 0.08 at the other site. These effective stress parameters were used in an effective stress stability analysis for two Norwegian and three Swedish quick clay landslides. These five slides were 40 to 67 years old. Therefore, geotechnical data are sparse, and pore pressure conditions prior to the slides are not well known. Consequently, somewhat approximate factor of safety calculations were carried out. The main objective of the study was to investigate the magnitude of the pore pressures needed to give a safety factor of unity for each landslide, and to discuss the realis of these pore pressures at each site.

The two Norwegian landslides at Baastad and Rissa required an artesian pressure, expressed as the rise in the groundwater level above ground level, of 1.5 and 1.8 m.

Corresponding values for the Swedish landslides, Gøta, Tuve and Surte, was found to be 3.6, 5.3, and 3.9, respectively. Since the occurrence of quick clay, in almost in all known cases, is a result of streaming ground water and increasing artesian pore pressure with depth, the values for the Norwegian landslides seem realistic. Due to lack of actual data, the values calculated for the Swedish slides are difficult to evaluate. However, measured artesian pore pressures of 50 – 70 kPa at a location in Gothenburg City, and reported artesian pressures up to 70 kPa in the southern part of the Göta River valley support the hypothesis of rather large artesian pore pressures at the location of the three landslides.

The slides at Surte and Tuve extended a long distance in front of the part included in the stability analysis. If these areas, if the stability analysis were run in a conventional way (i.e. based on solely the undrained shear strength), this would require unrealistic high pore pressures to explain a safety factor equal to 1.0. In this respect, a theory put forward is that the front parts of the landslide, because of a historic vertical unloading and horizontal loading under conditions of no lateral yield, have been brought into a condition of pure passive shear involving no shear stress acting on the horizontal and vertical planes. Under such circumstances, the clay blocks would act as compression members and fail like a card house simultaneously with the upper part of the slide.

Pore pressures have a dominating influence on calculated safety factors, especially in an effective stress analysis. Likewise, in order to have full control on effective stresses in an ADP analysis, one cannot neglect the pore pressures. Consequently, piezometer installations or pore pressure measurements (e.g. with the piezocone) should be included in all site investigations where quick clay is found.

In closing, it is appropriate to quote the last sentence in Bent Jacobsson's (1952) comprehensive paper on the landslide at Surte:

"The main conclusions to be drawn from the [Surte] slide are that a small slide can under certain conditions grow to a great extent, and that we have to take the pore water pressure into consideration in a greater degree than hitherto".

References

Aas, G. (1981). Stability of natural slopes in quick clays. Proc. Int. Conf. Soil Mech. Found. Eng. 11th ICSMFE, Stockholm, 1981, Proc. **3**: 333−339.

Aas, G., Lacasse, S., Lunne, T. and Høeg. K. (1986). Use of in Situ Tests for Foundation Design on Clay. ASCE. Conf. in Situ 86 Blacksburg, Virginia, USA, 1986, pp. 1−30.

Aas, G. and Lacasse, S. (2021a). Shear Strength of Soft Clay Expressed in Terms of Effective stresses. 1st paper in this publication.

Aas, G. and Lacasse, S. (2021b). Undrained Shear Strength of Overconsolidated Clays. 4th paper in this publication.

Alte B., Olsson, T., Sällfors, G. and Bergsten, H, (1989). *Djupdykking i Gøteborgleran.* Study of the Gothenburg clay Geological-geotechnical study of clay from great depths in kv. Guldet. Chalmers University of Technology, Gothenburg *(In Swedish).*

Berntsson, J. and Lindt G.B: (1981). *Analys av orsaken till Tuveskredets utbilning* (Analysis of the cause of the Tuve Landslide). SGI Rapport No 10 *(in Swedish).*

Berre, T. (1987). Triaxial and unconfined compression tests on lean Drammen clay with OCR = 40. Norwegian Geotechnical Institute, Oslo. Internal report 56105-01. 1987-06-17, 27 pp.

Bjerrum, L., Løken, T., Heiberg, S. and Foster, R. (1969). A field study of factors responsible for quick clay slides. Proc. Int. Conf. Soil Mech. Found. Eng. 7. Mexico, **2**: 531−540.

Bjerrum, L. (1973). Problems of soil mechanics and construction on soft clays. SOA report. International Conference on Soil Mechanics and Foundation Engineering, 8. Moscow 1973. Proc. **3**: 111−159.

Gregersen O. and Løken, T. (1979). The quick-clay slide at Baastad, Norway, 1974. *Engineering Geology.* **14** (2/3): 183−196.

Gregersen O. (1981). The quick clay landslide in Rissa, Norway; the sliding process and discussion of failure modes. roc. Int. Conf. Soil Mech. Found. Eng. 11. ICSMFE, Stockholm, 1981. **3**: 421−426.

Jacobsson, B. and Mohren E. (1952). The Landslide at Surte on the Gøta River September 29. 1950. Statens geotekniska institut (SGI). 5, p. 120.

Ladd, C.C. and Foott, R. (1974). New design procedure for stability of soft clays. American Society of Civil Engineers. *JGED*. **100**(GT7): 763−786.

Larsson R. and Jansson, M. (1982). The landslide at Tuve. November 30. 1977. SGI Rapport No 18.

Liu, Z.Q, L'Heureux, J.S., Glimsdal, S. and Lacasse, S. (2021). Modelling of mobility of Rissa landslide and following tsunami. *Computers and Geotechnics*. Scott Sloan Memorial Issue (in print).

Lundstrøm R. (1981). *Synspunkter på Tuveskredets utvecling innom passiva zonen* (Reflections on the development of the Tuve Landslide in the passive zone). SGI Rapport No 10 *(in Swedish)*.

NGI (1979). *Undersøkelse av prøver fra Tuveskredet, Göteborg. Skredfare og arealplanlegging.* (Laboratory investigations on clay from the Tuve slide). Norwegian Geotechnical Institute. Internal Report 52206-1, Oslo. (G. Aas 01.01 1979). Lecture NIF course. Ullensvang, Hardanger. (unpublished data, in Norwegian).

NGI (1988). Stability investigations at St. Jørgens Sjukhus, Gothenburg. Norwegian Geotechnical Institute. Internal Report 87058-01, Oslo. 22 January 1988. 49 pp.

NGI (2009). *Rv 717 Sund-Bradden–Tolking av grunnundersøkelser, karakteristiske materialparametere* (Interpretation of the soil investigations and design parameters on RV 717 Sund-Bradden). Norwegian Geotechnical Institute. Report 2009 1284-00-38-R. Trondheim. (E.Enlid/A.K. Lund) 2009-09-18. 132pp. (in Norwegian).

Odenstad, S. (1958). Jordskredet i Göta den 7. juni 1957 (The landslide in Göta, 7 June 1957). Geologiska føreningen i Stockholm. Førhandlingar Nr. 492. **80**(1): 76−86 *(in Swedish).*

Persson, H., Bengtsson, P.E., Lundstrøm, K. and Karlsson, P. (2011). Bedømning av grunnvatten-førhollanden før slenter langs Göta ælv. (Evaluation of the groundwater level before the sliding along the Göta River). GAU delrapport 7, Lindkøping *(in Swedish).*

YIELD STRESSES IN SOFT CONTRACTING CLAYS

Gunnar Aas[1] and Suzanne Lacasse[2]
[1]formerly Norwegian Geotechnical Institute (NGI); [2]NGI

Abstract

The undrained shear strength s_u along an arbitrary failure plane can be expressed as:

$$s_u = {}^1\!/_2(\sigma'_{ULS} - \sigma'_{LLS}) \quad (1)$$

where σ'_{ULS} and σ'_{LLS} denote the upper (U) and lower (L) effective, normal, compressive failure stresses acting at angles of +45 and −45° with the failure plane. These limiting stresses represent values that cannot be exceeded without yield occurring. In this paper, a study was done to investigate how the friction and attraction are mobilised by the plastic and elastic deformations to which the clay has been subjected. It is then possible to express undrained shear strength as a function of the consolidation stresses and two effective stress-strength parameters, the relative material attraction χ, and the effective material friction angle, $sin\varphi'_M$. The proposed theory forms the basis for constructing so-called yield envelopes for a clay, based on these strength parameters.

Introduction

It is well known today that active, undrained shear tests on soft clay undergo extremely small strains up to a certain stress level. This stress level represents a critical state that involves a transition from small elastic to large plastic strains. When exceeding this critical stress, the clay develops high pore pressures, a structural collapse and reduced strength. Such critical stress was found to be far less pronounced in passive undrained shear than in active undrained shear, where maximum shear resistance can appear at a deformation of several percent. The idea of the existence of such limiting or yield stresses has been discussed by several researchers before, for instance, Schofield and Wroth, 1968; Mitchell, 1970; Tavenas and Leroueil, 1977; Wood, 1980; Wroth and Houlsby, 1980; Graham and Houlsby, 1983; and Lau *et al.*, 1988 Many have presented so-called "yield envelopes", which define critical combinations of shear stress and normal effective stress under active and passive shear. These envelopes may be constructed on the basis of stress paths determined in undrained or drained triaxial and plane strain tests. The points on the yield envelope are defined as the start of increased strain rates in drained tests and ultimate shear stress in undrained tests. However, it has been difficult to find an explanation for what these critical limits represent in reality, with respect to factors like friction and attraction or cohesion).

The objective of the present study is to provide a physical explanation on the phenomena, and to express the yield values as a function of effective stresses and a set of (somewhat revised) effective stress strength parameters, the friction and attraction (Aas, 1986).

Mobilization of friction

To understand the principle for mobilizing of friction, one may look at the building up of active shear for an *in situ* clay element which has undergone an uniaxial vertical consolidation for the stresses σ'_{vo} and $K_o\sigma'_{vo}$., where σ'_{vo} is the effective vertical stress and K_o the coefficient of earth pressure at rest. This clay has not experienced any plastic strain in the lateral (horizontal) direction, and the horizontal stress has not contributed to the build-up of any frictional resistance. The vertical stress, however, has resulted in a vertical, plastic compression of the clay, and caused a mobilized friction along a 45° plane equal to $^1/_2\sigma'_{vo}\sin\varphi'_M$. The friction angle φ'_M is denoted *the material friction angle o*f the clay. The term "material" indicates that the strength parameter is believed to be a pure material constant and, hence, independent of stress level, stress direction and stress history.

The stress conditions for this clay represent the final stage of a yielding process and are dictated from a simple requirement of static equilibrium. Hence, the mobilized frictional resistance needs to be equal to the applied shear stress:

$$s_{uA} = {}^1/_2(\sigma'_{vo}\, s_{uA} - \sigma'_{ho}) = {}^1/_2\sigma'_{vo}\cdot\sin\varphi'_M \qquad (2)$$

which gives:

$$\sigma'_{ho}/\sigma'_{vo} = K_o = 1 - \sin\varphi'_M \qquad (3)$$

Equation (3) is the well-known Jaky formula (Jaky, 1948), expressing the coefficient of earth pressure at rest for a normally consolidated soil.

Activation of attraction

Most clays have in addition a contribution to shear strength due to attraction. This is believed to be resulting of net attractive forces acting between clay particles, like a tension reinforcement in the clay. The attractive forces increase with decreasing distance between the soil particles. Consequently, the attraction, σ'_a, is believed to reflect on the effective stresses to which the clay is subjected:

$$\sigma'_a = \chi\cdot\sigma'_{na} \qquad (4)$$

where χ is *the relative material attraction* and σ'_{na} the value of the effective stress in the direction normal to the attractive force. Activation of the attraction is restricted to conditions of effective stress unloading and does not occur in connection with increasing effective stresses.

Lower limiting stresses

Figure 1describes the process leading to the limiting stresses under undrained shear. The clay element described above is first at a state described by the term "Primary consolidation". As a result of the mobilization of friction, the clay has mobilized an active shear resistance equal to $^1/_2\sigma'_{vo}\,sin\varphi'_M$. The activation of the attraction makes it then possible for this clay to reduce the effective horizontal stress by an amount of $\chi\cdot\sigma'_h$ in active shear. This operation, which does not involve plastic strain, leads to a lower limiting stress, σ'_{LLSA}:

$$\sigma'_{LLSA} = \sigma'_{vo}\,(1 - \chi - sin\varphi'_M) \tag{5}$$

and an active undrained shear resistance, s_{uA}:

$$s_{uA} = {}^1/_2\sigma'_{vo}(\chi + sin\varphi'_M) \tag{6}$$

Figure 1 shows that if one adds a shear strain to the clay in order to mobilize friction due to also the horizontal stress, this results in high pore pressures, structural disturbance and failure, as shown in the uppermost and lowermost diagrams.

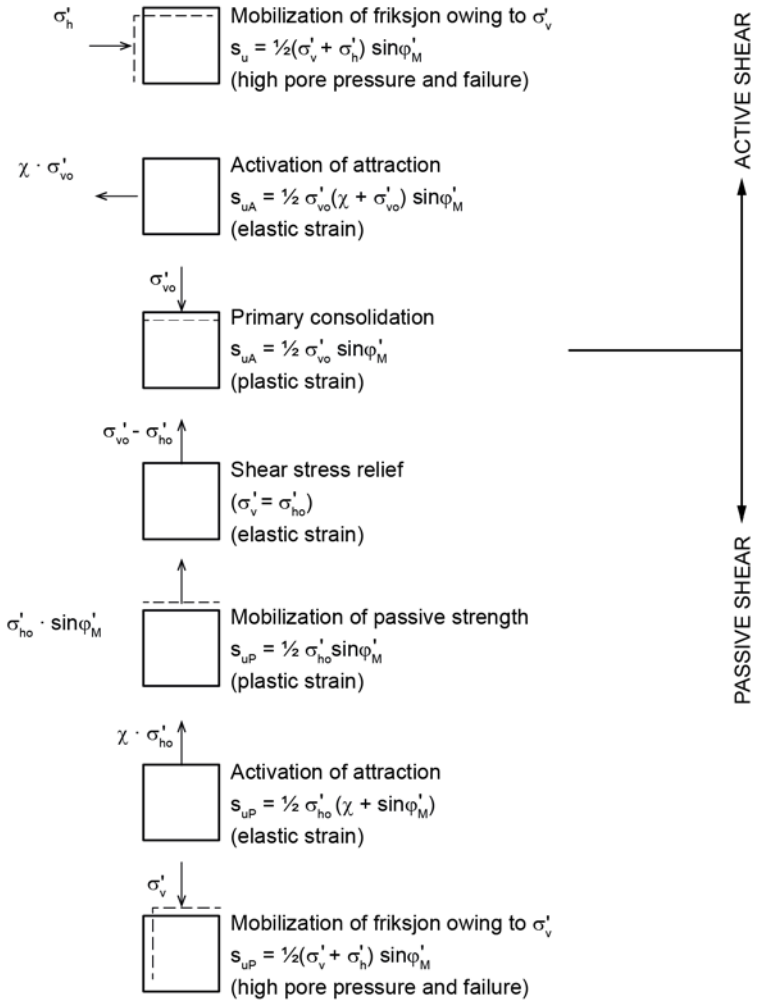

Figure 1. Mobilization of friction and attraction in active and passive shear.

Figure 1 also shows how one moves from the "Primary consolidation" condition to the lower limiting stress in passive shear. A shear stress relief resulting in $\sigma'_v = \sigma'_{ho}$ involves only elastic strain and has no influence on the clay's ability to mobilize friction. A further vertical unloading, however, will result in a condition just opposite to that in the active shear above in Figure 1. This leads to a uniaxial vertical plastic expansion. At the point where the effective vertical stress reaches the value of $\sigma'_v = K_0\sigma'_{vo}\,(1 - \sin\varphi'_M)$, the friction resistance is now balanced by the appearing passive shear stress, so that the friction resistance and the shear stress are both equal to $^1/_2\sigma'_{ho}\sin\varphi'_M$. The activation of the attraction will, in this case, lead to a lower limiting stress, σ'_{LLSP}:

$$\sigma'_{LLSP} = K_0\sigma'_{vo}\,(1 - \chi - \sin\varphi'_M) \tag{7}$$

Correspondingly, the passive undrained shear resistance, s_{uP}, becomes:

$$s_{uP} = {}^1/_2\sigma'_{vo}\,(\chi + \sin\varphi'_M) \tag{8}$$

In this case, a further straining in an attempt to mobilize friction, now due to the vertical stress, results in a structure collapse and reduced strength. The explanation on this behaviour in active and passive shear is believed to be that the transition from uniaxial to three-dimensional shear strain, represents a more brutal reorganization of the clay structure than experienced before.

Upper limiting stresses

There exists also a set of upper limiting stresses which cannot be exceeded, without resulting in yielding and, at the same time, increasing strain. For the young, normally consolidated clay above, the upper limiting stresses in active and passive shear are σ'_{vo} and $K_{0'}\sigma'_{vo}$, respectively. However, if the clay has undergone an additional uniaxial vertical deformation due to, for instance, ageing, weathering or mechanical overconsolidation, it will react like a young, normally consolidated clay stressed to a vertical stress σ'_{vE} greater than σ'_{vo}, and experience a strain equal to that of the normally consolidated clay.

Hence, the upper limiting stresses in active and passive shear become:

$$\sigma'_{ULSA} = \sigma'_{vE} \tag{9}$$

$$\sigma'_{ULSP} = \sigma'_{vE}\,(1 - \sin\varphi'_M) \tag{10}$$

Yield envelopes

Points on a yield envelope may be constructed in the following way:

One starts with the well-known Mohr Coulomb diagram and a clay for which the preconsolidation stress p'_c ($= \sigma'_{vE}$) and the effective stress strength parameters, χ and $\sin\varphi'_M$, are known. One then chooses a consolidation condition, including the stresses σ'_{vo} and σ'_{ho}, and indicates the tests and effective stress paths for cases where one of the principal stresses is kept constant while the other one is either increased or decreased. As illustrated in Figure 2:

- Unloading cases indicated by the stress paths $a-b$ and $a-c$ end on the χ-lines expressing the lower limiting stresses in active and passive shear, corresponding to Eq. (5) and (7).
- The stress path $a-d$ showing the result of an increase in horizontal effective stress, ends on the line expressing $\sigma'_v = \sigma'_{vE}\,(1 - \sin\varphi'_M)$ in accordance with Eq. (10).
- The stress path for the loading case $a-e$ (σ'_v increasing) ends on the line B−C in the diagram in Figure 2, which defines that the ratio $\Delta\sigma'_h/\Delta\sigma'_v$ equals $(1 - \sin\varphi'_M)$, stating the limit for pure uniaxial and elastic strain under loading (no attraction involved).
- For high values of both σ'_{vo} and σ'_{ho}, the stress path $f-g$ may end on the line expressing σ'_{vE}.

In the above examples, the vertical consolidation stress represents the major principal stress and does not exceed the value of $\sigma'_{vE}\,(1-\sin\varphi'_M)$. Under this condition, the lines surrounding the area ABCDEFA (in red letters in Fig. 2) constitute the yield envelope for the considered clay. However, the yield envelope is not a definitely unique property of a given clay, as it may vary somewhat depending of the stress path chosen. For instance, for a horizontal unloading case starting with a vertical consolidation stress close to p'_c, the stress path $h-i$ will end on the extended χ- line, due to activation of the attraction (line B-C' in red letters in Fig. 2).

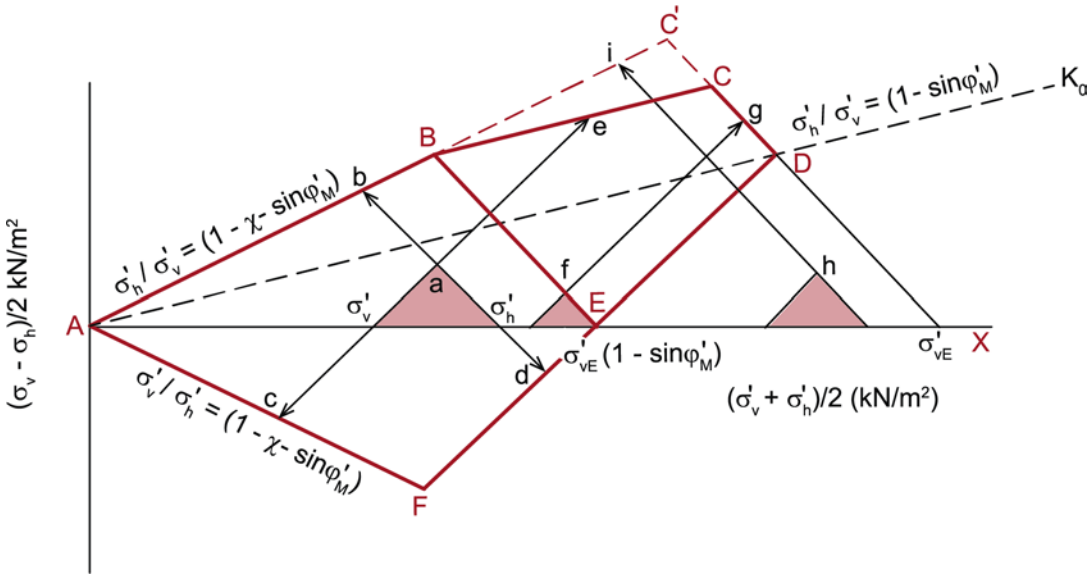

Figyre 2. A theoretical example of a yield envelope

Conditions that have an influence on the upper limiting stresses

Strain rate effect

Innumerable examples from the geotechnical literature have demonstrated that the undrained shear strength depends on strain rate, or, alternatively, the duration of failure load application. The above shear strength concept makes it possible to explain the strain rate effect in a rather simple way.

The secondary compression process involves a rate of settlement gradually decreasing with time. Consequently, the process could be related to strain rate, such that to a certain point of elapsed time, there corresponds a certain value of strain rate. This simply means that any aged clay would behave, in undrained shear, as a young, normally consolidated, if exposed to a strain rate exactly equal to the "current" value corresponding to the current age of the clay. If loaded faster than the "current" strain rate, the aged clay will show an apparent preconsolidation in triaxial and oedometer tests. Hence, recorded values of apparent preconsolidation stress, p'_c or upper limiting stress σ'_{ULSA}, are functions of how high the applied strain rate is in relation to the "age-governed" strain rate for the clay.

Figure 3 shows effective stress paths from four undrained, active triaxial tests on plastic Drammen clay, all reconsolidated to stresses below the *in situ* stresses (Berre, 1973). The applied rate of strain varied in the test series from 0.0015 to 35 % per hour. As can be seen, the lower limiting stress σ'_{ULSA} is the same in all tests, as it theoretically should be, and that it is an exclusive function of the *in situ* vertical effective stress.

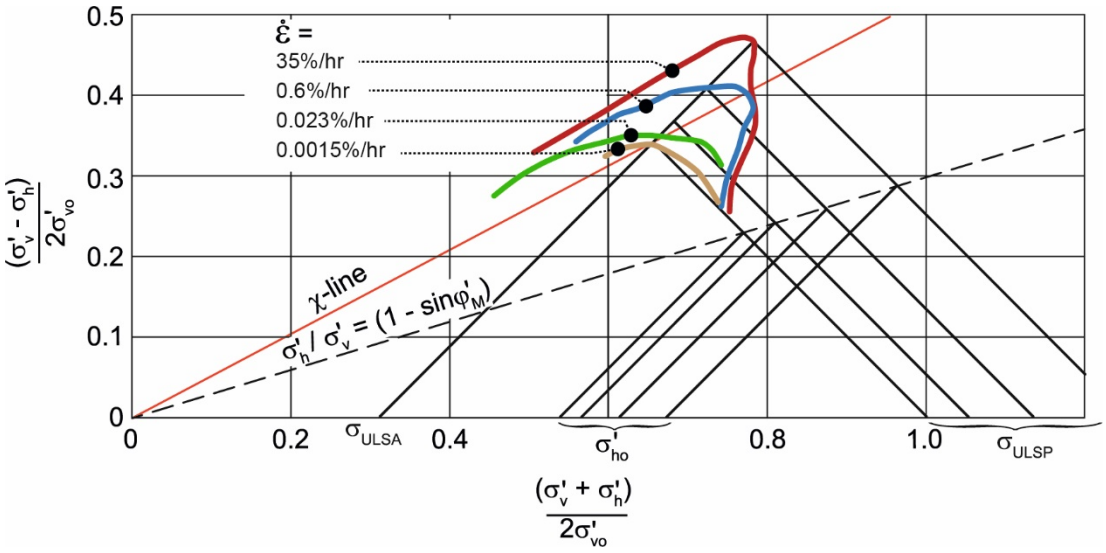

Figure 3. Effects of secondary compression on apparent in situ effective stresses and undrained, active triaxial strength (plastic Drammen Clay)

The slowest test indicates a p'_c-value approximately equal to σ'_{vo} and, hence, a nearly young, normally consolidated clay. The other tests indicate increasing values of apparent horizontal effective stress and p'_c (or σ'_{ULSA}) with increasing strain rate. These tests thus seem to demonstrate clearly that the strength parameters $\sin\varphi'_M$ and χ are fundamental with respect to strain rate.

The effects of secondary compression described above involve that recorded values of *in situ*, horizontal effective stress also are strain dependent.

Sampling disturbance

Figure 4 illustrates the significant difference in the effective, active stress paths of Ellingsrud clay for a test specimen cut from a block samples and a test specimen from a 95-mm steel tube

sample. The specimens tested were from depths 7.3 and 13.1m. The tests on tube samples gave for this clay 25−30% lower undrained, active shear strength than the tests on block samples. The block samples were taken with the University of Sherbrooke cylindrical block sampler (Lefebvre and Poulin, 1979).

The explanation for the effect of disturbance is that the upper limiting stress in active shear indicated by the top point of the stress path for the block samples reduces significantly in the tube samples. This reduction nullifies the effect of ageing appearing in the block sample tests. Hence, it can be hypothesized that the disturbance and strength reduction in the piston sample, in this extremely quick and nearly attraction-free clay, is due to a plastic elongation of the tube sample in the vertical direction. Such an elongation will have a directly opposite effect to that of secondary compression on the upper limiting stresses in undrained shear.

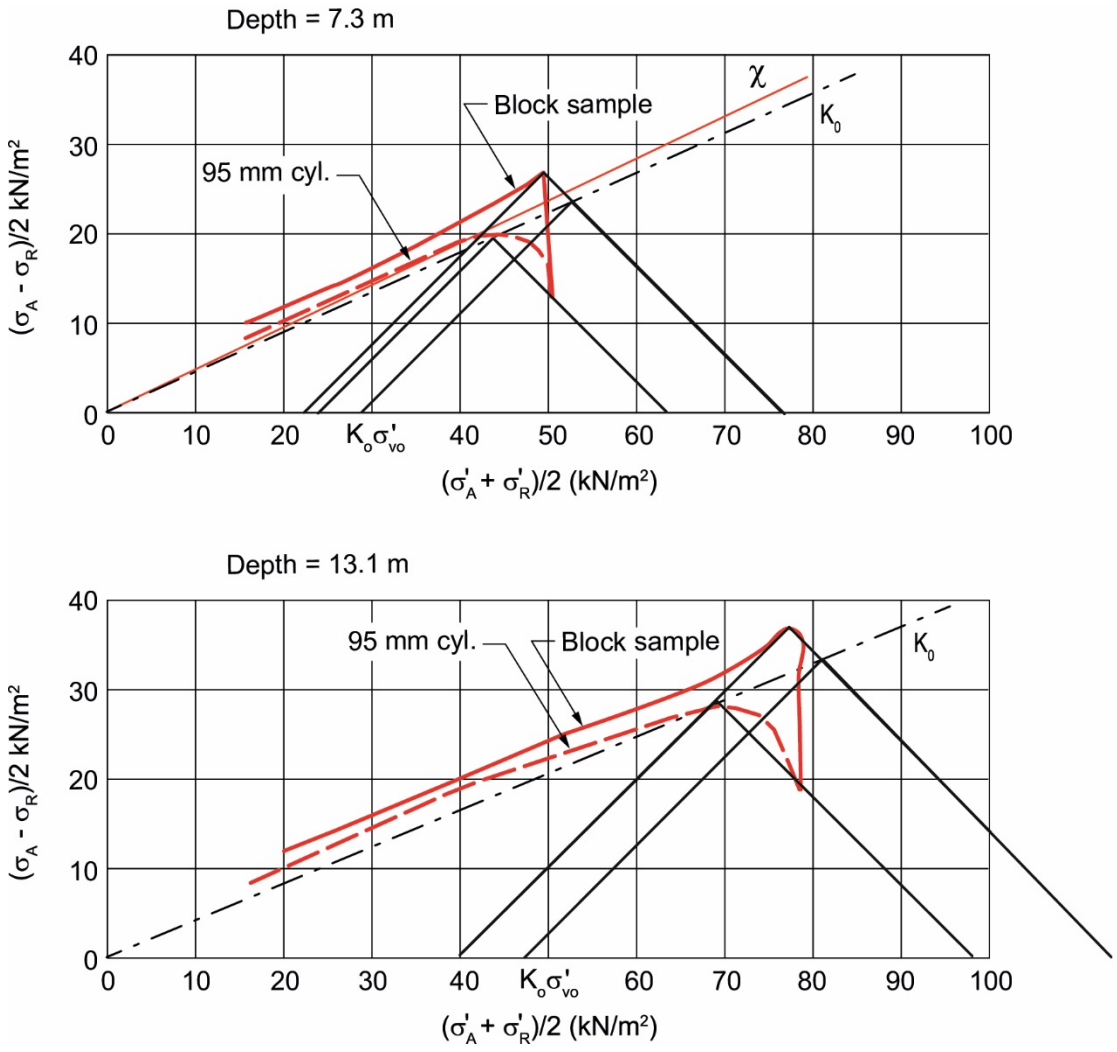

Figure 4. Effective stress paths from undrained, active triaxial tests on 95-mm and block samples on Ellingsrud clay (Lacasse et al., 1985).

Examples of yield envelopes

Backebol Clay

Figure 5 shows the results from a series of oedometer and drained triaxial and plane strain tests for the determination of the yield envelope for the Backebol clay (Larsson, 1981). In the shear tests, one of the principal stresses was kept constant while the other one was either increased or decreased. Full symbols represent the yield values, and open symbols the failure values. Failure was possible to be determine in unloading tests only. It should be remembered that a test procedure involving effective stress unloading alone provides a necessary condition to activate the attraction of the clay.

At the sampling depth for this test series, the effective vertical stress was about 30 kPa, whereas the preconsolidation stress, p'_c, recorded in oedometer tests was 48 kPa. Effective horizontal stress measured with Gløtzl-cells and pressuremeter was 25 kPa. The clay was highly plastic (I_p = 56%) and showed signs of weathering at the sampling depths.

With the effective stress strength parameters $sin\varphi'_M$ = 0.35 and χ = 0.40 for the Backebol clay, all the yielding and failure points in Figure 5 may be fitted to a yield envelope consisting of:

- the upper limiting stress in active shear, σ'_{vE};
- the upper limiting stress in passive shear, $\sigma'_{vE}\,(1 - sin\varphi'_M)$; and
- the two χ-lines.

These test results represent an extremely good confirmation of the ideas on which the yield envelope was based upon in Figure 2.

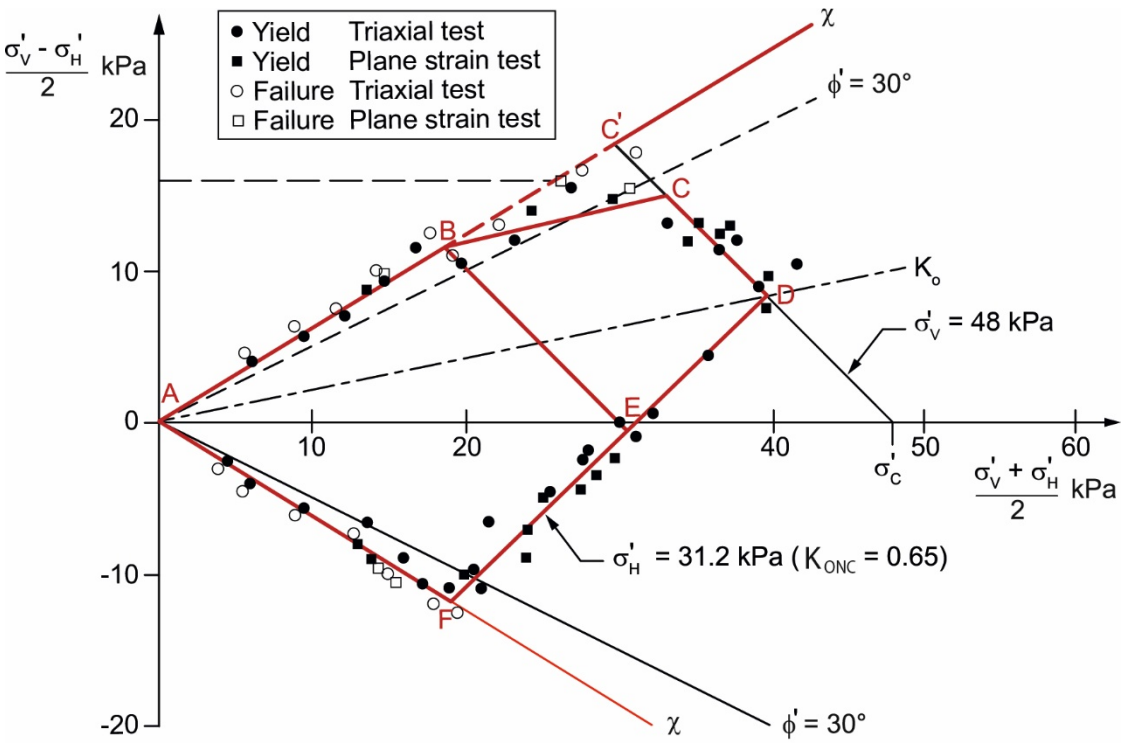

Figure 5. Yield envelope for Backebol clay-

Drammen Clay

Figure 6 shows a yield envelope constructed for a plastic Drammen clay (Berre, 1975). The specimen were first consolidated to the same effective stresses as the clay had been exposed to *in situ* (Point 1 in Fig. 6). The following drained triaxial tests were then performed:

1) The vertical stress was kept constant, and the horizontal stress was decreased (path *1−2*)
2) The vertical stress was increased, and the horizontal stress was kept constant (path *1−3*).
3) Both vertical and horizontal stresses were increased, such that the specimen area remained constant (K_0-test, path *1−4*).
4) The vertical stress was kept constant, and the horizontal stress was increased (path *1−5*).
5) The vertical stress was decreased, and the horizontal stress was kept constant (path *1−6*).

Points 2 and 6 are failure in the unloading tests as the stress paths reach the upper and lower yield envelopes respectively. The vertical stress at Point 4 equals the upper yield stress p_c' *(=* σ'_{vE}*)*. The calculated K_0-value in the current study deviates from the value suggested by Berre (1975), and indicated by the line 1−4 in Figure 6.

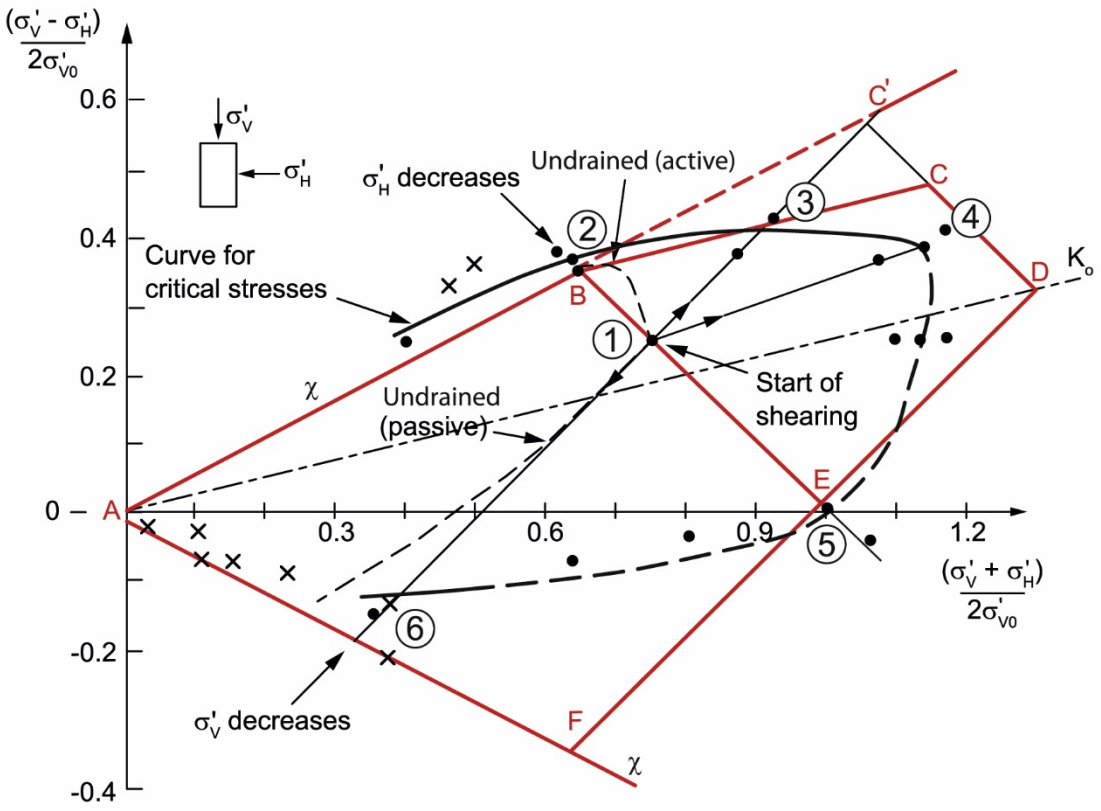

Figure 6. Yield envelope for Drammen plastic clay.

Tests by Ramanatha (1975) on the same plastic Drammen clay (I_p = 34%) looked at drained triaxial active and passive tests on undisturbed clay under relatively low effective stresses. These results shown as cross marks in Figure 6. These fall closely to the yield envelope from the undrained tests.

With the effective stress strength parameters $sin\varphi'_M = 0.37$ and $\chi = 0.34$ for the plastic Drammen clay (I_p = 34%), the yielding and failure points in Figure 6, in spite of a limited number of test results, can be fitted to a yield envelope consisting of:

- the upper limiting stress in active shear, p'_c;
- the upper limiting stress in passive shear, $p'_c\ (1 - -sin\varphi'_M)$; and
- the two χ-lines.

The diagram in Figure 6 deviates from the original version published by Berre (1975) in that the χ-lines now replace similar lines which indicated a friction angle equal to 30°.

New Jersey Clay

Figure 7 shows the yield envelope constructed for the marine plastic New Jersey clay (I_p = 43%). The clay had an overconsolidation ratio of 3 to 4. The shear testing program involved, among others, undrained active and passive triaxial and plane strain tests on undisturbed clay samples.

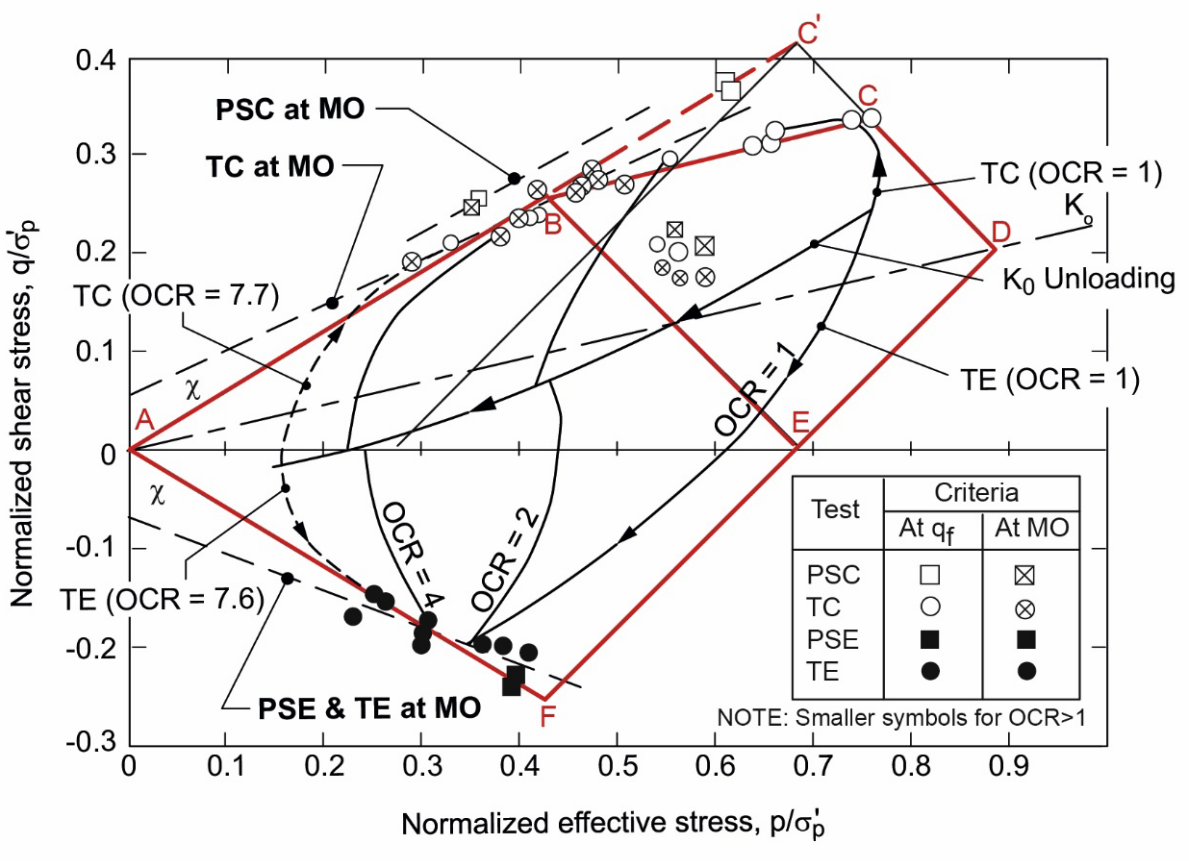

Figure 7. Yield envelope for New Jersey plastic clay (Koutsoftas and Ladd, 1984)
TC and TE: triaxial compression (active) and extension (passive) tests;
PSC and PSE: plane strain compression (active) and extension (passive) tests;
At q_f = at peak shear stress; At MO = at maximum obliquity;
$q = (\sigma_1 - \sigma_3)/2$; $p = (\sigma'_1 + \sigma'_3)/2$; σ'_p = preconsolidation stress; OCR = overconsolidation ratio.

Based on the SHANSEP approach (Ladd and Foott, 1974; Ladd *et al.*, 1977), developed to minimize the effects of sampling disturbance on the normalised shear strength parameters, all specimens were consolidated well beyond the *in situ* preconsolidation stress and then unloading to varying overconsolidation ratios. For compression (active) testing, the vertical stress was increased. For extension (passive) tests, the vertical stress was decreased. Both tests maintained constant cell pressure.

In Figure 7, four sets of active and passive effective stress paths are shown, where the last ones ended on the passive χ-line, while the active tests seem to land on the B–C line (see also Fig. 2). The points for two failure criteria are shown: at maximum shear stress (q_f) and at maximum obliquity (MO, where the ratio of the major and minor principal streeses σ'_1/σ'_3) is maximum).

The calculated effective stress shear strength parameters are $sin\varphi'_M = 0.37$ and $\chi = 0.39$ for the New Jersey plastic clay.

Boston Blue Clay

Figure 8 shows then yield envelope adapted to the test results for Boston Blue clay. The clay had approximately 50% clay size (less than two μm particle size) and a plasticity index of 21%.

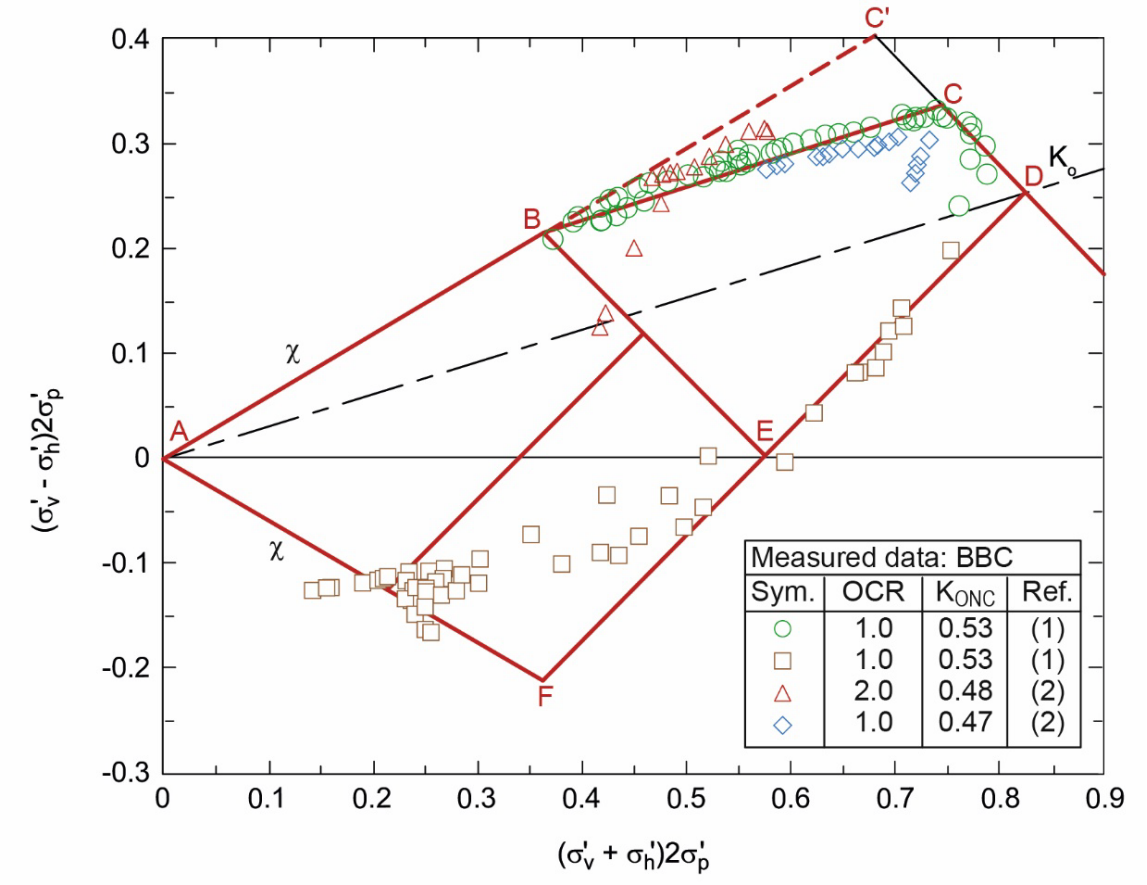

Figure 8. Yield envelope for Boston Blue clay
σ'_p = preconsolidation stress; OCR = overconsolidation ratio; K_{0NC}=K_0 for normally consolidated clay (data after Jamiolkowski et al., 1985; O'Neill, 1985)

Batches of resedimented Boston Blue clay were prepared by consolidating a clay slurry under conditions that resulted in strength and consolidation properties similar to those of natural Boston Blue Clay. The consolidated cake was extruded and stored in transformer oil prior to testing. Specimen were then cut from the cake and subjected to consolidated undrained plane strain tests under a maximum effective consolidation stress of about 40 kPa. The test program included tests run on samples with nominal overconsolidation ratios (ratios) of 1, 2 and 4.

The calculated effective shear strength parameters were $sin\varphi'_M$ = 0.46 and χ = 0.29.

James Bay, B-6 Marine Clay

At 12 meter depth, the James Bay, B-6 marine clay had a natural water content of about 40%, a plasticity index of 10%, a sensitivity of 280 and a clay fraction (less than 2 μm particle size) of 71%. The clay was overconsolidated, probably partly due to weathering.

Figure 9 shows the results from active and passive triaxial tests on normally consolidated specimens of this brittle clay.

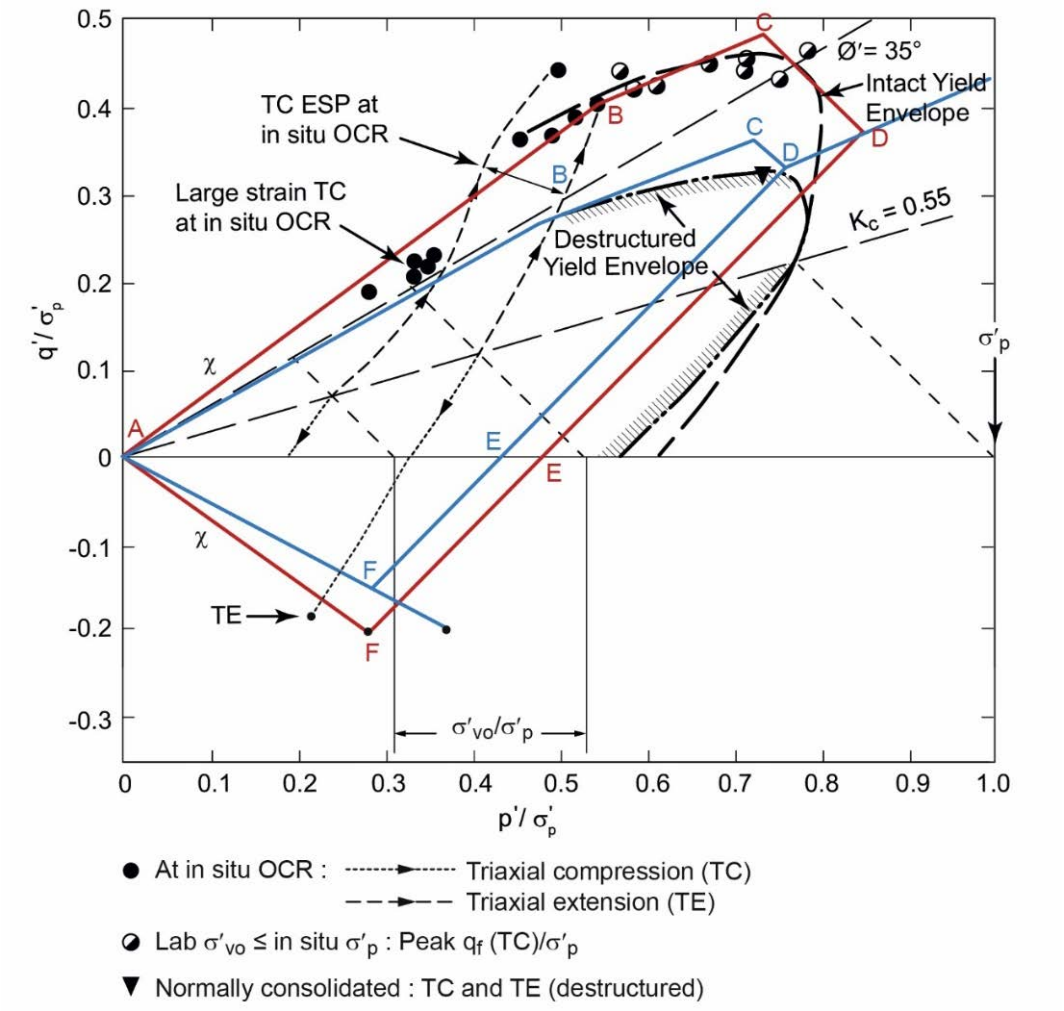

Figure 9. Yield envelopes for the James Bay B-6 Marine Clay.
Polygon ABCDEFA (red) is for the undisturbed clay. Polygon ABCDEFA (blue) is for the disturbed clay.
ESP = effective stress path (data after Jamiolkowski et al., 1985).

The following consolidation conditions, based on a stipulated value of K_0 = 0.55 were used:

1) Consolidation to $\sigma'_{vc} = \sigma'_{vo}$ on specimens at five depths, to measure the behaviour of "intact clay" at the *in situ* overconsolidation ratio (OCR), which varied from 1.8 to 3.3.
2) Consolidation to σ'_{vc}/σ'_p between 0.6 and 1.0 at two depths to measure the effect of recompression on intact clay.
3) Consolidation to σ'_{vc} ranging from 1.3 to 3 times the *in situ* preconsolidation stress σ'_p to measure the behaviour of "de-structured" clay (Leroueil *et al*., 1979).

The yield envelopes on Figure 9 were constructed on the basis of the active triaxial peak strengths and effective stress paths. The following additions were done: the revised yield envelopes were drawn for both the undisturbed and the de-structured clay. With the help of passive triaxial effective stress paths from a sample at depth 12 m (Koutsoftas and Ladd, 1984), it was possible to add also the passive parts to the envelopes.

The calculated effective stress shear strength parameters were $sin\varphi'_M$ = 0.60 and χ = 0.26 for the undisturbed clay, and $sin\ \varphi'_M$ = 0.60 and χ = 0.12 for the disturbed clay. The large reduction in attraction can be due to a certain destruction of the clay fabric, leading to a reduction of effective clay particle contacts.

James Bay, Olga Clay

The clays from the James Bay district are often described as overconsolidated due to some type of brittle cohesive bonds, due to, e.g., cementation. Earlier experience indicates that such bonds might be destroyed as a result of de-structuration or the application of stresses well above the preconsolidation stress. Test results for a second James Bay clay deposit (NGI, 1977a; 1977b) might throw further light on this phenomenon. The Olga Clay had a plasticity index of 10%.

Figure 10 presents the results of laboratory tests conducted on block samples of Olga clay from about 7 m depth. Leftmost in the diagram, the effective stress paths from active and passive plane strain and triaxial tests on specimens reconsolidated to the *in situ* stresses are shown. The result from a vane test at a corresponding depth is also shown.

The plane strain tests, supported by the 'net vane strength' data ($s_{uV} - s'_{uV}$), give the following effective strength parameters: $sin\varphi'_M$ = 0.45 and χ = 0.31. The parameters s_{uV} and s'_{uV} denote the average vane shear strength and the average remoulded vane shear strength. The difference in the Olga strength values compared with the B-6 Marine Clay above is a result of different plasticity, 25% versus 10%. The two types of active tests (triaxial and plane strain tests) gave nearly identic result, whereas the triaxial test in passive shear gave a very low value, probably due to testing shortcomings.

Figure 10 also contains active, effective stress paths from an active/plane strain and a triaxial test, where both specimens were consolidated under a vertical stress equal to $3.5\sigma'_{vo}$. This consolidation stress exceeded the apparent preconsolidation stress measured in an oedometer tests. It is interesting to note that these tests suggest a normally consolidated clay exhibiting the same effective stress shear strength parameters $sin\varphi'_M$ and χ as the weathered clay. At least for this clay, the test results indicate that the shear strength can be expressed on the basis of a set of two “true” strength parameters and the existing effective stress conditions.

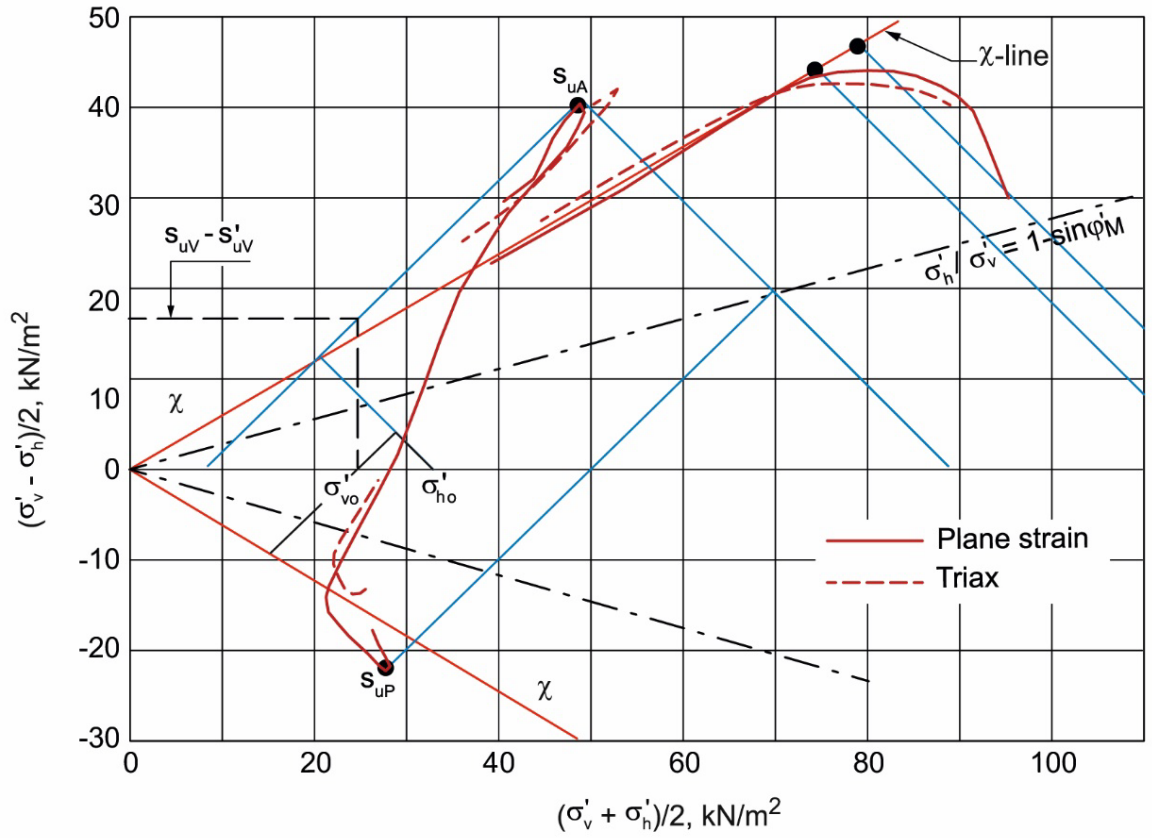

Figure 10. Determination of effective stress strength parameters for Olga clay at depth 7 m.

Effective shear strength parameters

The effective stress shear strength parameters for the six clays reported above were compared with an earlier published relationship (Aas *et al*, 1986; Aas and Lacasse, 2021) between the effective stress shear strength parameters and the clay's plasticity index. Figure 11 shows that the results from these new clay sites agree well with the earlier publications. Table 1 summarizes the values of the effective stress shear strength parameters obtained for the six clays in this paper. Except for the undisturbed cemented James Bay B-6 clay, the sum of the effective stress parameters $\chi + \sin\varphi'_M$ is between 0.71 and 0.76, with an average of 0.74, in agreement with the data presented earlier in Aas and Lacasse (2021a; b).

Table 1. Effective stress shear strength parameters for the six clays investigated in this paper

Clay	Attraction parameter, χ	Friction parameter, $\sin\varphi'_M$	Sum $\chi + \sin\varphi'_M$
Backebol	0.40	0.35	0.75
Plastic Drammen	0.34	0.37	0.71
Plastic New Jersey	0.39	0.37	0.76
Boston Blue	0.29	0.46	0.75
James Bay B-6 ("undisturbed")	0.26	0.60	0.86
James Bay B-6 ("disturbed")	0.12	0.60	0.72
Olga	0.31	0.45	0.76

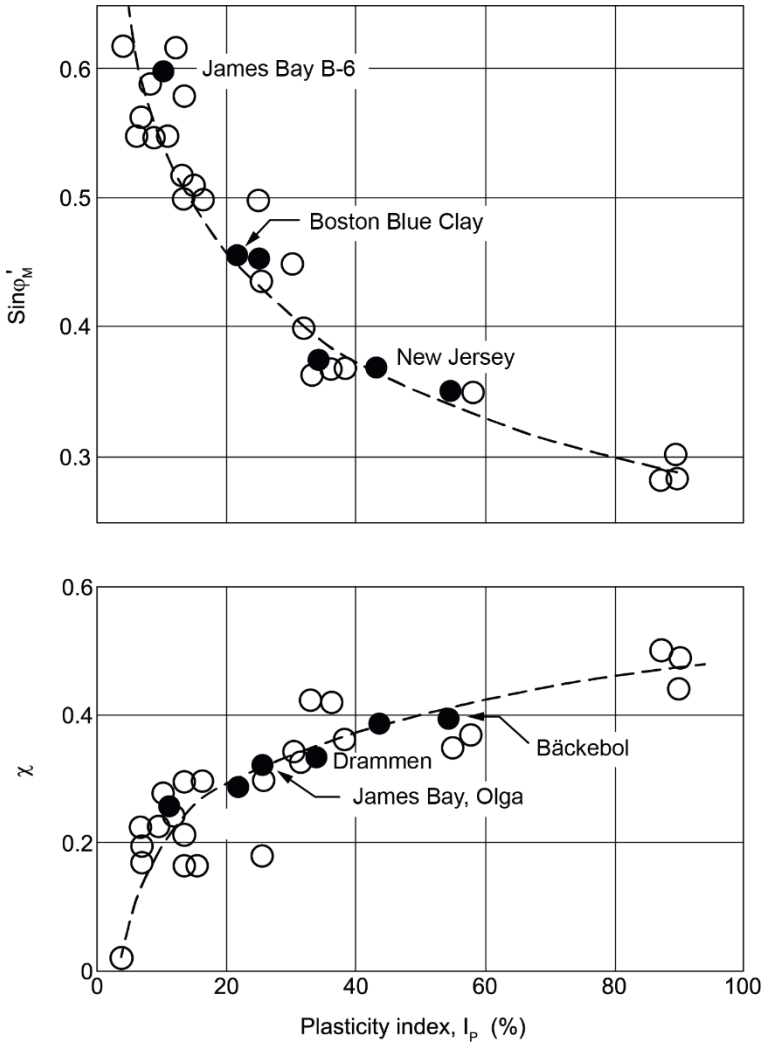

Figure 11. Friction and attraction effective stress parameters as functions of plasticity index, I_p.

Conclusions

Yield stress has often been described as a shear stress limit for a clay, representing failure or a sudden transition from small elastic to large plastic strains. It is important, however, to recognise that the general definition of a so-called yield envelope is not about strain magnitude. The yield envelope should be rather linked to relations between deformations and mobilization of the effective shear strength parameters of the clay, attraction χ and friction angle $sin\varphi'_M$. The activation of the attraction is restricted to unloading cases, and the mobilization of friction follows strict rules with respect to appearing simultaneously with plastic deformations. Actually, yielding occurs before friction has been mobilized due to the horizontal stress under active shear and the vertical stress under passive shear.

The upper boundaries of a yield envelope depend on the rate of strain and the degree of sample disturbance. The test results in this paper indicate, however, that the rate of strain and disturbance only affect the upper limiting stresses, and have no influence on the lower limiting stresses.

A yield envelope, as suggested in this paper, can be used to determine the preconsolidation stress and the effective stress shear strength parameters of the clay; or vice versa, the yield envelope can be constructed on the basis of the above mentioned soil parameters. Five examples on yield envelopes constructed from the literature, were analysed. It was possible to demonstrate a common yield envelope pattern for the five different clays.

The effective stress shear strength parameters determined for these clays fit well with the model presented by Aas and Lacasse (2021), expressing the attraction χ and friction angle $sin\varphi'_M$ parameters as a function of the plasticity index, I_p. Although the values of $\chi + sin\varphi'_M$ vary somewhat for the six clays, the sum of the two parameters χ and $sin\varphi'_M$ was invariably close to 0.8 as observed earlier.

References

Aas, G. (1986). In situ investigation techniques and interpretation for offshore practice. Recommended interpretation of vane tests. Final report. Norwegian Geotechnical Institute, Oslo. Report 40019-24. 1986-09-08.

Aas, G. and Lacasse, S. (2021a). Shear Strength of Soft Clay in Terms of Effective Stresses. 1st paper in this NGI publication.

Aas, G. and Lacasse, S. (2021b). Undrained Shear Strength of Overconsolidates Clay. 4th paper in this NGI publication.

Aas. G., Lacasse S., Lunne, T. and Høeg, K. (1986). Use of in situ teats for foundation design on clay. Use of In Situ Tests in Geotechnical Engineering. Proc. In Situ '86, ASCE. Blacksburg, VA, USA. pp. 1−30.

Berre, T. (1973). Effect of rate of strain on the stress-strain relationship for undrained triaxial tests on plastic Drammen clay. Norwegian Geotechnical Institute, Oslo. Internal report, 50301-4.

Berre, T. (1975). Bruk av triaksial- og direkte skjærforsøk til løsning av geotekniske problemer. Nordisk geoteknikermøde. København 1975. Foredrag pp. 199−211. (Also publ. In Norwegian Geotechnical Institute Publication 110, Oslo).

Graham, J., and Houlsby, G.T.H. (1983). Anisotropic elasticity of a natural clay. *Geotechnique*. **33**: 165−180.

Jaky, J. (1948). On the bearing capacity of piles. International Conference on Soil Mechanics and Foundation Engineering, 2. Rotterdam 1948. Proc. **1**: 100−103.

Koutsoftas, D.C., and Ladd C.C. (1984). Design Strength of an Offshore Clay. *JGED ASCE*. 111 (2): 337−355. https://doi.org/10.1061/(ASCE)0733-9410(1985)111:3(337).

Jamiolkowski, M., Ladd, C.C:, Germaine, J.T. and Lancellotta, R. (1985). New developments in field and laboratory testing of soils. SOA report, International Conference on Soil Mechanics and Foundation Engineering, 11. San Francisco. Proc. **1**: 57−153.

Lacasse, S., T. Berre and G. Lefebvre (1985). Block sampling of sensitive clays. International Conference on Soil Mechanics and Foundation Engineering, 11. San Francisco 1985. Proc. **2**: 887−892.

Ladd C.C. and Foot R. (1974). New design procedure for stability of soft clays. J*ournal of the Geotechnical Engineering Division*. ASCE. **100**(7): 763−786.

Ladd, C.C., R. Foott, K. Ishihara, F. Schlosser and H.G. Poulos (1977). Stress-deformation and strength characteristics: SOA report. 9th Int. Conf. Soil Mechanics and Foundation Engineering, Tokyo. Proceedings. **2**: 421−494.

Larsson, R. (1981), Drained behaviour of Swedish clays. Swedish Geotechnical Institute, Linkøping. Report 12. 157 pp.

Lau, K.A, Graham, J. and Crooks, J. (1988). Yield envelopes: identification and geometric properties. *Geotechnique*. **38**. 125−134. 10.1680/geot.1988.38.1.125.

Lefebvre, G. and Poulin, C. (1979). A new method of sampling in sensitive clay. *Canadian Geotechnical Journal*, **16** : 226−233.

Lefebvre, G., Ladd, C.C. and Pare J.J. (1988). Comparison of field vane and laboratory undrained shear strength in soft sensitive clay. ASTM Symposium: Vane shear strength testing in soils: Field and laboratory studies. ASTM STP 1014. 233−24.

Leroueil, S., Tavenas, F., Brucy, F., La Rochelle, P., and Roy, M. (1979). Behaviour of destructured natural clays. *ASCE, J of GED*, **105**(GT6): 759−778.

Mitchell, R.J. (1970). On the yielding and mechanical strength of Leda clay. *Canadian Geotechnical Journal*. **7**: 297−312,

O'Neill, D. (1985). Undrained strength anisotropy of an overconsolidated thixotropic clay. SM thesis. MIT, Cambridge, MA USA. 359 pp.

NGI (1977a). James Bay, Canada. Results of triaxial and direct simple shear tests on block samples taken at Olga site in 1977. Norwegian Geotechnical Institute. Contract Report 76050-2. Oslo, 26 Oct. 1977.

NGI (1977b). James Bay, Canada. Results of plane strain tests on block samples taken at Olga and Rupert site in 1977. Norwegian Geotechnical Institute. Contract Report 76050-4. Oslo, 9 Dec. 1977.

Ramanatha Iyer, T. S. (1975), The behaviour of Drammen plastic clay under low effective stresses. Canadian Geotechnical Journal. 12(1): 70−83.

Schofield, A. and Wroth, C.P (1968). Critical State Soil Mechanics. McGraw-Hill. ISBN: 978-0641940484

Tavenas, F. and Leroueil, S. (1977). Effect of stress and time on yielding of clays. 9th Int. Conf. Soil Mechanics and Foundation Engineering, Tokyo. Proc. **1**: 319−326.

Wood, D.M. (1980). Yielding of soft clays at Backebol, Sweden. *Geotechnique.* **30**: 49−65.

Wroth, C.P. and Houlsby, G.T. (1980). A critical state model for predicting the behaviour of clays. Proc. Workshop on Limit Equilibrium, Plasticity and Generalised Stress-Straining in Geotechnical Engineering. Montréal, Canada. pp. 592-627.

OSLO 2022

ISBN 978-82-546-1009-1